Clinical Applications of Perfusion-Weighted Magnetic Resonance Imaging in Neurological Disorders

---

Dr Yasser Falah

Thesis submitted to the University of Nottingham for the degree of Doctor of Philosophy

May 2019

Disclaimer

I, Yasser Falah, confirm that the work presented in this thesis is original. Information from other references has been indicated in the thesis and acknowledgments if taken from other sources.

Acknowledgments

I am honoured to have worked with many people during my PhD whom without this work would not have been possible. I would like to thank:

- All the patients and healthy controls who kindly participated in my projects.
- My first supervisor, Dr Nikos Evangelou, for giving me the opportunity to work within his team. I learned a lot from his experience, knowledge, and judgement. I am grateful for his support and mentorship which helped me immensely throughout the research years.
- My second supervisor, Dr Molly Bright, for her support and guidance. I am thankful for her help with scanning participants, imaging analysis, and publishing my work. Her continuous input in guiding my development and progress was crucial in helping me complete my projects.
- Professor Cris Constantinescu, Dr Bruno Gran, and the MS Neurology Consultants at QMC for their support, advice, and helpful feedback.
- Professor Penny Gowland and Dr Susan Francis, School of Physics collaborators, for their guidance in planning the MS projects, validating data results, and reviewing publications.
- Dr Robert Dineen for the RCVS study imaging analysis.

- Dr Richard Dury who worked with me on the MS projects and helped in organising the scanning sessions and analysing the imaging data during and after his PhD studies. His input in validating scanning protocols and making sure the technical aspects are addressed was crucial for the timely completion of the projects.
- Dr Chris Tench for his valuable advice on the statistical analysis of data.
- Dr Paul Morgan for his advice on imaging analysis.
- Dr Amal Samaraweera, Dr Rasha Fahim, Megi Clarke, Joe Paul, and the QMC Neurology Registrars for their help in patients recruitment and advice on using imaging software programmes and other IT systems.
- Mrs Nanci Frakich for her assistance with laboratory related work.
- The MS Specialist Nurses at Queen's Medical Centre who recruited most of the patients for the MS projects.
- The generous funding from the "Mason Medical Research Trust" for the RCVS project.
- Rulla, my beloved wife, who helped me to overcome the challenges I encountered throughout my clinical and research career. I am blessed to have your endless support and for that I will always be grateful.

- My Mum and Brothers for being there for me. Your blessings are the reason why I have achieved my goals, I hope I have made you proud.
- Dr Adnan Al-Araji, my Neurology Teacher and Mentor, for his guidance throughout my medical career. He inspired me to become a better neurologist and researcher.

Finally, I would like to dedicate my work to my late father, Professor Muhammed Alrawi (RIP); I will always be grateful to him for giving me what it takes to be where I am today.

Yasser Falah

Preface

The research presented in this thesis represents my passion for developing magnetic resonance imaging (MRI) techniques in neurological disorders. Arterial spin labeling (ASL), a non-contrast MRI method, is used as a tool to characterise different patients groups with the view to develop understanding of disease processes, confirm diagnosis, and monitor progression.

In chapter two, 7 tesla (T) ASL MRI is used to measure cortical lesions perfusion in Multiple Sclerosis (MS) and compare that to local and global normal appearing grey matter. To our knowledge, this is the first study to date addressing this issue using 7T ASL.

To assess the reproducibility of ASL and its reliability compared to the gold standard perfusion weighted MRI method, dynamic susceptibility contrast (DSC), the study detailed in chapter three was performed. This is the first longitudinal 7T ASL study to date in MS.

Reversible cerebral vasoconstriction syndrome (RCVS) is a poorly understood condition; perfusion MRI can be a useful tool complementing anatomical and vascular scans. The study described in chapter four assessed a cohort of patients who presented with recurrent thunderclap headache suggestive of RCVS using 3T ASL to validate its clinical use.

Chapter five summarises the projects I performed and highlights the aspects which need addressing before ASL can be used in clinical practice such as standardised protocols and automated imaging analysis. While 7T ASL offers invaluable opportunity to study cerebral perfusion in various neurological disorders, there are certain requirements and implications which researchers should be aware when planning studies. A multi-centre collaboration to develop ASL protocols and test their application in clinical setting is a great prospect for future work.

Publications and presentations from this thesis

1- Ultra-high-field arterial spin labelling MRI for non-contrast assessment of cortical lesion perfusion in multiple sclerosis.

Richard J. Dury*, **Yasser Falah***, Penny A. Gowland, Nikos Evangelou, Molly G. Bright, Susan T. Francis.

Eur Radiol (2019) 29: 2027-2033.

https://doi.org/10.1007/s00330-018-5707-5

(*****joint first authorship).

2- Test-retest reliability of 3D-EPI Pulsed Arterial Spin Labelling at 7T in Multiple Sclerosis.

Y. Falah, R.J. Dury, P.A. Gowland, N. Evangelou. S.T. Francis, M.G. Bright.

Poster presentation at the 34th Congress of the ECTRIMS, Berlin, October 2018.

3- Reproducibility and quality assessment of a 3D-EPI Pulsed Arterial Spin Labelling scheme at 7 T in a clinical cohort.

R. Dury, **Y. Falah**, P.A. Gowland, N. Evangelou. S.T. Francis, M.G. Bright.

Poster presentation at the Joint Annual Meeting ISMRM-ESMRMB, Paris, June 2018.

4- Assessment of perfusion in grey matter cortical lesions in Multiple Sclerosis using high-resolution ASL at 7T.

R.J. Dury, M.G. Bright, **Y. Falah**, P.A. Gowland, N. Evangelou, S.T. Francis.

Poster presentation at the 32st Congress of the ECTRIMS, London, September 2016.

5- Assessment of grey matter cortical lesions in Multiple Sclerosis using high resolution ASL at 7T.

Richard Dury, **Yasser Falah**, Molly G. Bright, Penny A. Gowland, Nikos Evangelou, Susan T. Francis.

Poster presentation at the 25th ISMRM annual meeting, Singapore, May 2016.

Contents

Disclaimer ii

Acknowledgments iii

Preface vi

Publications and presentations from this thesis viii

List of Tables xiv

List of Figures xv

List of Abbreviations xx

Chapter 1: Introduction 1

1.1 Magnetic Resonance Imaging 1

1.1.1 MRI acquisition 1

1.1.2 Perfusion imaging 7

1.1.3 Ultra-high field MRI 17

1.1.4 Limitations 19

1.1.5 Future prospective 21

1.2 Multiple Sclerosis 22

1.2.1 Causes of MS 22

1.2.2 Pathogenesis of MS 23

1.2.3 Diagnostic criteria 25

1.2.4 Cortical lesions in MS 26

1.2.5 Perfusion in MS 28

1.2.6 MRI in MS 32
1.2.7 Perfusion MRI in MS 37
1.2.8 Clinical implications for using perfusion MRI in MS 42
1.2.9 Future perspective 48
1.3 Reversible Cerebral Vasoconstriction Syndrome 50
1.3.1 Pathophysiology 50
1.3.2 Clinical features 53
1.3.3 Diagnostic criteria 54
1.3.4 Imaging 55
1.3.5 Perfusion MRI in RCVS 56
1.3.6 Treatment 57
1.4 Hypothesis 59
1.4.1 Objectives 59
Chapter 2: Ultra-High-Field Arterial Spin Labeling MRI for Non-Contrast Assessment of Cortical Lesion Perfusion in Multiple Sclerosis 61
2.1 Introduction 61
2.2 Objectives 63
2.3 Methods 64
2.4 Results 71
2.4.1 Cortical lesions identification 71

2.4.2 Perfusion in CLs 73

2.4.3 Local NAGM zones 74

2.4.4 Clinical data 75

2.5 Discussion 77

Chapter 3: 7T Arterial Spin Labeling MRI in Multiple Sclerosis: Reproducibility and Comparison with Dynamic Susceptibility Contrast 80

3.1 Introduction 80

3.2 Objectives 82

3.3 End points 83

3.4 Methods 83

3.5 Results 88

3.5.1 Global grey matter perfusion 88

3.5.2 Regional grey matter perfusion 92

3.5.3 Global white matter perfusion 104

3.5.4 White matter lesion perfusion 105

3.5.5 Clinical data 105

3.6 Discussion 110

Chapter 4: Arterial Spin Labeling MRI in Reversible Cerebral Vasoconstriction Syndrome: Longitudinal perfusion study 114

4.1 Introduction 114

4.2 Objectives 118

4.3 Endpoints 118

4.4 Eligibility criteria 119

4.5 Methods 119

4.6 Results 125

4.6.1 Anatomical data 125

4.6.2 Perfusion data 128

4.7 Discussion 136

Chapter 5: Conclusion 139

5.1 ASL in MS 139

5.2 ASL in RCVS 142

Chapter 6: Bibliography 144

List of Tables

Table 1 Perfusion MRI techniques 16

Table 2 Benefits and challenges of ASL 17

Table 3 No evidence of disease activity parameters 36

Table 4 Perfusion MRI studies in MS 39

Table 5 RCVS diagnostic criteria 54

Table 6 Cortical lesions and lesion volume for each MS patient ... 71

Table 7 Inclusion and exclusion criteria for MSGadASL study 84

Table 8 RCVS study patients' clinical data 120

Table 9 MRA scans findings 126

List of Figures

Figure 1 Precession 2

Figure 2 Longitudinal (T_1) relaxation 3

Figure 3 T1-weighted contrast 4

Figure 4 Transverse (T_2) relaxation 5

Figure 5 T2-weighted contrast 6

Figure 6 Example of CL, ASL map, and NAGM zones mask 70

Figure 7 Example of leuco-cortical lesion 72

Figure 8 Example of intracortical lesion 73

Figure 9 CBF in cortical lesions, local normal appearing grey matter, and cortical grey matter 74

Figure 10 CBF in cortical lesions compared to surrounding normal appearing grey matter zones. 75

Figure 11 Correlation between age and global cortical GM CBF 76

Figure 12 Correlation between EDSS and global cortical GM CBF . 76

Figure 13 Correlation between MFIS and global cortical GM CBF .. 77

Figure 14 Bland-Altman plot for ASL in MS patients 89

Figure 15 Bland-Altman plot for ASL in healthy controls 89

Figure 16 Correlation between ASL GM CBF data in MS patients .. 90

Figure 17 Correlation between ASL GM CBF data in healthy controls 90

Figure 18 Bland-Altman plot for ASL and DSC in MS patients 91

Figure 19 Correlation between mean GM CBF measurements using ASL and DSC in MS patients 91

Figure 20 Comparison of regional GM CBF between ASL visit 1 and 2 in MS patients 92
Figure 21 Correlation between right ACA ASL GM CBF data in MS patients 93
Figure 22 Correlation between left ACA ASL GM CBF data in MS patients 93
Figure 23 Correlation between right MCA ASL GM CBF data in MS patients 94
Figure 24 Correlation between left MCA ASL GM CBF data in MS patients 94
Figure 25 Correlation between right PCA ASL GM CBF data in MS patients 95
Figure 26 Correlation between left PCA ASL GM CBF data in MS patients 95
Figure 27 Comparison of regional GM CBF between ASL visit 1 and 2 in healthy controls 96
Figure 28 Correlation between right ACA ASL GM CBF data in healthy controls 97
Figure 29 Correlation between left ACA ASL GM CBF data in healthy controls 97
Figure 30 Correlation between right MCA ASL GM CBF data in healthy controls 98
Figure 31 Correlation between left MCA ASL GM CBF data in healthy controls 98

Figure 32 Correlation between right PCA ASL GM CBF data in healthy controls 99
Figure 33 Correlation between left PCA ASL GM CBF data in healthy controls 99
Figure 34 Comparison of regional GM CBF between ASL visit 1 and DSC in MS patients 100
Figure 35 Correlation between right ACA GM CBF data in MS patients 101
Figure 36 Correlation between left ACA GM CBF data in MS patients 101
Figure 37 Correlation between right MCA GM CBF data in MS patients 102
Figure 38 Correlation between left MCA GM CBF data in MS patients 102
Figure 39 Correlation between right PCA GM CBF data in MS patients 103
Figure 40 Correlation between left PCA GM CBF data in MS patients 103
Figure 41 Correlation between mean WM CBF measurements using ASL and DSC in MS patients 104
Figure 42 Correlation between age and ASL GM CBF in MS patients 106
Figure 43 Correlation between age and ASL GM CBF in healthy controls 106

Figure 44 Correlation between disease duration and ASL GM CBF in MS patients 107
Figure 45 Correlation between EDSS and ASL GM CBF in MS patients 107
Figure 46 Correlation between age and DSC GM CBF in MS patients 108
Figure 47 Correlation between disease duration and DSC GM CBF in MS patients 109
Figure 48 Correlation between EDSS and DSC GM CBF in MS patients 109
Figure 49 RCVS study participation timeline 123
Figure 50 Distal narrowing in the left anterior cerebral artery (participant 1, visit 1)..... 126
Figure 51 Resolution of the left anterior cerebral artery narrowing (participant 1, visit 2)..... 127
Figure 52 Narrowing of the right middle cerebral and basilar arteries (participant 2, visit 1) 127
Figure 53 Resolution of the right middle cerebral artery narrowing (participant 2, visit 2)..... 128
Figure 54 Resolution of the basilar artery narrowing (participant 2, visit 2)..... 128
Figure 55 Participant 1 regional/global GM rCBF across visits.... 131
Figure 56 Participant 2 regional/global GM rCBF across visits.... 132
Figure 57 Participant 4 regional/global GM rCBF across visits.... 133

Figure 58 Participant 1 regional/left MCA rCBF across visits 134

Figure 59 Participant 2 regional/left MCA rCBF across visits 135

Figure 60 Participant 4 regional/left MCA rCBF across visits 136

List of Abbreviations

ACA	Anterior cerebral artery
AIF	Arterial input function
ASL	Arterial spin-labeling
ATT	Arterial transit time
bSSFP	Balanced steady-state free precession
CASL	Continuous arterial spin-labeling
CBF	Cerebral blood flow
CBV	Cerebral blood volume
CIS	Clinically isolated syndrome
CLs	Cortical lesions
CNS	Central nervous system
CO_2	Carbon dioxide
CoV	Coefficient of variation
CSF	Cerebrospinal fluid
CT	Computed tomography
CTA	Computed tomography angiography
CVR	Cerebrovascular reactivity
DCE	Dynamic contrast enhanced
DIR	Double Inversion Recovery
DMTs	Disease modifying therapy drugs
DSC	Dynamic susceptibility contrast
DWI	Diffusion weighted imaging
E-1	Endothelin-1
EDSS	Extended Disability Status Scale
EPCs	Endothelial progenitor cells
FAIR	Flow-alternating inversion recovery
FLAIR	Fluid attenuation inversion recovery
FOV	Field of View
FSS	Fatigue Severity Scale
Gd	Gadolinium
GM	Grey matter

HCs	Healthy controls
ICHD-3	International classification of headache disorders, 3rd edition
IHS	International Headache Society
IRIS	Immune reconstitution inflammatory syndrome
MCA	Middle cerebral artery
MD	Mean diffusivity
MFIS	Modified Fatigue Impact Scale
MPRAGE	Magnetization Prepared Rapid Acquisition Gradient
MRA	Magnetic resonance angiography
MRI	Magnetic resonance imaging
MS	Multiple sclerosis
MTT	Mean transit time
NAGM	Normal appearing grey matter
NAWM	Normal appearing white matter
NEDA	No evidence of disease activity
PASL	Pulsed arterial spin-labeling
PCA	Posterior cerebral artery
pCASL	Pseudo-continuous arterial spin-labeling
PET	Positron emission tomography
PLD	Post-label delay
PML	Progressive multifocal leukoencephalopathy
PPMS	Primary progressive multiple sclerosis
PRES	Posterior reversible encephalopathy syndrome
PSIR	Phase-sensitive inversion recovery
PWI	Perfusion-weighted imaging
rCBF	Relative cerebral blood flow
RCVS	Reversible cerebral vasoconstriction syndrome
RF	Radiofrequency
ROI	Region of interest
RRMS	Relapsing remitting multiple sclerosis
SAH	Subarachnoid haemorrhage
SNR	Signal-to-noise ratio
SPECT	Single-photon emission-computed tomography
SPMIC	Sir Peter Mansfield Imaging Centre

SPMS	Secondary progressive multiple sclerosis
SWI	Susceptibility weighted imaging
T	Tesla
TCD	Transcranial doppler ultrasonography
TE	Echo Time
TR	Repetition Time
WM	White matter
WMLs	White matter lesions

Chapter 1: Introduction

1.1 Magnetic Resonance Imaging

The introduction of Magnetic resonance imaging (MRI) to clinical practice more than three decades ago has transformed our understanding of many conditions that affect the human body. The use of MRI in diagnosing and monitoring neurological conditions has proven crucial to achieve better outcomes. Advances in MRI development have helped to address many questions raised by clinicians dealing with diseases affecting the central nervous system (CNS), its arterial blood supply, and venous drainage system.

MRI is a safe and radiation free technique compared to other types of imaging such as X-ray, computed tomography (CT), and positron emission tomography (PET). This offers the option of performing imaging at multiple time points which is valuable in conditions such as brain tumours, multiple sclerosis (MS) and other neuro-inflammatory brain disorders.

1.1.1 MRI acquisition

The MR signal used to generate images comes from hydrogen nuclei which each contains a single proton with positive electrical charge. Protons have a "spin" property which produces a positively

charged magnetic field with random orientation. Applying an external magnetic field, referred to as "B_0", causes protons to align either parallel or antiparallel to B_0. As a result, protons act as little bar magnets. Precession is the term used to describe the spinning of group of protons in a certain way (Figure 1). Sum magnetisation, referred to as "M_0", represents the parallel precessing of protons in relation to B_0. It is not possible to measure the person's magnetic force as he/she lies in the scanner parallel to B_0. A magnetisation lying at an angle to B_0 is needed. Radiofrequency (RF) pulses are produced by RF coils and they are switched on and off to trigger protons alignment out of B_0. RF pulses need to have same frequency as the precessional frequency of the protons; this is called resonance; which is the reason behind the term "magnetic resonance imaging" (Currie et al. 2013).

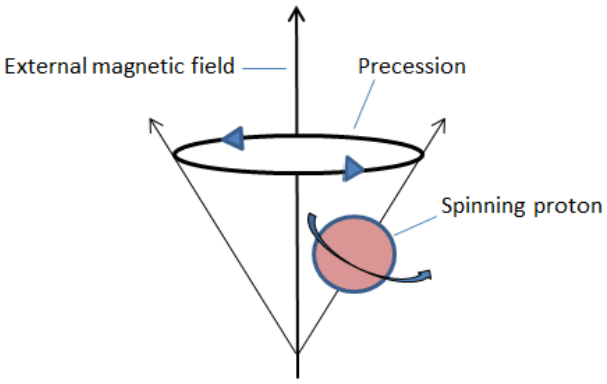


Figure 1 Precession

1.1.1.1 T_1 relaxation

The applied RF pulses induce an energy exchange state between the spinning protons and the surrounding matter or lattice. Reversal of the net magnetisation to the equilibrium orientation in the applied field direction is called "spin-lattice relaxation rate". The time dependence of the recovery is represented by a single exponential function with time constant "T_1" which is the "spin-lattice or longitudinal relaxation time" (Gore et al. 1981) as shown in Figure 2 (Pooley 2005).

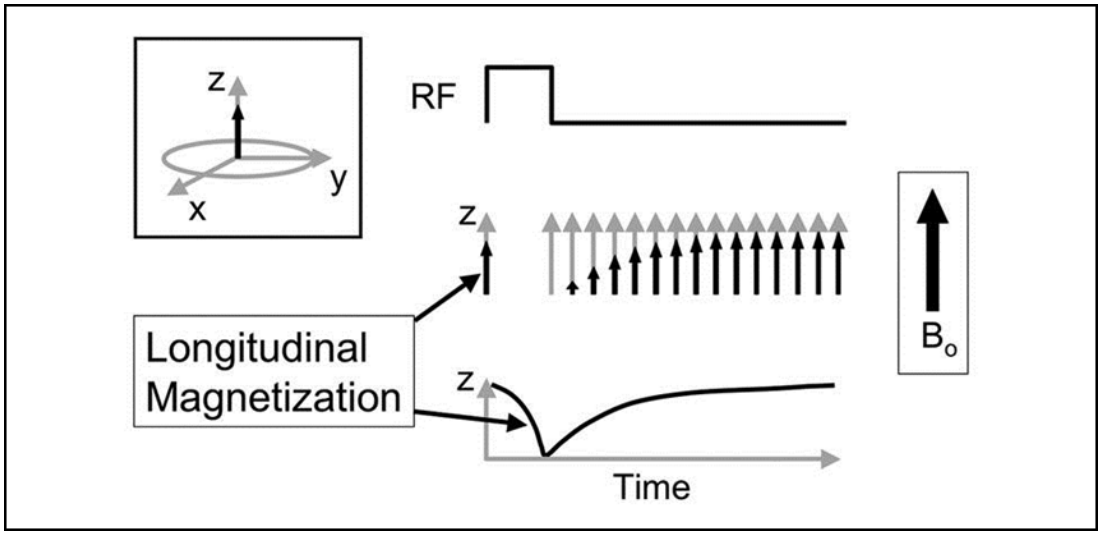


Figure 2 Longitudinal (T_1) relaxation
(Reproduced with permission from Pooley 2005)

Protons from different tissues have different rate at which longitudinal relaxation grows back; this is the source of contrast seen in T1-weighted images. Cerebrospinal fluid (CSF) has a long T_1 time (relaxes slowly and appears dark), grey matter (GM) has

an intermediate T_1 (relaxes at an intermediate rate and appears as shades of grey), and white matter (WM) has short T_1 time (relaxes rapidly and appears light in colour). Because there are different relaxation times, a good time to acquire an image can be identified when the signal intensities are widely separated as shown in Figure 3 (Pooley 2005).

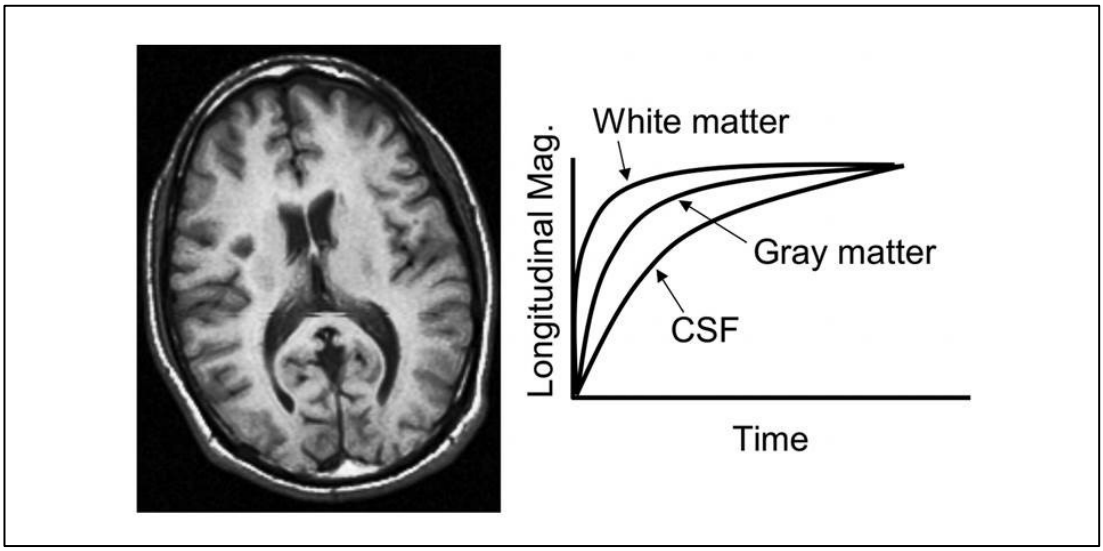


Figure 3 T1-weighted contrast
(*Reproduced with permission from Pooley 2005)*

1.1.1.2 T_2 relaxation

A scanned tissue contains nuclei with different atomic environments causing slightly different resonance frequencies when an external magnetic field is applied. Magnetic influence of nuclei on the adjacent ones causes broadening or splitting of the absorption or emission lines are called "spin-spin interactions". The

mixed emitted radiation frequencies are seen as decay in voltage. The time constant for this decay is the "spin-spin or transverse relaxation time, T_2" (Gore et al. 1981) as shown in Figure 4 (Pooley 2005).

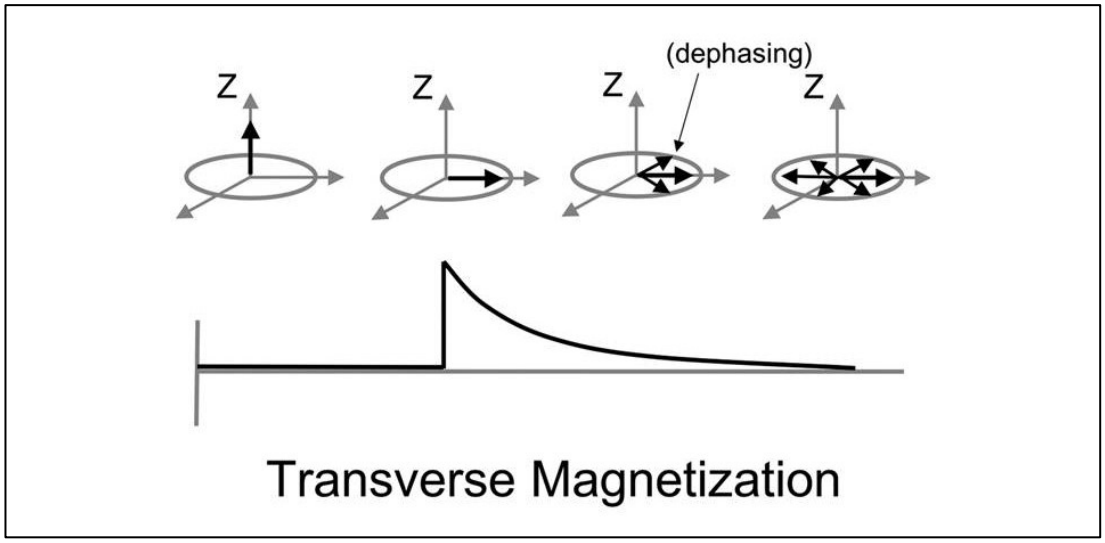


Figure 4 Transverse (T_2) relaxation
(*Reproduced with permission from Pooley 2005)*

T2-weighted image is created using the differences in tissue transverse relaxation time; CSF has a long T_2 time, GM has an intermediate time, and WM has a short time. T2 image is produced with high contrast between tissues when the relaxation magnetisation curves are widely separated; CSF appears light, GM is light grey, and WM is dark in T2-weighted images as shown in Figure 5 (Pooley 2005).

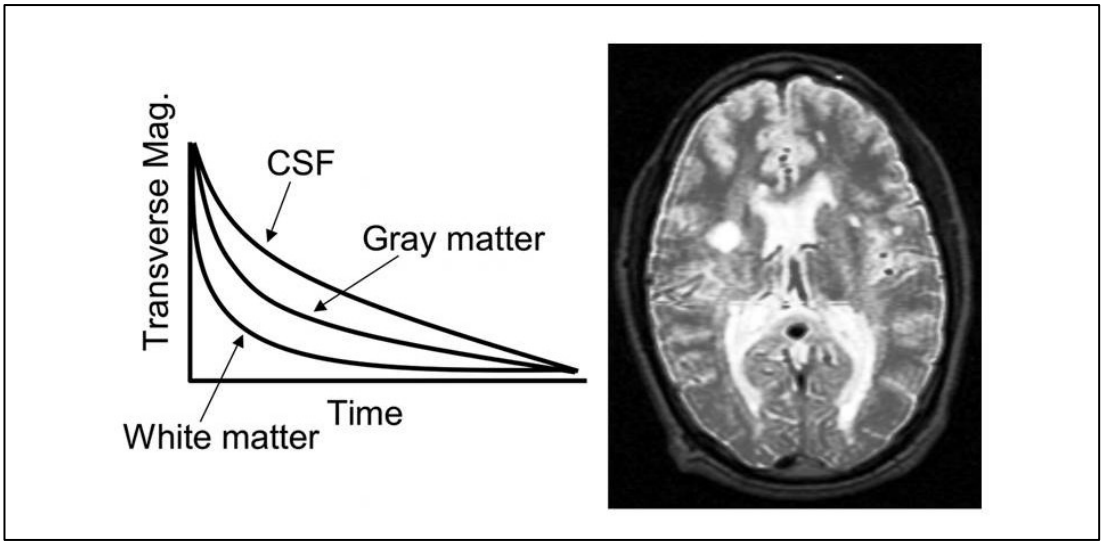


Figure 5 T2-weighted contrast

(*Reproduced with permission from Pooley 2005)*

1.1.1.3 T_2* relaxation

This is a relatively new MRI technique. While T_2 relaxation acquires a spin echo signal, T_2* relaxation acquires a gradient echo signal. This requires high uniformity of the magnetic field. T_2* can detect small changes in the magnetic field uniformity which in turn is useful to detect small lesions (Tang et al. 2014).

T_2* relaxation determines image contrast with gradient-echo sequences and represents the basis for many MRI applications such as susceptibility weighted imaging (SWI) and perfusion imaging. T2*-based contrast is used in SWI to exploit the magnetic susceptibility differences of the blood, iron, and calcification in the imaged tissue (Chavhan et al. 2009).

1.1.2 Perfusion imaging

Cerebral perfusion is defined as the volume of blood flowing through a given volume of tissue per minute (Keston, Murray, and Jackson 2003). Distinguishing bulk blood flow, through major arteries and veins, from perfusion is of significant importance (Jahng et al. 2014). Studying cerebral perfusion, mostly in research setting, has helped detecting, characterising, and monitoring neurological conditions (Essig et al. 2013); like stroke (Markus 2004), Parkinson's disease (Firbank et al. 2003), Alzheimer's dementia (Binnewijzend et al. 2014), epilepsy (Pizzini et al. 2013), and MS (Wuerfel et al. 2004).

Different techniques have been used to assess brain perfusion such as single-photon emission-computed tomography (SPECT), PET, and MRI.

1.1.2.1 Non-MRI perfusion imaging

SPECT and PET are the best-known techniques to measure perfusion other than MRI. Other CT techniques such as Xenon-enhanced computed tomography and dynamic perfusion-computed tomography are also used (Wintermark et al. 2005). These techniques have been used in research, and to less extent in clinical practice, for few decades. In patients with thalamic ischaemia and painful dysesthesia, SPECT demonstrated reduced

perfusion in ipsilateral cerebral cortex. This is believed to be due to tissue damage resulting in loss of neuronal activity and consequent cortical dysregulation (Lee, Choi, and Chung 1989). In patients with Alzheimer's disease, perfusion PET imaging showed hypoperfusion and reduced metabolic activity in functionally relevant brain regions (Rodriguez-Vieitez et al. 2016).

SPECT and PET have the advantage of being reliable functional imaging techniques, widely used in clinical practice especially in the field of neurodegenerative diseases such as dementia (Silverman 2004). They can demonstrate changes in brain tissue, not seen on MRI, in early stages of the disease process. In addition, both techniques are available for clinicians to use in clinical practice.

The use of a radioactive tracer renders tomography imaging techniques non suitable for monitoring chronic conditions due to risk of accumulative radiation (Wintermark et al. 2005). Doppler ultrasound is a low cost non-invasive, contrast-free, technique which can be repeated as often as clinically indicated (Wintermark et al. 2005). Transcranial doppler ultrasonography (TCD) can measure blood flow but not tissue perfusion. It is based on the principle of the "Doppler effect". According to this principle, the Doppler probe emits ultrasound waves which are transmitted through the skull and reflected by moving red blood cells within the intracranial blood vessels (Purkayastha and Sorond 2012). The technique is limited by being operator dependant, and by other

factors that affect blood vessels integrity such as age, comorbidities, blood pressure, Carbon Dioxide (CO_2) content, collateral flow, vessel anatomy, and response to medications. It is believed that TCD is useful in identifying middle cerebral artery (MCA) changes but no other intracranial vessels (Washington, Zipfel, and Hemorrhage 2011). As a result, ultrasound techniques have limited role in clinical conditions where major blood vessels are not involved or affected in the disease process.

In diseases like MS, where MRI is required as a structural imaging technique for diagnosis and monitoring, perfusion MRI is a more suitable option as can be added to routinely performed sequences allowing for assessment of brain structure and perfusion in one imaging session.

1.1.2.2 Perfusion MRI

MRI as a developing imaging method has an excellent safety record. MRI has been used to assess perfusion for more than two decades with first measurements of human cerebral blood flow (CBF), a marker of cerebral perfusion, using MRI dating back to 1970 (Morse and Singer 1970). One of the main advantages of MRI is that it can measure blood flow in large vessels as well as brain tissue perfusion; phase contrast angiography allows robust measurement of blood flow in the carotid arteries for example (Peng et al. 2015). This has the potential to transform our

understanding of the pathophysiology of various neurological diseases, improve the diagnostic process, and boost the knowledge toward better therapeutics and follow up (Essig et al. 2013). MRI offers the advantage of being both structural and functional imaging modality compared to tomography techniques.

Two main MRI approaches are used to measure perfusion based on whether contrast agent is used or not (Jahng et al. 2014). The first group includes dynamic susceptibility contrast (DSC)-MRI and dynamic contrast enhanced (DCE)-MRI, while the second is arterial spin-labeling (ASL) (Essig et al., 2013).

1.1.2.2.1 DSC and DCE

DSC-MRI is one of the most widely used MRI perfusion techniques. A paramagnetic contrast agent, like those containing gadolinium (Gd) chelates, is injected intravenously causing magnetic field distortion. DSC is based on the susceptibility changes resulting from the bolus formed by the contrast. It is also known as bolus tracking MRI as it uses very rapid imaging to catch the first pass of the contrast (Jahng et al. 2014). The rapid loss of MR signal on T2- or T2*-weighted images is used to measure the contrast concentration changes between individual voxels (O'Connor et al. 2011). An important factor in DSC is the arterial input function (AIF) which reflects the contrast agent concentration in the feeding vessel to the region of interest (ROI) at a given time and needs to

be chosen as close as possible to the ROI (Wuerfel, Paul, and Zipp 2007), this is affected by the shape of the injected bolus, cardiac output, cerebral vascular configuration and resistance.

DCE-MRI is referred to as "permeability" MRI; serial T1-weighted images are acquired before, during, and after an exogenous contrast agent is injected (Essig et al. 2013). It allows quantitative measurement of microvascular permeability which is specifically helpful in brain tumour assessment (O'Connor et al. 2011) and MS lesions (Ingrisch et al. 2012).

Overall, contrast MRI modalities offer higher signal-to-noise ratio (SNR) than ASL with better temporal and spatial resolution (Essig et al. 2013). They calculate cerebral blood volume (CBV) and mean transit time (MTT) as well as CBF (less accurate than ASL) (Jahng et al. 2014). CBV is determined by integrating each voxel tissue concentration time curve, while CBF is determined by the curve deconvolution with an AIF (Wuerfel, Paul, and Zipp 2007). DSC perfusion imaging assumes that the contrast agent remains intravascular (Rashid et al. 2004) which is not the case when blood-brain barrier is broken like in many neurological pathologies.

DSC and DEC-MRI are contrast based techniques and this limits their use in people with difficult intravenous access, renal impairment, and in children. A limitation to use of DSC-MRI is the susceptibility artefacts caused by air, blood, bone, and calcification.

DCE-MRI images acquisition is complex and there is no available easy to use post processing software (Essig et al. 2013).

Contrast based MRI is of limited use if longitudinal scanning is needed. There is evidence from post-mortem studies of Gd deposition in the brain especially in globus pallidus and dentate nucleus (2016). Gd is a rare earth heavy toxic metal. The ion radius is close to that of Calcium and this may block the activity of some Calcium dependent enzymes and channels resulting in problems in nerve conduction and muscle contractions. To prevent this, Gd is injected in a tightly bound form with strong chelate molecules. However, a phenomenon called "transmetallation" may occur, releasing Gd which deposits in various body tissues such as brain, bone, and skin. It is known that some chelate molecules, such as Gadoteridol (ProHance), hold onto Gd better than others (Murata, Gonzalez-Cuyar, et al. 2016).

1.1.2.2.2 ASL

This technique uses magnetically labelled blood as an endogenous tracer. It includes the subtraction of a 'label' image (obtained by magnetic blood labelling) from a 'control' image (obtained without labelling) (Jahng et al. 2014).

ASL has three main types; continuous (CASL), pulsed (PASL), and pseudo-continuous (pCASL). In CASL, arterial blood water is continuously labelled by prolonged RF pulse until tissue

magnetisation reaches a steady state. PASL uses short RF pulse to label arterial blood in a single point in time. Imaging is then performed after a period of time allowing the labelled blood to reach the tissue of interest (Essig et al. 2013). While CASL has better SNR, PASL is more straightforward to implement and offers high tagging efficiency (Wu et al. 2011). In PASL, labelling is performed once in a 10-15 cm slab proximal to the imaged slices. A source of reduced efficiency is the increased transit time caused by the gap needed between the labelled blood and the image slices (Petersen et al. 2006). To combine the advantages of both CASL and PASL, pCASL has been developed in the last decade. It offers longer bolus tagging than CASL (higher SNR) and higher labelling efficiency than PASL (Wu et al. 2007).

CBF is measured by ASL based on two factors; the assumption that the endogenous tracer (labelled blood water) is freely diffusible and elimination of static tissue signal completely (Petersen et al. 2006). Quantification of perfusion using MRI signals in ASL depends on many factors such as the inversion efficiency, T_1 relaxation time for both blood and tissue, flow effects in and out of the brain tissue, blood-tissue partition coefficient of water, and vascular signal contamination. Two images are acquired in ASL; one represents the labelling of the incoming blood and the other with no labelling. The subtracted images from control to label represent "perfusion-weighted imaging (PWI)". Proton density and

T_1 relaxation rates of tissue and inflowing blood, and their respective differences, are central to the relationship between the PWI signal and actual CBF. ASL measures perfusion by assuming the blood water and tissue water exchange happen instantly; the tagged arterial blood water acts as a free diffusible tracer. By fitting a haemodynamic model to CBF data acquired at multiple delay times, it is also possible to obtain tagged blood arrival time at a voxel and the exchange time from intra- to extra-vascular space (Jahng et al. 2014).

One of the disadvantages of ASL is low SNR especially at lower field strength scanners. In a study by Wang et al. comparing 4 tesla (T) MRI with 1.5T, it was found that higher MRI field can maximise SNR gain (Wang et al. 2002). The acquisition procedure is complex and scanning time is longer than other techniques resulting in potential movement artefacts (Essig et al. 2013). ASL may not accurately estimate perfusion; when used in acute stroke patients, ASL overestimated hypoperfusion in the ischaemic areas (Huang et al. 2013), this could be caused by errors in labelling efficiency which is crucial so all signals from perfusing blood can be included (Jahng et al. 2014). This issue can be addressed by developing labelling pulses that improve efficiency.

Measuring WM perfusion using ASL is challenging due to several factors; WM has much lower CBF compared to GM, the SNR is low as WM exhibits long transit times (causes more relaxation of

labelled spins before they arrive at the tissue of interest), and lastly small contamination from a much higher perfused GM can result in significant error in quantifying WM CBF. To address these challenges, technical changes are needed in the acquisition and post scanning analysis steps which could lead to longer scanning time and noisy data (Zhang et al. 2016).

Partial volume effect, caused by mixed contribution of different tissues in the imaged voxel, can be significant as ASL due to the low spatial resolution (Asllani, Borogovac, and Brown 2008), this can be corrected by post scan processing. Static tissue signals affect the subtraction of control and labelled images; background suppression techniques are used to tackle this problem using multiple inversion recovery pulses. Arterial transit time (ATT) is a source of error as it differs across the brain (long in distal branches). Most ASL scans are acquired using a single post-label delay (PLD) time to reduce total scanning time, however this acquisition approach cannot characterise the transit delay of the labelled blood to the tissue. Because the ATTs will vary, the CBF value in each voxel can be underestimated or overestimated. Acquisition of multiple images with different PLD time can improve the accuracy of estimating transit times, and thus perfusion (Jahng et al. 2014).

Table 1 lists the three MRI techniques and describes the main differences between them (Jahng et al. 2014). Table 2 summarised the benefits and challenges related to ASL use.

Table 1 Perfusion MRI techniques

	DSC	**DCE**	**ASL**
Bolus	Tracking	Passage	Tagging
Acquisition	First pass of contrast	Accumulation of contrast	Tagged arterial blood
Exogenous Contrast	Intravenous bolus of Gd-based agent	Intravenous bolus of Gd-based agent	None
Tracer	Non-diffusible blood pool tracer	Permeability limited diffusible tracer	Diffusible tracer
Mechanism	T_2/T_2* relaxation	T_1 relaxation	Magnetically labelled blood
Signal	Decreased	Increased	Image subtraction
Parameters CBF: flow rate of volume of blood per cerebral tissue (ml/100g/min) CBV: volume of flowing blood per cerebral tissue (ml/100g) MTT: CBV/CBF (seconds)			

Table 2 Benefits and challenges of ASL

Benefits: ➢ Contrast free technique ➢ Allows serial CBF measurements to measure dynamic changes or response to interventions ➢ Complementary to functional MRI methods by adding "CBF" as a physiological parameter ➢ Useful in infants, children, pregnant women, and those with poor IV access
Challenges: ➢ Labelling efficiency ➢ Static tissue signal contribution ➢ CBF quantification errors ➢ ATT variability across the brain ➢ Partial volume errors

1.1.3 Ultra-high field MRI

Structural brain imaging has improved in quality through increasing resolution. The transformation from 1.5T to 3T MRI has improved tissue contrast; which can help in identifying cortical pathology, cortical volume measurement and differentiation of WM and GM, essential markers in conditions like MS to monitor disease activity, lesions load, and progression. Increasing MRI field

strength can boost the SNR and offer high spatial resolution structural imaging (Duyn 2012).

Ultra-high field MRI produces high quality images which reflect the gross pathological specimens (Nakada 2007); this offers great opportunities in studying diseases like MS where detecting new lesions, assessing the brain cortex, and monitoring subtle dynamic changes over time have become a field of growing interest in the era of "no evidence of disease activity (NEDA)". 7T MRI is able to detect cortical involvement in MS, including cortical lesions (CLs), with strong correspondence to that reported by histology in terms of distribution (Mainero et al. 2009); this has transformed MRI from a standard imaging modality to one which can reflect, in detail, the changes previously only visible on autopsy brain samples. Improving CLs detection in MS can help in clinical practice; in diagnosing MS as CLs are now included in the diagnostic criteria (Thompson et al. 2018) or monitoring disease activity and progression (Kilsdonk et al. 2016).

At 7T, T1-weighted imaging demonstrates hyper-intense delineation of cerebral vasculature, facilitating the focus on vascular pathology as well as brain structural imaging (Maderwald et al. 2008). Functional MRI has benefited from increased field strength at 7T to get better signal from motor cortex (van der Zwaag et al. 2012). Prolonging on of T_1 times at 7T improves vessel-to-background contrast in magnetic resonance angiography

(MRA) (Umutlu et al. 2014), this improves the anatomical and pathological assessment of intracranial and extra-cranial blood vessels.

1.1.4 Limitations

The use of some modern MRI techniques has not yet been well established in clinical practice due to many factors. Historically, there has been a lack of awareness between referring clinicians of the importance of these techniques. One of the current challenges is that non-expert radiologists may not have good exposure to advanced MRI scans which accounts for lack of experience (Essig et al. 2013).

There are several technical limitations to the use of perfusion MRI. Compared to other MRI techniques, perfusion scans can have a lower SNR, resulting in longer scans or reduced spatial coverage or resolution. WM has less perfusion compared to GM leading to less sensitivity in detecting abnormality. However, this may be addressed by measuring dynamic changes and variability in regional CBF/CBV differences using contrast based perfusion MRI (Holland et al. 2012).

Cerebral perfusion is correlated with age; approximately 0.5% reduction per year in GM perfusion is seen in ASL-MRI studies (Amann et al. 2012). This needs to be considered when analysing

perfusion levels in imaging studies and could represent a limiting factor in characterising people with comorbidities which may affect CBF.

The majority of completed studies measuring cerebral perfusion are not longitudinal, and therefore it is generally not possible to compare perfusion maps over time. Unlike PET and SPECT, MRI is ideal for longitudinal studies as there are no radiation concerns. While perfusion brain imaging is a growing field of interest, investigating the optic nerve or spinal cord with similar technique has not been addressed.

Ultra-high field imaging has several limitations which range from technical to physiological and biological factors. The material (like wires and conductors) needed to make the scanners differ in high field scanners and they can be difficult and expensive to make. RF pulse transmission in high field is altered compared to lower field scanners; this can have significant practical implications. The strength of the magnetic field is a major factor in the amount of heat produced within the tissues during imaging; this may limit the range of experiments on humans. Physiological aspects like movement in the B_0 field and tissue heating induced by RF power deposition are limiting factors to ultra-high field imaging. Symptoms like metallic taste, nausea, and vertigo have been reported temporarily by patients at 7T and higher field strengths; this can be addressed by minimising the head motion inside the

magnet. Optimising the RF coils and pulses can reduce the heat effect without the risk of affecting SNR by dropping sequences or shortening scanning time (Duyn 2012). Another disadvantage is the lack of techniques and sequences which can be tested and applied using lower field scanners which are widely used in clinical practice.

1.1.5 Future prospective

Improvements in perfusion MRI techniques can be achieved by using high-field systems which offer higher resolution and shorter scanning times. Standardising protocols across centres will have significant impact on optimisation of MRI performance and interpretation. MRI, as an important para-clinical biomarker in MS, has the potential to transform from an "imaging" tool (producing qualitative data) to a "measuring" (quantitative) one (Essig et al. 2013). ASL-MRI has the potential to be the technique of choice since contrast media is not required allowing for safe longitudinal monitoring of conditions with dynamic brain perfusion changes.

1.2 Multiple Sclerosis

MS is a chronic inflammatory disease of the CNS (Compston and Coles, 2008). There are three main types of MS; relapsing remitting (RRMS), primary progressive (PPMS), and secondary progressive (SPMS). RRMS patients may progress with time without relapses and accumulate disability and develop SPMS. It is a major cause of disability in adulthood with significant impact on mobility, mental state, and occupation (Coles 2009).

1.2.1 Causes of MS

Multiple factors have been implicated in MS; both genetic and environmental factors play a role in disease risk. The risk ranges from 2-3% in first-degree relatives to 1% in second-degree and third-degree relatives (Compston and Coles 2008). The association between alleles of the major histocompatibility complex and MS, strongest in northern Europeans, was identified in the 1970s (DR15, DQ6, and the corresponding genotypes DRB1*1501, DRB5*0101, DQA1*0102, and DQB2*0602) (Terasaki et al. 1976, Compston, Batchelor, and McDonald 1976, Olerup and Hillert 1991). Other genotypes found to increase risk of MS include HLADRB1*17 (less pathogenic than HLA-DRB1*15) and HLA-DRB1*08 (more than doubles the risk associated with a single copy of HLA-DRB1*15). Some genes may protect against MS;

HLADRB1*14 (completely cancels HLADRB1*15 effect when inherited together), HLADRB1*01, and HLADRB1*10 (only act in the presence of HLA-DRB1*15) (Hoppenbrouwers and Hintzen 2011). Several environmental risk factors are studied extensively and shown to affect MS incidence, such as Infectious Mononucleosis (an Epstein-Barr virus infection) (Belbasis et al. 2015), smoking (Riise, Nortvedt, and Ascherio 2003), vitamin D level (Munger et al. 2006) , and latitude (Simpson et al. 2011). Despite our wide knowledge of risk factors behind MS, the definite cause remains interestingly unknown.

1.2.2 Pathogenesis of MS

Demyelinated plaques represent the hallmark of MS pathology, but they do not fully explain the disease symptomatology. Autopsy data showed that focal demyelinated plaques are present in all MS types. While active inflammatory lesions dominate WM in acute and relapsing MS patients, normal appearing white matter (NAWM) diffuse injury and cortical demyelination are the hallmark of progressive MS (Kutzelnigg et al. 2005). Oligodendrocytes are responsible for myelin sheaths synthesis and maintenance in the CNS. Loss of myelin and reduction of oligodendrocytes are two processes seen within MS plaques (Zajicek et al. 1992).

MS pathological process seems to start with autoreactive lymphocytes migrating across the blood-brain barrier due to loss of regulatory pathways allowing these cells to trigger an immune response in the brain (Compston and Coles 2008). MS plaques are caused in part by failure of local regulatory mechanisms and dominated by perivascular CD8+ T-cells infiltrates (Compston and Coles 2008). Inflammation is driven by subtypes of T-cells which secrete interleukin-17 under interleukin-23 control (Langrish et al. 2005). Both interleukins 17 and 22 damage the blood-brain barrier and allow T-helper 17 cells to penetrate the brain and kill neurons (Kebir et al. 2007, Tzartos et al. 2008). Lymphocytes (T and B cells), macrophages, and plasma cells accumulate, and pro-inflammatory cytokines recruit naïve microglia resulting in amplified immune response. Activated microglia and oligodendrocyte-myelin unit contact is established and a lethal signal through cell surface bound tumour necrosis factor α is delivered (Zajicek et al. 1992). This results in the extensive axonal injury seen in acute demyelinating plaques (Kuhlmann et al. 2002). In SPMS, lesions show demyelination, diffuse axonal injury, and neuronal degeneration associated with tau accumulation (Anderson et al. 2008). Diffuse microglial activation within brain parenchyma caused by expansion of focal lesions results in NAWM and cortical demyelination (Kutzelnigg et al. 2005). B-lymphoid follicles, found in the meninges, cause intrathecal antibody production and cortical

damage (Magliozzi et al. 2013). PPMS patients tend to have reduced brain lesions load, less inflammation, and absence of lymphoid follicles (Compston and Coles 2008). However, cortical involvement, with increasing lesions volume and cortical atrophy, is seen extensively in progressive stage of the disease (Calabrese et al. 2012, Filippi et al. 2013) and can well explain the clinical progression without significant cerebral inflammation.

MS plaques remyelinate in one fifth of MS patients (Patrikios et al. 2006) usually during the acute inflammatory phase, but also in progressive MS, when myelin debris is phagocytically removed (Compston and Coles 2008).

1.2.3 Diagnostic criteria

Diagnosing MS requires the identification of clinical symptoms and paraclinical parameters supportive of the diagnosis. Since the introduction of the McDonald Criteria (McDonald et al. 2001), there have been three revisions aimed to improve the sensitivity and specificity of the criteria (Polman et al. 2005, Polman et al. 2011, Thompson et al. 2018). The role of MRI in diagnosing MS is significant; establishing dissemination space through multi-focal CNS involvement or dissemination in time by demonstrating old and new lesions is possible using MRI.

Difficulties in applying the criteria arise from atypical clinical presentations and non-specific lesions on MRI which can lead to misdiagnosis. Another aspect which is controversial in clinical practice is identifying the secondary progressive phase of the disease; reported worsening of clinical disability independent from relapses is widely used as a parameter. Experts in the field believe that there is growing need for more robust paraclinical parameters such as imaging biomarkers to aid the diagnostic process and help monitoring disease progression.

1.2.4 Cortical lesions in MS

MS was thought to be primarily a WM inflammatory disease. However, histological and imaging studies have established that there is extensive involvement of the GM, including the cerebral cortex, by the inflammatory and degenerative processes (Kidd et al. 1999, Popescu and Lucchinetti 2012) especially in the later stages of relapsing MS and the progressive phase of the disease (Calabrese et al. 2008, Calabrese et al. 2015). It has been shown that CLs volume, beside age and cerebellar cortical volume, may predict the probability of RRMS patients developing SPMS (Calabrese et al. 2013).

There are three types of CLs: leucocortical (34%), intracortical (16%), and subpial lesions (50%) (Bø et al. 2003, Peterson et al.

2001). The later type of lesions, usually seen in autopsy brain samples, is best identified using special MRI sequences at ultra-high-field (Pitt et al. 2010).

It was believed that CLs develop predominately as a result of disease progression related neurodegeneration and axonal damage; however a recent study described "cortical relapses" in patients who presented with new atypical symptoms, suggestive of a relapse, and found to have active CLs on special MRI sequences, double inversion recovery (DIR) and phase-sensitive inversion recovery (PSIR), explaining the atypical presentation (Puthenparampil et al. 2016), this indicate that CLs may develop independent from WM pathology. Moreover, meningeal inflammation seems to be correlated with development of subpial CLs (Kutzelnigg et al. 2005) indicating that cortical pathology in MS is not purely caused by spreading damage from adjacent WM.

The growing interest in using CLs seen on MRI to aid the diagnostic process (Filippi et al. 2010) has been addressed in the latest revision of the McDonald criteria by Thompson et al. (Thompson et al. 2018) with cortical and juxta-cortical lesions counted as same area.

CLs are associated with cognitive dysfunction in MS; Calabrese et al found that MS patients with cognitive deficits have more CLs and more severe cortical atrophy than cognitively preserved patients

(Calabrese et al. 2009). This makes CLs a promising biomarker to monitor disease progression.

Measuring CLs perfusion is an exciting prospect to help develop understanding of their role in disease process and addressing the question of "how the lesions pathological changes correlate to the surrounding normal appearing brain tissue".

1.2.5 Perfusion in MS

Perfusion is a vital biological process which refers to delivery of oxygen and other nutrients by blood flow to tissues at the capillaries level (Jahng et al. 2014). It is a crucial indicator of tissue function and viability which is why it became a major focus for research scientists (Kim 2012).

Brain perfusion in MS patients may be reduced, increased, or unchanged based on the disease activity, clinical course, and affected cerebral region. Three decades ago, SPECT, and PET were used to measure perfusion in MS showing hypoperfusion in WM and cortical GM (Brooks et al. 1984). NAWM perfusion is shown to be reduced in different MS subtypes regardless of presence of progression (Law et al. 2004, Ge et al. 2005, Adhya et al. 2006, Saindane et al. 2007, Inglese et al. 2008), this is believed to be a consequence of reduced metabolic demand due to axonal damage (ElSankari et al. 2013). Few studies found increased perfusion in

NAWM in RRMS and SPMS patients (Rashid et al. 2004, Bester et al. 2015), this is thought to be secondary to ongoing inflammation in high inflammatory MS cases.

Perfusion in GM is found to be reduced in all MS subtypes (Rashid et al. 2004, Inglese et al. 2008, Varga et al. 2009). This may be a consequence of WM damage and resulting disconnection between the cerebral cortex and the subcortical structures (De Keyser et al. 2008).

Perfusion in MS lesions depends on how acute they are; active lesions have increased perfusion (Haselhorst et al. 2000, Wuerfel et al. 2004) which may start before contrast enhancement seen on imaging. Reduced perfusion seen in chronic lesions (Holland et al. 2012, Peruzzo et al. 2013) is usually attributed to neurodegeneration.

Patients with clinically isolated syndrome (CIS), believed to be the first presentation of MS, have different perfusion levels based on lesions age, areas involved, and disease activity. They tend to have reduced CBF in NAWM and normal appearing grey matter (NAGM) (Varga et al. 2009, Narayana et al. 2014, Papadaki, Simos, Mastorodemos, et al. 2014, Papadaki, Simos, Panou, et al. 2014). This represents clear evidence that changes in perfusion start early in the disease process and may represent an integral part of the MS pathophysiology.

An important aspect of why perfusion is a field of interest in MS is whether hypoperfusion is a primary or a secondary phenomenon and whether this can be modified to change disease course. Mean diffusivity (MD) measures the magnitude of diffusion of water molecules and it is reduced in acute ischaemia because of cellular swelling. MD normalises after the acute phase then increases due to tissue necrosis (De Keyser et al. 2008). In MS patients, there was a significant correlation between hypoperfusion and reduced MD (Saindane et al. 2007) which indicates a role for ischaemia in tissue damage. This is supported by the fact that GM hypoperfusion is seen in early MS before brain atrophy begins (Debernard et al. 2014). Early MS lesions show loss of myelin-associated glycoprotein from inner myelin membranes and adjacent NAWM which is seen also in ischaemic stroke insults suggesting that hypoxia occur is a factor in MS lesions development (Juurlink 2013). "Virtual hypoxia" has been proposed as the mechanism by which hypoxia happen in MS lesions; this refers to the energy deficit that happen due to increased energy demand and mitochondrial failure to synthesise ATP rather than absence of oxygen (Trapp and Stys 2009).

Astrocytes are important in regulating blood flow in the brain. The astrocytic end-feet occupy parts of the intracerebral blood vessels surface. They are involved in the ions balance between the perivascular space and vascular smooth muscle cells. Impairment

of the ions balance results in alteration of CBF. Astrocytes possess a wide variety of neurotransmitter receptors such as β2-adrenergic receptors which are found to be deficient in MS lesions and might be responsible for CBF reduction in WM (De Keyser et al. 2008).

Perivascular damage due to MS plaques was thought to be causing hypoperfusion. This should result in focal or patchy reduced perfusion like that seen in cerebral vasculitis, but this is not the case in MS where more global hypoperfusion is seen together with pathological findings of absence of micro-vessel thrombosis and other structural abnormalities (D'haeseleer et al. 2015).

Endothelin-1 (E-1), a potent vasoconstrictive peptide produced by endothelial cells and distributed in human body, was found to be elevated in MS patients' venous blood (Haufschild et al. 2001) and CSF (Speciale et al. 2000). This is thought to cause arteriolar vasoconstriction and reduced blood flow when released by reactive astrocytes in MS plaques (D'haeseleer et al. 2013). Another study on MS patients did show reduced E-1 in MS patients plasma (Jankowska-Lech et al. 2015) arguing against the consistency of this marker. E-1 is shown to be elevated in reactive astrocytes in other brain pathologies such as reversible cerebral vasoconstriction syndrome (RCVS) (Hammad et al. 2013), Alzheimer's disease, ischaemic stroke, traumatic injury, and viral infections (Nie and Olsson 1996, Ostrow, Langan, and Sachs 2000) indicating lack of specificity. Using E-1 antagonist, Bosentan, D'haeseleer et al were

successful in restoring CBF in MS patients to healthy controls (HCs) values. The therapeutic implications of this interesting finding are still unexplored (D'haeseleer et al. 2013).

Chronic venous insufficiency was thought to be playing a role in altering brain blood flow and subsequently MS pathogenesis (Zamboni et al. 2009, Zivadinov et al. 2011), but this was disproved by high-field SWI showing no evidence for venous stasis (Ge et al. 2009) and phase contrast MRI demonstrating no venous flow abnormality in MS patients (ElSankari et al. 2013). Moreover, MR venogram demonstrated no structural anomalies in cerebral venous anatomy of MS patients compared to HCs (Wattjes et al. 2011).

We conclude that perfusion seems to be an important factor in MS pathogenesis. Measuring perfusion in MS patients may help in making decisions on how to better manage people at risk of high disease activity or developing progressive MS.

1.2.6 MRI in MS

Para-clinical parameters and markers have developed extensively in recent years. MRI remains the gold standard investigation to diagnose MS and look for evolving changes throughout the disease course. However, conventional MRI lacks specificity in differentiating between the various pathological processes that

happen throughout the disease course and this led to extensive research into various modalities and techniques to help understand these processes and develop new therapeutic (Essig et al. 2013).

The common MRI techniques used in MS are: T1-weighted, T2-weighted, fluid attenuation inversion recovery (FLAIR), and contrast enhanced T1-weighted imaging.

1.2.6.1 T1-weighted imaging

MS lesions have different intensities when seen on T1-weighted imaging. Hypo-intense lesions or "black holes" are correlated with disease progression and disability (Truyen et al. 1996).

The use of lesions load on T1-weighted imaging is limited by the difficulty to identify the lesions which may appear grey in colour similar to the background NAWM resulting in considerable inter-observer variation. The significance of T1 lesion volume and the correlation with clinical outcomes is inconsistent between studies (Stevenson and Miller 1999) with more evidence toward lack of correlation with cognitive symptoms and disability.

1.2.6.2 T2-weighted imaging

Lesions (plaques) seen on T2-weighted imaging are essential to diagnose all MS types (Polman et al. 2011). The lesions appearance using this technique is not specific and may represent

various pathological stages such as demyelination, axonal loss, or remyelination (Lassmann 1998, Barkhof et al. 2003).

Measuring disease burden in MS is commonly measured by the total brain lesion volume on T2-weighted scans. Serial assessments of T2 lesions are used to identify CIS conversion to MS, measure MS disease progression, inflammation activity, response to therapy, and in some instances to differentiate MS from other non-progressive WM disease processes. The clinical correlation between disability scales and T2 lesion load is not very high; the total lesion volume does not reflect the location of the lesions (some affected brain areas are more significant and symptomatic) and does not include the spinal cord (highly associated with MS related disability). Moreover, T2-weighted imaging does not differentiate between various MS types or reflect NAWM changes (Stevenson and Miller 1999).

1.2.6.3 FLAIR

FLAIR sequence is a T2-weighted technique which nulls fluid like CSF allowing for subtle periventricular white matter lesions (WMLs) to be seen on background of dark CSF and hypo-intense WM. MS plaques have the highest intensity followed by GM, WM, and CSF. FLAIR imaging is also useful in detecting spinal cord involvement

and differentiating lesions with ambiguous signal intensity on T2-weighted imaging (Hashemi et al. 1995).

1.2.6.4 PSIR

PSIR is a T1-weighted MRI sequence that combines negative and positive longitudinal magnetisation in the image providing greater range of signal intensity, provides better GM/WM contrast, and confirms presence of CLs in MS (Sethi et al. 2012, Mougin et al. 2016). PSIR is shown to be more accurate than other techniques, like DIR, in confirming the exact location of CLs in relation to GM/WM junction (Sethi et al. 2013). While PSIR is not included in routine clinical scans, there is growing evidence that it can provide crucial information not only on brain involvement in MS but also the spinal cord (Poonawalla et al. 2008) if combined with other relevant sequences.

1.2.6.5 Contrast enhanced T1-weighted imaging

Contrast enhanced imaging is widely used in identifying and monitoring disease activity in MS. It uses a paramagnetic agent which crosses damaged blood-brain barrier and enhances during T_1 relaxation. This technique is found to be more sensitive compared to CT based contrast imaging used before MRI invention (Miller et al. 1988). Contrast enhancing lesions are central to the diagnosis

of MS in cases with one clinical attack (confirm dissemination in time) (Polman et al. 2011). Gd-enhancing lesions have crucial role in deciding on effectiveness of disease modifying therapy drugs (DMTs) in RRMS and SPMS with relapses (Giovannoni et al. 2015). They are also widely used in clinical trials developing new DMTs. Lack of Gd-enhancing lesions is one of the parameters of the new concept of NEDA (Table 3) which has gained acceptance among MS neurologists as a target for MS therapeutics (Giovannoni et al. 2015).

Table 3 No evidence of disease activity parameters

Clinical	1- No relapses
	2- No disability progression
MRI	3- No new T2 lesions
	4- No new Gd-enhancing lesions

Finally, Gd-enhanced imaging can help in the diagnosis of MS mimics such as progressive multifocal leukoencephalopathy (PML) caused by some DMT drugs (Honce, Nagae, and Nyberg 2015) and cerebral sarcoidosis (Christoforidis et al. 1999).

1.2.7 Perfusion MRI in MS

Advanced MRI development in the twenty first century has facilitated measuring brain perfusion; which helps in the understanding of the pathophysiological processes that happen in normal and abnormal appearing brain areas in different stages of MS and potentially predict the evolving abnormalities early. The use of contrast and non-contrast MRI techniques has been reported in literature with variable findings depending on the technique used, MS subtype, and the assessed brain area (Table 4).

Haselhorst et al. published the first cross-sectional study to investigate different MS lesions, using DSC-MRI, showing that acute MS lesions have increased perfusion compared to contralateral NAWM (Haselhorst et al. 2000). Regional changes in WM perfusion occur before acute lesion formation; elevation in CBV and CBF is seen prior to increase of diffusivity with change in blood flow. After the initial peak due to vasodilation induced by acute inflammation, perfusion declines gradually thereafter when gliosis and hypometabolism occur. Ge at al found that perfusion increased in some chronic non-enhancing lesions as well as acute lesions indicating that inflammation is playing a major role in MS pathophysiology. Together with proximity of lesions to venules, these studies confirm the role of vasculature in the inflammation process (Wuerfel et al. 2004, Ge et al. 2005).

Variability in regional cerebral perfusion is believed to affect the distribution of WMLs in MS. NAWM tend to have better perfusion than WM regions where lesions develop. Also, the ability of brain tissue to repair/remyelinate is affected by perfusion which is why some MS lesions remain chronic or large especially in deep WM close to the ventricles where perfusion is low. This may explain why SPMS lesions are found in areas with low perfusion compared to RRMS (Holland et al. 2012). NAWM CBF and CBV are reduced, more in progressive MS than RRMS, compared to HCs (Adhya et al. 2006, Ge et al. 2005, Inglese et al. 2008, Debernard et al. 2014).

GM including the deep GM structures such as the thalamus and basal ganglia have less perfusion in MS patients compared to controls. Most cortical MS lesions have lower CBV and CBF than NAGM. This observation is more pronounced in progressive MS than in RRMS possibly supporting the concept of degeneration being the predominant pathological process rather than inflammation (Inglese et al. 2008, Peruzzo et al. 2013, Debernard et al. 2014).

Perfusion MRI can be used to measure cerebrovascular reactivity (CVR) which is a useful index for assessing cerebral vascular function and measuring the haemodynamic response to vasodilator stimuli. Marshall et al proved for first time that CVR is impaired in MS when measured using ASL-MRI with hypercapnia being a stimulus. Interestingly, global GM CVR significantly decreased after

CO_2 challenge and correlated with brain atrophy and lesions volume (Marshall et al. 2014) raising the possibility that this is one of the causes of the neurodegeneration in MS.

It is clear from reading the literature on perfusion MRI in MS that there are discrepancies between the studies. Showing increased or reduced perfusion in certain brain regions and variability between MS subtypes is thought to be related to the link between cerebral perfusion and disease activity. However, it is well known that technical difficulties can be a source of error leading to inaccurate conclusions. There is also the effect of patients demographics and treatment status which are not accounted for in most of the studies. The number of participants in many studies is small hence lack of statistical significance required to generalise the conclusions on population level.

Table 4 Perfusion MRI studies in MS

Author Year	Cohort	MRI technique	Field strength (T)	Main perfusion changes in MS patients
(Haselhorst et al. 2000)	17 RRMS, 7 SPMS, 1 PPMS	DSC	1.5	Increased in active WMLs, reduced in chronic WMLs
(Law et al. 2004)	17 RRMS, 17 controls	DSC	1.5	Reduced in NAWM
(Rashid et al. 2004)	21 RRMS, 14 SPMS, 12 PPMS, 13 Benign, 34 controls	CASL	1.5	Increased in NAWM (RRMS & SPMS). Reduced in the thalamus (PPMS & SPMS)

(Wuerfel et al. 2004)	20 RRMS	DSC	1.5	Increased in active WMLs (prior to the blood brain barrier breakdown)
(Ge et al. 2005)	17 RRMS	DSC	1.5	Increased in active WMLs, reduced in NAWM and most of chronic lesions
(Adhya et al. 2006)	11 RRMS, 11 PPMS, 11 controls	DSC	3.0	Reduced in NAWM (more in PPMS)
(Inglese et al. 2007)	11 RRMS, 11 PPMS, 11 controls	DSC	3.0	Reduced in NAGM (more noticeable in PPMS)
(Saindane et al. 2007)	14 RRMS, 17 controls	DSC	1.5	Reduced in normal appearing corpus callosum
(Inglese et al. 2008)	18 RRMS, 14 PPMS, 11 controls	DSC	3.0	Reduced in deep GM
(Varga et al. 2009)	12 CIS, 12 Early RRMS, 12 controls	DSC	3.0	NAWM: Reduced in CIS and RRMS. NAGM: Reduced in RRMS
(Amann et al. 2012)	123 RRMS, 42 SPMS	PASL	1.5	Reduced in NAGM (more in PPMS)
(Aviv et al. 2012)	37 SPMS, 10 controls	DSC	3.0	Reduced in NAGM
(Holland et al. 2012)	454 Early RRMS, 580 Late RRMS, 215 SPMS	MRI with SPECT perfusion atlas	1.5	Reduced in chronic WMLs
(Ingrisch et al. 2012)	17 RRMS, 2 SPMS	DCE	3.0	Increased in WMLs (more in active than chronic)
(Papadaki et al. 2012)	30 CIS, 30 RRMS, 30 controls	DSC	1.5	Reduced CBF in deep GM in CIS and RRMS. Reduced CBF in NAWM in RRMS.
(Francis et al. 2013)	45 SPMS	DSC	3.0	Reduced in NAGM

(Ota et al. 2013)	18 RRMS, 8 SPMS, 1 PPMS, 24 controls	pCASL	3.0	Reduced in NAGM
(Peruzzo et al. 2013)	44 RRMS	DSC	1.5	Reduced in most CLs except few outliers
(Steen et al. 2013)	16 RRMS, 9 Progressive MS, 10 controls	pCASL	3.0	Reduced in NAWM
(Debernard et al. 2014)	25 RRMS, 25 controls	pCASL	3.0	Reduced in NAGM
(Li et al. 2014)	7 RRMS, 7 controls	DSC	3.0	Increased in active WMLs, reduced in T1-hypointense lesions
(Narayana et al. 2014)	5 CIS, 34 RRMS, 6 SPMS, 20 controls	pCASL	3.0	Reduced in areas where T1-hypointense lesions lie, variable for T2-hyperintense lesions
(Paling et al. 2014)	35 RRMS, 33 controls	PASL	3.0	Increased in NAWM. Reduced in NAGM
(Papadaki, Simos, Mastorodemos, et al. 2014)	30 CIS, 43 controls	DSC	1.5	Increased in NAWM and deep GM
(Papadaki, Simos, Panou, et al. 2014)	40 CIS, 30 controls	DSC	1.5	Increased in NAWM and deep GM
(Bester et al. 2015)	13 HI-RRMS (high inflammatory), 20 LI-RRMS (low inflammatory)	DSC	3.0	Increased in NAWM in HI-RRMS, reduced in LI-RRMS
(Sowa et al. 2015)	66 RRMS, 2 PPMS, 1 SPMS	DSC	1.5	Reduced in chronic WMLs

(Hojjat, Cantrell, et al. 2016)	39 RRMS, 19 controls	DSC	3.0	Reduced in NAWM and NAGM more than WMLs and CLs respectively
(Hojjat, Kincal, et al. 2016)	39 RRMS, 19 controls	pCASL	3.0	Reduced in anatomically significant cortical areas of cognitively impaired patients
(Vitorino et al. 2016)	39 RRMS, 10 controls	DCS	3.0	Regional frontal cortical perfusion deficits in RRMS, with more widespread hypoperfusion in those with cognitive impairment
(Doche et al. 2017)	23 RRMS, 16 controls	pCASL	3.0	Reduced perfusion in thalamic regions is associated with disability
(Ingrisch et al. 2017)	24 RRMS, 16 controls	DCE	3.0	No hypoperfusion in NAWM
(Sowa et al. 2017)	66 RRMS	DSC	1.5	Lower baseline perfusion is associated with higher disease severity and activity at 1 year
(Yin et al. 2018)	30 MS patients	DCE	3.0	Increased perfusion in contrast enhancing WMLs compared to non-enhancing lesions and NAWM

1.2.8 Clinical implications for using perfusion MRI in MS

1.2.8.1 Ischaemic vs demyelinating lesions

Differentiating between ischaemic and demyelinating lesions on MRI remains a challenge for clinicians and radiologists. In acute demyelinating lesions, increased metabolic activity results in hyperperfusion (Li et al. 2014) which may help in the diagnostic process. Perfusion imaging is probably less helpful in chronic

lesions, both ischaemic and demyelinating, as both types show hypoperfusion.

Zivadinov et al. used DCE-MRI to study lesions in patients with MS, acute, and chronic stroke. MTT was significantly prolonged in lesions and surrounding NAWM in stroke patients, both acute and chronic, when compared to acute demyelinating lesions in the MS patients. This confirms that there are haemodynamic differences in the pathological processes in these conditions both in the affected brain area and surrounding tissue (Zivadinov et al. 2008). Whether we can use these findings to draw conclusions on population basis is a research question to be addressed.

1.2.8.2 Early detection of high-inflammatory lesions

Perfusion imaging can detect regional changes of active inflammation prior to detectable enhancing lesions. Wuerfel et al. used DSC-MRI in RRMS patients and found a regional increase in CBF and CBV detected in new lesions up to three weeks prior to contrast enhancement (Wuerfel et al. 2004). This can help, even in absence of contrast enhancing lesions, to identify changes early in the diagnostic process of patients with MS and direct treatment options accordingly. Using DSC-MRI, Bester et al. demonstrated an increase in NAWM CBV and CBF in high-inflammatory patients (at least one contrast enhancing lesion in 3 out of 4 scans). This has significant clinical implications, both diagnostic and therapeutic, as

perfusion imaging can be used as a surrogate marker to demonstrate ongoing global inflammation in normal appearing brain areas (Bester et al. 2015).

In CIS patients, perfusion MRI demonstrated increased WM perfusion (Papadaki et al. 2012, Papadaki, Simos, Mastorodemos, et al. 2014, Papadaki, Simos, Panou, et al. 2014) indicating active inflammatory process, this may help in the future when considering therapeutic interventions without waiting for a relapse. However, one study showed that CIS patients have reduced perfusion in WM and GM similar to that seen in non-active RRMS cases (Varga et al. 2009) which could represent early neuronal loss in CIS and non-progressive MS patients. This could change the view on "watch and wait" strategy followed by neurologists around the globe when dealing with inactive CIS or RRMS population since a delay in modifying the disease process may result in irreversible cognitive deficits or disability progression linked with neurodegeneration.

1.2.8.3 Differentiating between MS subtypes and aiding prognosis

Using ASL-MRI in patients with different MS subtypes, WM perfusion was observed to increase with lesion load in the SPMS group, indicating the role of inflammation in some SPMS patients with active disease. When compared to controls, RRMS and SPMS

patients demonstrated increased WM perfusion indicating high metabolic activity. Decreased perfusion was found in cortical and deep GM structures in PPMS and SPMS groups consistent with neuronal loss and reduced metabolic activity (Lycke et al. 1993, Rashid et al. 2004). These findings can help us differentiate MS subtypes based on perfusion changes observed in different brain areas.

MS lesions have distinctive characteristics, and some are correlated with more disability. A study which assessed different lesion types showed reduced perfusion in T1-hypointense lesions and increased perfusion in active lesions. These perfusion changes were correlated significantly with brain atrophy which in turn reflected severity of clinical disability with high Extended Disability Status Scale (EDSS) score (Li et al. 2014). This supports using perfusion imaging for prognostic purposes in MS management.

1.2.8.4 Correlation between hypo-perfused areas and neurological deficits

Using SPECT, Lycke et al found that hypoperfusion in the frontal GM significantly correlated with neurological disability, low frontal GM and WM perfusion correlated with cognitive impairment, and low CBF in the occipital regions correlated with visual dysfunction in 19 MS patients (Lycke et al. 1993).

Correlation between fatigue and reductions in CBF/CBV in the thalami and basal ganglia has been demonstrated in RRMS and PPMS patients. Visuospatial and executive dysfunction has also been associated with decreases in deep GM CBF in MS patients (Inglese et al. 2008). SPMS patients with cognitive impairment exhibited reduction in frontal lobe GM CBV when compared to non-impaired SPMS cases (Aviv et al. 2012). These findings support the prospect of using perfusion MRI studies in evaluating MS patients with cognitive symptoms and can be used to assess response to potential therapeutic interventions.

Cortical involvement in MS has gained attention with the development of MRI techniques in the last decade. It is now believed that CLs represent an important aspect of the disease process in MS (Bagnato et al. 2006). Cortical atrophy and CLs seen early in MS patients are associated with physical and cognitive impairments independent from WM inflammatory activity (Calabrese, Atzori, et al. 2007, Calabrese et al. 2010). CLs perfusion has not studied extensively due to the limitations of the techniques used. Peruzzo et al used DSC-MRI in 2013 to demonstrate hypoperfusion in majority of CLs in RRMS patients (Peruzzo et al. 2013), there were few lesions with increased perfusion probably due to ongoing inflammatory process. Considering the safety of contrast media in MRI research, developing ASL-MRI to answer the question of: "What happens to

CLs perfusion in MS?" is a prospect worth investigating. GM involvement in MS is known to correlate with cognitive symptoms such as fatigue and memory difficulty. If proven that CLs undergo hypoperfusion, it could be possible to enhance perfusion using therapeutic interventions to assess their benefit on cognition in MS.

1.2.8.5 MS mimics

MRI offers a valuable tool in differentiating MS from its mimics. Perfusion MRI can provide significant information on typical MS plaques and atypical ones like tumefactive demyelinating lesions (Cha et al.). Using DSC-MRI, tumefactive MS lesions showed significantly lower CBV values compared to intracranial neoplasms and primary cerebral lymphomas (Cha et al. 2001). One major advantage of using perfusion MRI in this field is allowing clinicians to avoid unnecessary interventions such as brain biopsy to confirm the nature of the lesion. More research is needed on larger cohort and using non-contrast techniques if possible, to allow longitudinal observation.

PML can happen in MS patients as a complication of using DMTs. In a case of natalizumab-associated PML, perfusion MRI demonstrated significantly increased blood flow to the lesion. These changes returned to normal in advance of significant anatomical changes on conventional MRI sequences two weeks after initiating treatment (Elster 2013). Using ASL-MRI, it was shown that the edges of PML

lesions demonstrated significantly greater levels of hyperperfusion in patients with progressive disease compared to survivors (Khoury et al. 2013). Perfusion MRI can provide a useful tool to aid diagnosis, monitor response to treatment, and assess disease prognosis.

1.2.9 Future perspective

Perfusion MRI as a new biomarker in MS can help develop more understanding of disease pathogenesis and transform our approach in assessing disease activity, localisation of affected areas, monitoring progression, and deciding on effectiveness of therapy (Ge 2006, Holland et al. 2012).

Studies to time of writing did not investigate the effect of DMTs on perfusion in MS which could be a contributing factor to the heterogeneity found between MS patients from different disease types. Future studies need to assess effect of DMTs on cerebral perfusion.

Cortical involvement in MS is difficult to quantify using conventional MRI sequences; perfusion MRI can assess cortical changes by measuring local and regional perfusion. This offers great opportunity to study correlation of altered perfusion and clinical outcomes in MS and finding solutions to modify perfusion.

Perfusion MRI can be performed using contrast (DSC and DCE) and non-contrast (ASL). These have different strengths and weaknesses, and it will be important to consider how both techniques perform in MS imaging studies. In chapters two and three I am presenting my work on use of 7T perfusion MRI in MS. I aim to address three major aspects which are not adequately covered in the literature: CLs perfusion compared to NAGM using ASL, reproducibility of ASL in MS patients and healthy individuals, and how ASL and DSC perform when done simultaneously in MS patients.

1.3 Reversible Cerebral Vasoconstriction Syndrome

RCVS is a group of conditions characterised by prolonged but reversible multifocal narrowing of the cerebral arteries (Calabrese, Dodick, et al. 2007). It presents typically as acute severe headache, usually recurrent and thunderclap in character, with or without additional symptoms and signs (Ducros et al. 2007). Case reports have been published as early as the 1960s in various clinical settings. Biopsies show no evidence of histopathological abnormality in the affected blood vessels. While RCVS can happen spontaneously, around half of the cases occurs postpartum or following the intake of vasoactive drugs. RCVS has also been described in conditions such as migraine and other headache disorders, eclampsia/pre-eclampsia, unruptured cerebral aneurysms, and as a complication of various surgical interventions (Ducros 2013, Mehdi and Hajj-Ali 2014).

1.3.1 Pathophysiology

The pathophysiology of RCVS is not clearly understood. One crucial factor may be a disturbance in the cerebral vascular tone control, which may happen spontaneously or secondary to various exogenous or endogenous factors (Calabrese, Dodick, et al. 2007).

Genetic factors were linked to the severity of RCVS in a study of 90 patients; the Brain-Derived Neurotrophic Factor gene Val66Met polymorphism, known to be involved in neurogenesis and synaptic plasticity, exhibited a protective role against severe vasoconstriction. The same gene was found to play a role in the pathophysiology of unstable angina (Chen et al. 2011).

8-iso-prostaglandin F2α, an isoprostane produced by the non-enzymatic free radical peroxidation of arachidonic acid, is a marker of oxidative stress. This compound has a complex relationship with endothelial dysfunction and sympathetic over-activity, which is thought to be a factor in pathogenesis of RCVS. Urine levels of 8-iso-prostaglandin F2α were found to be significantly higher in RCVS cases during ictal phase compared to other primary headache disorders presenting with acute severe attacks or HCs, and the levels were correlated with the severity of vasoconstriction (Chen, Chung, et al. 2013). Another study by the same group demonstrated autonomic dysfunction in RCVS during the ictal stage, with improvement encountered after remission but still abnormal compared to controls. Patients had decreased heart rate variability, decreased parasympathetic modulations, and heightened sympathetic activity. While these could be associated phenomena with cerebral vasoconstriction, the authors assert they are biological markers for RCVS (Chen, Yang, et al. 2013).

Bone marrow-derived endothelial progenitor cells (EPCs) are involved in regeneration and maintenance of the endothelium (Chen et al. 2011). Circulating EPCs are inversely correlated with endothelial repair capacity and cardiovascular risks. Their number is considered a surrogate marker of vascular function (Hill et al. 2003). EPCs are classified according to the endothelial marker they express. Blood $CD34^{+}KDR^{+}$ EPCs measured in patients with RCVS inversely correlated with severity of vasoconstriction; reduced numbers of circulating cells were found in RCVS patients compared to controls, particularly in patients with severe vasoconstriction, indicating that oxidative stress and sympathetic over-activity in RCVS accelerate consumption of circulating EPCs (Chen et al. 2014).

E-1, a potent vasoconstrictor, was studied in 7 RCVS patients; during the ictal phase plasma E-1 was significantly higher compared to controls. E-1 level then decreased to average HC levels after resolution of vasoconstriction indicating its involvement in the pathogenesis of RCVS (Hammad et al. 2013).

Elevated levels of placental growth factors, like sFlt-1 and TGF-beta1, have been found in cases with postpartum RCVS (Stary et al. 2014).

1.3.2 Clinical features

RCVS affects women more than men, and typical age is between 20 to 50 years. It commonly presents as recurrent sudden onset severe headaches, referred to as "thunderclap headache" (Calabrese, Dodick, et al. 2007). It is estimated that half of RCVS cases are idiopathic while the rest are secondary ((IHS) 2013) . As a clinical term, RCVS covers a wide range of clinical presentations (Ducros et al. 2007), including what is known as "Call-Fleming syndrome" (Call et al. 1988), postpartum cerebral angiopathy (Bogousslavsky et al. 1989), benign angiopathy of the CNS (Hajj-Ali et al. 2002), drug-induced angiopathy (Martin, Rogers, and Kavanaugh 1995), migrainous vasospasm (Serdaru et al. 1984), idiopathic thunderclap headache (Liao et al. 2003), and thunderclap headache with vasospasm (Dodick et al. 1999).

Headache in RCVS is associated with multiple symptoms that may mimic migraine including nausea, vomiting, photophobia, visual blurring, and sometimes confusion (Sattar, Manousakis, and Jensen 2010). Focal neurological deficits are seen in 8 to 43% and seizures in 1-17% of cases (Mehdi and Hajj-Ali 2014). Adverse complications associated with RCVS may manifest based on the degree of vasoconstriction; cortical subarachnoid haemorrhage (SAH) is seen in one third of patients, ischaemic infarction in 6-39%, and concomitant posterior reversible encephalopathy syndrome (PRES) in 9-38% (Miller et al. 2015a). RCVS may also

present as parenchymal brain haemorrhage in 20% of cases (Bernard and Rivera 2015).

1.3.3 Diagnostic criteria

The Headache Classification Committee of the International Headache Society ((IHS)) published the International Classification of Headache Disorders, 3rd edition (Chen et al.) ((IHS)) in 2013 (Table 5).

Table 5 RCVS diagnostic criteria

A. Any new headache fulfilling criterion C
B. RCVS has been diagnosed
C. Evidence of causation demonstrated by at least one of the following: 1. Headache, with or without focal deficits and/or seizures, has led to angiography (with 'strings and beads' appearance) and diagnosis of RCVS 2. Headache, has either or both of the following: a. Recurrent during <=1 month, and with thunderclap onset b. Triggered by sexual activity, exertion, Valsalva manoeuvres, emotion, bathing and/or showering 3. No new significant headache occurs >1 month after onset

D. Not better accounted for by another ICHD-3 diagnosis, and aneurysmal SAH has been excluded by appropriate investigations

"Headache probably attributed to RCVS" is used for patients who present with a headache typical of RCVS, triggered by sexual activity, exertion, Valsalva and/or emotion, without demonstrable vasoconstriction on catheter angiography ((IHS) 2013).

1.3.4 Imaging

The hallmark of RCVS is vasoconstriction seen on vascular imaging scans, which reverses within 3 months. Prevalence of radiological vasoconstriction in RCVS is 90% and typically appears as diffuse segmental constriction lasting 4-12 weeks (Sattar, Manousakis, and Jensen 2010). Imaging is often negative in first 4-5 days (Mortimer et al. 2013). Mean time to detect abnormality on vascular imaging is 8 days after headache onset (Bernard and Rivera 2015). RCVS usually resolves by 1 month after presentation (Ducros et al. 2007).

Digital subtraction angiography is the gold standard technique to diagnose RCVS but it is an invasive procedure with a considerable risk of complications including stroke (Leffers and Wagner 2000). MRA shows vasoconstriction in 60-70% of patients (Lee, Ramadan, and Bamford 2013, Calic, Cappelen-Smith, and Zagami 2015).

Standard CT and MRI brain are helpful to show RCVS complications such as bleeding, ischaemia, and PRES (usually MRI is the diagnostic modality in PRES) (Lee, Ramadan, and Bamford 2013, Dilli 2014). CT angiography (CTA) is considered as good as MRA in terms of sensitivity (Dodick 2002), but the radiation involved with CT means it is not an ideal technique for repeated monitoring. TCD has been used successfully to show flow changes in RCVS and monitor reversibility (Ducros et al. 2007).

1.3.5 Perfusion MRI in RCVS

Perfusion MRI imaging has not been extensively studied in RCVS; a literature search revealed only two case reports at the time of writing. Rosenbloom and Singhal reported a case of RCVS induced by carotid endarterectomy following a frontal lobe ischaemic stroke. Perfusion MRI showed unilateral hypo-perfusion, mainly affecting internal watershed areas with superficial cortical regions being relatively spared. There is no data on the perfusion changes in the affected areas following resolution of vasoconstriction on angiography, as the perfusion MRI was not repeated (Rosenbloom and Singhal 2007). In a second report, ASL-MRI was performed on a 50-year-old man with RCVS who presented with severe recurrent headaches and neurological deficits (localising to the right hemisphere). ASL-MRI demonstrated significant hypo-perfusion in

the right parieto-occipital lobe, but no infarct was seen on diffusion imaging. At 12 weeks, there was complete resolution of cerebral vasoconstriction on angiography and normal perfusion findings on ASL-MRI (Komatsu et al. 2014). As described above, it is already well-documented that cerebral vasoconstriction may not be seen on brain imaging depending on timing of the scan and technique used.

Perfusion MRI imaging can offer an additional tool to confirm RCVS. ASL-MRI is a non-invasive radiation and contrast-free technique that can be performed at multiple time points to monitor changes in perfusion over the time of RCVS resolution and assess response to potential therapeutics.

1.3.6 Treatment

Management of RCVS depends on clinical presentation. There is no enough evidence to support any pharmacological intervention to aid resolution of RCVS. Calcium channel blockers, like nifedipine, nimodipine and verapamil, have been used in RCVS usually for 4 to 8 weeks (Sattar, Manousakis, and Jensen 2010). Evidence behind this practice comes from SAH induced vasospasm trials. Reported efficacy of nimodipine in RCVS ranges from 64% (Ducros et al. 2007) to 83% (Chen et al. 2006). Unfortunately, this does not apply to complicated ischaemic or haemorrhagic cases probably

due to the hypotensive effect of calcium channel blockers (Chen, Fuh, and Wang 2010). Other side effects include nausea, dizziness, flushing, and tachycardia. Magnesium sulphate has shown promising results in few trials on patients with postpartum RCVS (Singhal 2004, Singhal and Bernstein 2005). Corticosteroids have also been tried with variable results and often given with other medications (Call et al. 1988).

1.4 Hypothesis

In this thesis, ASL-MRI has been developed as a tool for characterising several patient cohorts, with the aim of enhancing the understanding of disease processes, defining pathophysiological changes, aiding diagnosis, and monitoring progression.

To assess ASL repeatability and reproducibility, in MS patients and HCs, ASL has been performed at two time-points. Establishing ASL as a reliable method requires direct comparison with the gold standard DSC-MRI; MS patients were scanned using both techniques to address this issue.

RCVS is a poorly understood condition; perfusion MRI can be a useful tool complementing the angiogram scan which can be normal initially in some cases. I studied a cohort presenting with recurrent thunderclap headache suggestive of RCVS using 3T pCASL and MRA to validate the technique use.

1.4.1 Objectives

1- Investigate perfusion changes in CLs and NAGM in MS using 7T ASL-MRI.

2- Assess ASL reproducibility in MS patients and HCs. Also, compare ASL with DSC-MRI in MS patients at 7T.

3- Investigate cortical perfusion, using 3T ASL, in suspected cases of RCVS and assess correlation with vascular changes on MRA.

Chapter 2: Ultra-High-Field Arterial Spin Labeling MRI for Non-Contrast Assessment of Cortical Lesion Perfusion in Multiple Sclerosis

2.1 Introduction

CLs in patients with MS are associated with physical disability (Calabrese et al. 2012) and cognitive impairment (Calabrese et al. 2009); however, little is known about the formation and development of CLs due to their typically small size (Pitt et al. 2010) and the insufficient sensitivity and spatial resolution offered by conventional imaging modalities. Emerging techniques using ultra-high-field MRI can significantly improve the detection of CLs compared to 3T scanners (Nielsen et al. 2012), and can advance our understanding of how these lesions develop or resolve over time.

Techniques including DIR (Geurts et al. 2005) and PSIR (Mougin et al. 2016) and can identify CLs and track changes of their structure. However, it is also desirable to understand changes in physiology that may precede or dictate these structural changes. To date, the haemodynamic changes within CLs have been characterised using DSC MRI, revealing that local haemodynamic change with the

status of the lesion: chronic CLs exhibit reduced perfusion (Haselhorst et al. 2000, Peruzzo et al. 2013, Hojjat, Kincal, et al. 2016), whereas in acute lesions increased perfusion has been reported (Haselhorst et al. 2000). Reports of changes in perfusion prior to lesion formation and contrast enhancement (Wuerfel et al. 2004) suggest that studies of local haemodynamics may predict such tissue damage, possibly identifying a critical window for therapeutic intervention.

To characterise rapid changes during periods of disease activity and CL development, patients must be scanned repeatedly and frequently. DSC MRI, although is considered the clinical gold-standard for assessing haemodynamic changes, is not well suited to such longitudinal studies. Recent concerns over dose-dependent deposition of Gd-based contrast agents in the brain caution against frequent repeated exposure (Kanda et al. 2014, Kanda et al. 2015, McDonald et al. 2015, Radbruch et al. 2015). This has led to multiple publications by the U.S. Food and Drug Administration and the European Medicines Agency in recent years.

ASL MRI provides an alternative method for quantifying local tissue perfusion that requires no injection of exogenous contrast. ASL has already been successfully used to measure perfusion deficits in cortical GM in early stages of MS compared to HCs, demonstrating its clinical sensitivity (Debernard et al. 2014). CL perfusion has been examined using pCASL at 3T and DSC to validate the results:

there was poor agreement in perfusion quantification (r=0.23) between the methods (D'Ortenzio et al. 2016), highlighting the challenges in making robust ASL perfusion measurements in small CLs compared to larger regions, especially at coarser spatial resolution. The inherently low contrast-to-noise ratio of ASL techniques is substantially improved when scanning at ultra-high-field (here defined to be 7T) (Gardener, Gowland, and Francis 2009), allowing data to be collected at higher spatial resolution. However, there are numerous challenges when performing ASL at 7T that require optimisation of the imaging protocol (Teeuwisse, Webb, and van Osch 2010). In this chapter, we assess the feasibility of using an optimised, ultra-high-field, high-spatial resolution, low-distortion ASL acquisition (Hall et al. 2010) to quantify perfusion in chronic CLs, demonstrating proof of concept that this technique is suitable for characterising local haemodynamic pathology in MS.

2.2 Objectives

Primary objective: Test a 7T ASL-MRI protocol to measure perfusion in CLs and NAGM.

Secondary objectives:

1- Investigate whether perfusion in CLs is different from local and global NAGM.
2- Assess whether perfusion in NAGM is dependent on proximity from CLs.
3- Perform exploratory, pilot correlations between cortical GM perfusion and clinical outcomes (EDSS, Fatigue Severity Scale (FSS), Modified Fatigue Impact Scale (MFIS)).

2.3 Methods

This cross-sectional prospective study was approved by the local research ethics authority. Twelve MS patients (7 RRMS, 4 PPMS and 1 SPMS); 4 women, 8 men; median age: 50 years (range 35 to 64); median EDSS: 5.5 (range 2.0 to 7.0); median disease duration 5 years (range 4 to 22 years) were recruited after giving written informed consent. All patients were selected based on having known pre-existing CLs from scans of two prior studies (Mougin et al. 2016, Samaraweera et al. 2017). The first study tested the PSIR technique for improved CL detection and the second examined the "central vein sign" in WMLs; neither of these earlier studies acquired ASL data or quantified perfusion. Both studies completed prior to the end of December 2014. Access to these earlier scans and evaluation of CLs was allowed as part of their consent. All scanning for this study took place between

September and December 2015, at least 8 months after the identification of CLs in the previous studies. As such, all CLs in this study are considered chronic.

MRI acquisition:

MRI was performed using a 7T Phillips Achieva scanner (Philips Medical Systems, Best, The Netherlands) using a 32-channel receive coil. To identify CLs, a whole-head PSIR scan was performed using a tailored adiabatic inversion pulse to ensure efficient inversion in areas of RF inhomogeneities found at ultra-high field (Hurley et al. 2010). The PSIR images were acquired at high spatial resolution (0.6 mm isotropic) to minimise partial volume effects in small CLs, allowing accurate boundary detection.

ASL data were acquired using a flow-alternating inversion recovery (FAIR) ASL scheme with in-plane pre-saturation using WET (Water suppression Enhanced through T1 effects) scheme and a sinc post-saturation pulse. A balanced steady-state free precession (bSSFP) readout was used to achieve high spatial resolution ($1.2x1.2x3mm^3$) with minimal distortions, essential for accurate co-registration of small CLs. A single axial imaging slice was positioned to transect one or more CLs identified from the PSIR acquisition. Single-phase ASL data were collected at PLDs of 1400 and 1800 ms to determine tissue perfusion. In addition, multi-phase ASL was acquired using a Look-Locker bSSFP readout

comprising 8 PLDs of 200, 550, 900, 1250, 1600, 1960, 2300, and 2650 ms (40 label-control pairs, to estimate ATT and locate intravascular signal contributions). An M_0 image was acquired for both single- and multi-phase bSSFP acquisitions to allow absolute perfusion quantification.

Data analysis: Analysis was performed jointly by me and Dr Richard Dury (University of Nottingham). Two subjects were not analysed due to substantial head movement artefacts.

Cortical lesion identification: CLs were identified from the PSIR modulus image during the scanning session in order to position the ASL slice appropriately. CLs were selected as any hypointense demarcated lesions within the cortical ribbon, as described by Mougin et al (Mougin et al. 2016). Masks were produced using MIPAV ((Medical Image Processing, Analysis, and Visualization), Center for Information Technology, National Institutes of Health, Bethesda, Maryland).

Image co-registration: The ASL and PSIR sequences were acquired back-to-back, to minimise misalignments between these data acquisitions. However, in two patients there was significant movement between the ASL and PSIR scans. In order to accurately locate the CLs in ASL dataspace, the PSIR data were co-registered

to the ASL data. Due to the limited coverage of the ASL scan, automated co-registration techniques were not appropriate. Instead, the PSIR slices corresponding to the ASL slice were identified and corrective rotations were applied manually as needed using FSL FLIRT (Jenkinson et al. 2002). The CL masks were then co-registered to the ASL data by applying these transformations.

ASL pre-processing: The ASL data were brain extracted and motion corrected using 2D in-plane co-registration using FSL MCFLIRT (Smith 2002), and any label-control pairs that contained >1.2 mm translational movement (the in-plane resolution of the ASL voxels) were discarded. The label images were subtracted from the corresponding control images, and these difference images were averaged for each PLD using a Huber M-estimator to remove outlier signals and generate robust perfusion-weighted images (Maumet et al. 2014).

Perfusion quantification: The base M_0 images were co-registered to the average ASL label image using FSL FLIRT. A T1 map was obtained by fitting the label images from the multi-phase ASL data to a Look-Locker saturation recovery curve. The T_1 of the arterial blood was estimated by fitting an inversion recovery to the signal in the sagittal sinus and correcting for oxygenation (Blockley et al. 2008).

The multi-phase ASL data were fit to the model described by Francis et al (Blockley et al. 2008) to produce a transit time map. This method also fits for perfusion; however, the SNR of the multi-phase ASL data is considerably lower than that of the single-phase ASL data (Francis, Bowtell, and Gowland 2008). Thus, this transit time map, the T1 map, and the fitted value for the T_1 of arterial blood were used with the averaged single-phase data in a model fit, as described by Gardener et al (Gardener, Gowland, and Francis 2009), to quantify perfusion in ml/100g tissue/min. To optimise this fit, the starting parameters were chosen by comparing the voxel-by-voxel ASL signal to a lookup table of modelled ASL signals. Parameters producing the best estimate (assessed using the sum of square differences) were used to initialise a Nelder-Mead simplex direct search implemented in MATLAB (The MathWorks, Inc., Natick, MA, USA).

CL perfusion was calculated by averaging the voxel-wise perfusion values inside the CL mask. A mask of local GM was created by dilating the CL mask to a radius of 12 mm, then restricting to this to a GM mask obtained from segmenting the PSIR image using FSL FAST (Smith 2002). The mean perfusion value inside this region, with the CL removed, was defined as "local NAGM" perfusion. Finally, the average perfusion in total "cortical NAGM", with the CLs removed, was also computed.

Lesion eligibility: To ensure a sufficient sample size of voxels representative of the lesion, CLs were selected for analysis if the lesion volume was more than three ASL voxels (12.96mm^3) and no vascular contamination was found. Vascular artefacts can be reduced by dephasing signal from larger arteries label at the time of imaging by the insertion of vascular crushing gradients directly after the excitation pulse or a motion sensitized T2-preparation module (Alsop et al. 2015).

As vascular crushing could not be applied in this bSSFP ASL acquisition, fitted perfusion values were influenced by both perfusion and intravascular blood flow contamination in the voxel. A histogram of local NAGM perfusion values was created and fitted to a mixture model of Gaussians (allowing for multiple undetermined perfusion and inflow signal sources); any voxel containing a perfusion peak value of five times greater than the global cortical GM perfusion peak was assumed to be dominated by vascular inflow, and this was used to create a vascular inflow mask. CLs overlapping with this mask were discarded.

NAGM zones: Four concentric rings of GM surrounding the CL were formed by dilating the lesion by radii of 6, 12, 18, and 24mm using MATLAB. Average CBF was measured within the CL, across cortical GM and within the NAGM zones using MATLAB (Figure 6).

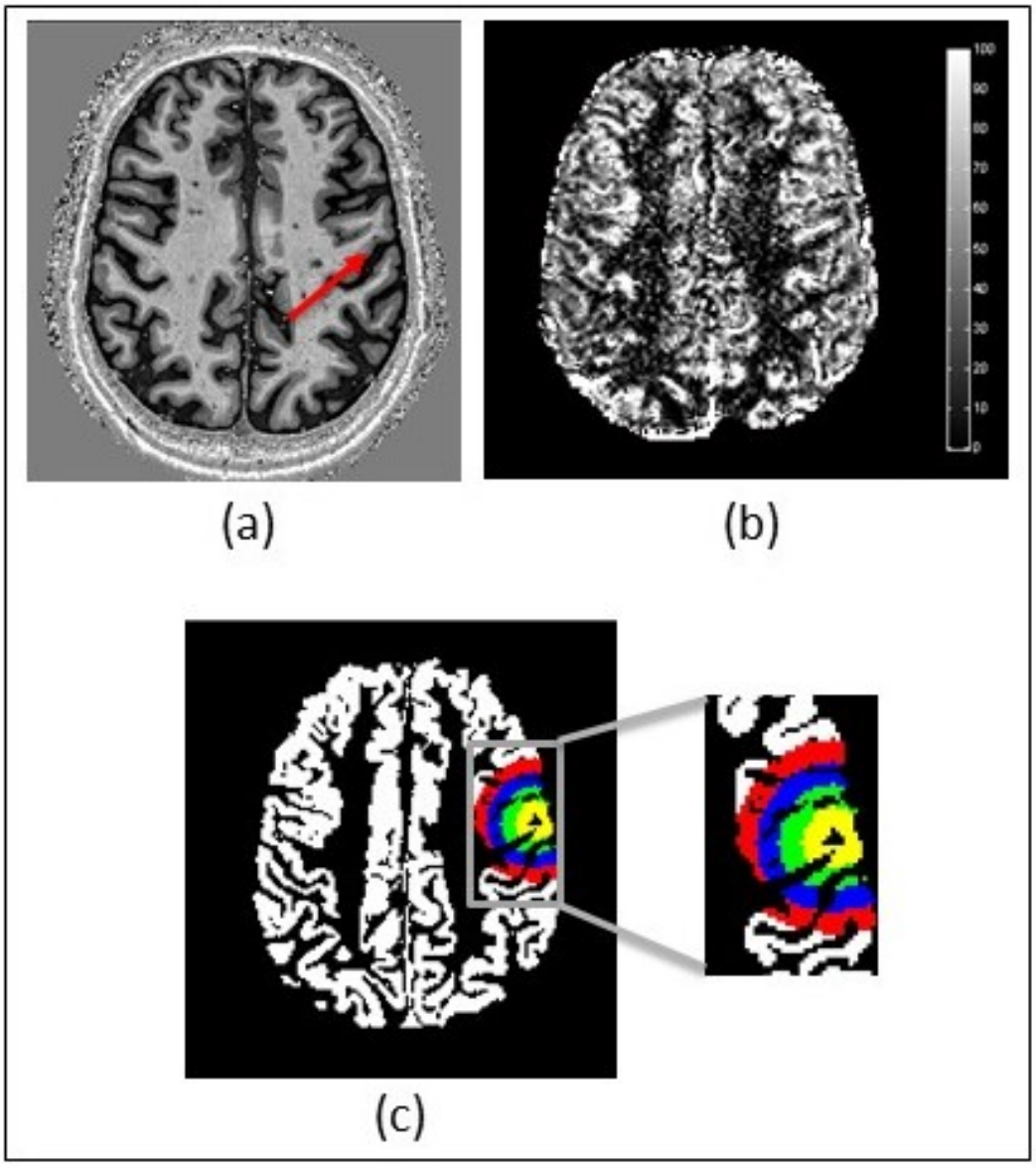


Figure 6 Example of CL, ASL map, and NAGM zones mask

(a) PSIR image showing a cortical lesion. (b) ASL map showing CBF range (ml/100g/min). (c) Grey matter mask with CL and local normal appearing grey matter and the surrounding NAGM zones

Statistical analysis: Paired two-sample t-tests examined differences in CBF (significance threshold $p<0.05$). Pearson's correlation coefficient r was used to assess relationships between each patient's mean CBF in global cortical GM and age, disease duration,

EDSS, and fatigue scores. Statistical analyses were performed using Minitab 17 (State College, PA: Minitab, Inc. (www.minitab.com)).

2.4 Results

Data from two participants were discarded due to head movement that moved CLs out of the ASL imaging volume. All remaining acquisitions were of sufficient quality to extract perfusion maps.

2.4.1 Cortical lesions identification

In total, 40 CLs were initially identified in the PSIR scans that overlapped with the ASL slice acquisition (Table 6). After applying the eligibility criteria, 27 lesions were selected for analysis (9 lesions were excluded due to small volume and 4 contained arterial contamination). Approximately three-quarters of lesions were leuco-cortical (n=21) (Figure 7) and one-quarter were intracortical (n=6) (Figure 8).

Table 6 Cortical lesions and lesion volume for each MS patient

Patient	No. Lesions	Lesion volume (mm^3)
1	4	27.86†, 21.60†, 8.42*, 16.63
2	5	13.18†, 15.12, 47.09, 14.04
3	1	17.50

4	3	44.50, 17.50, 19.44
5	3	17.71, 30.02, 26.35†
6	6	29.38, 8.64*, 17.93, 15.55, 6.48*, 21.17
7	4	22.03, 14.90, 25.49, 16.42
8	5	15.98, 15.34, 7.13*, 19.44, 15.98†
9	7	12.96, 7.56*, 8.86*, 8.86*, 8.42*, 14.26, 25.49
10	2	12.53*, 18.36
Lesions (*) with a cortical volume of < 12.96 mm^3 were discounted from analysis, along with those CLs (†) which had large vessel contribution.		

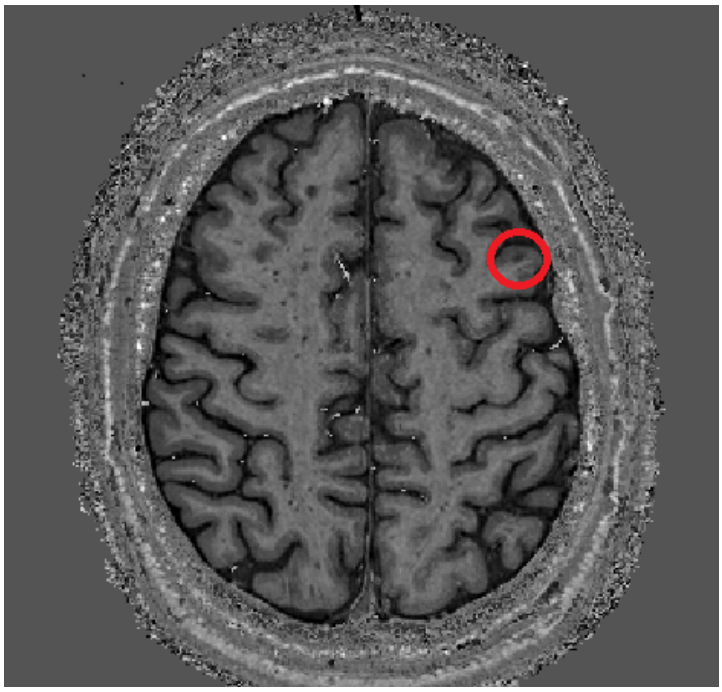


Figure 7 Example of leuco-cortical lesion

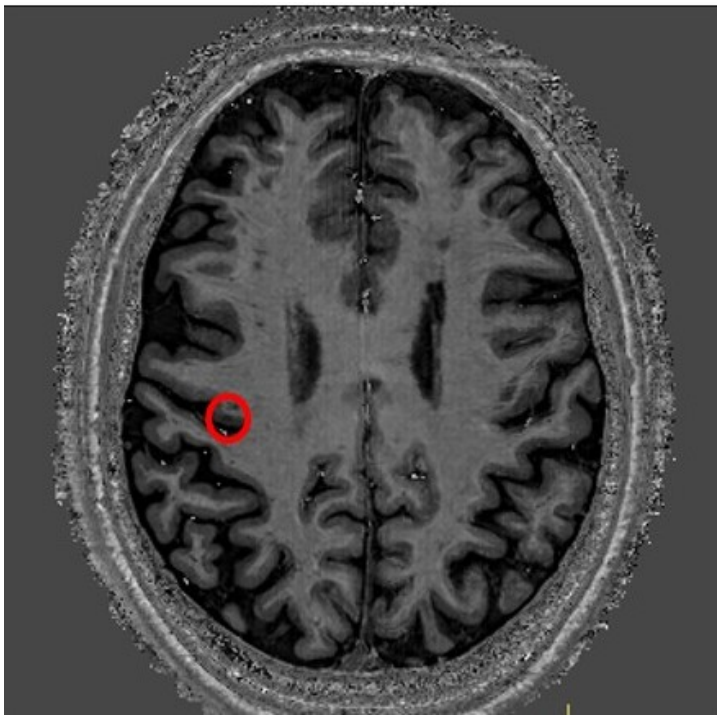


Figure 8 Example of intracortical lesion

2.4.2 Perfusion in CLs

The mean perfusion was 40±24 ml/100g/min in CLS, 53±12 ml/100g/min in local NAGM, and 53±8 ml/100g/min in global cortical GM. When comparing perfusion inside a given lesion to the associated local NAGM, CL perfusion was significantly lower by 23±9% (mean ± standard error, p=0.013), and significantly lower than global cortical GM by 26±9% (mean ± standard error, p=0.006) (Figure 9). The majority of CLs with increased perfusion (n=6) were seen in RRMS cases and only one lesion was seen in a PPMS patient. Four out of the 6 intracortical lesions (66%) and 3 out of 21 leuco-cortical lesions (14%) were hyperperfused.

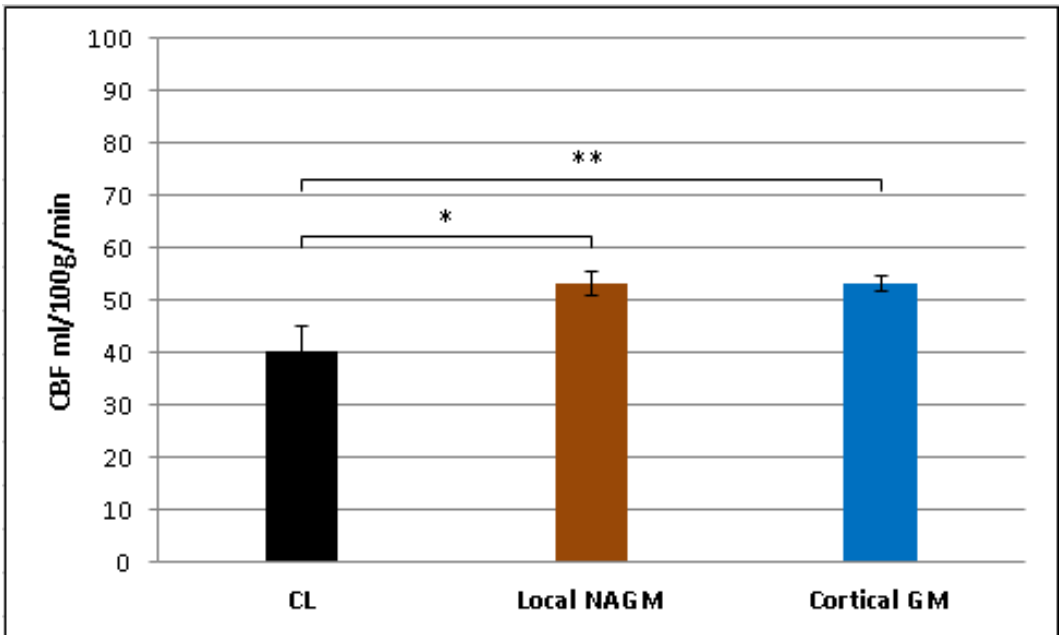


Figure 9 CBF in cortical lesions, local normal appearing grey matter, and cortical grey matter

2.4.3 Local NAGM zones

CLs showed significant hypoperfusion compared to all surrounding NAGM zones (Figure 10), p=0.009, p=0.03, p=0.007, p=0.02 respectively, but no significant difference between individual NAGM zones was observed.

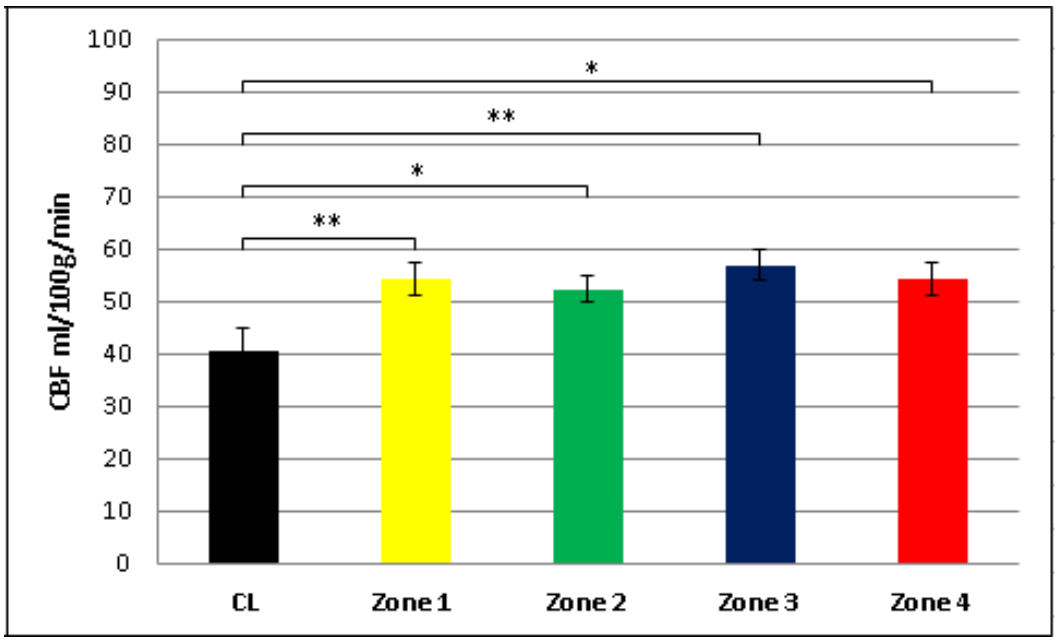


Figure 10 CBF in cortical lesions compared to surrounding normal appearing grey matter zones.

2.4.4 Clinical data

There was a trend for patients with older age (Figure 11), higher EDSS (Figure 12), and higher MFIS score (Figure 13) to have reduced global cortical GM CBF (r=-0.46, -0.61, and -0.45 respectively) but this lacked statistical significance (p=0.18, 0.06, and 0.19 respectively). Neither disease duration nor FSS scores were correlated with cortical GM CBF levels.

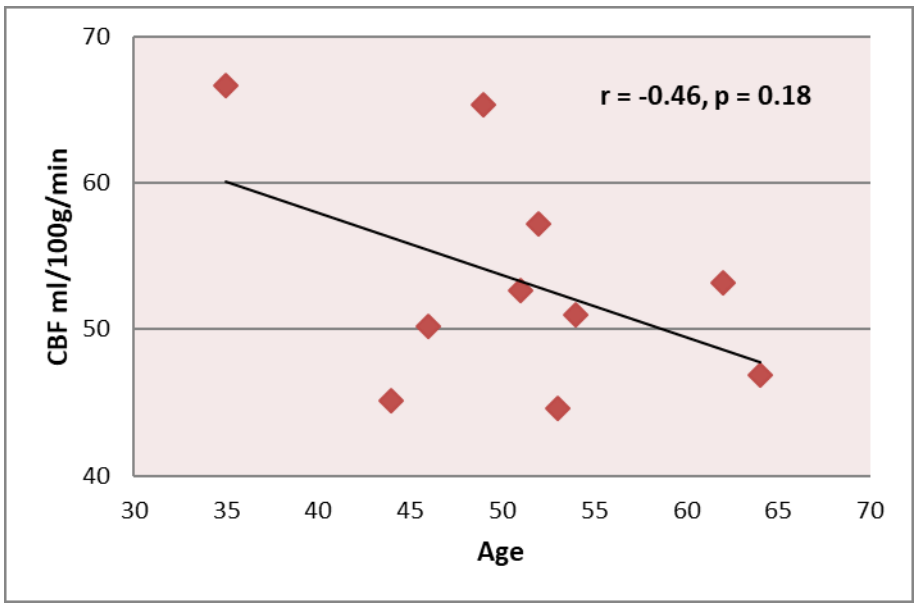


Figure 11 Correlation between age and global cortical GM CBF

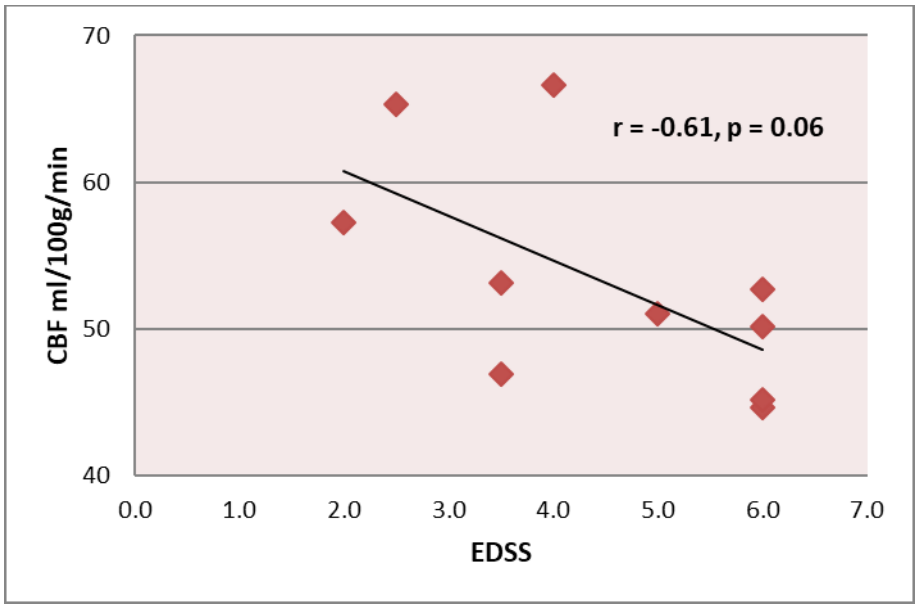


Figure 12 Correlation between EDSS and global cortical GM CBF

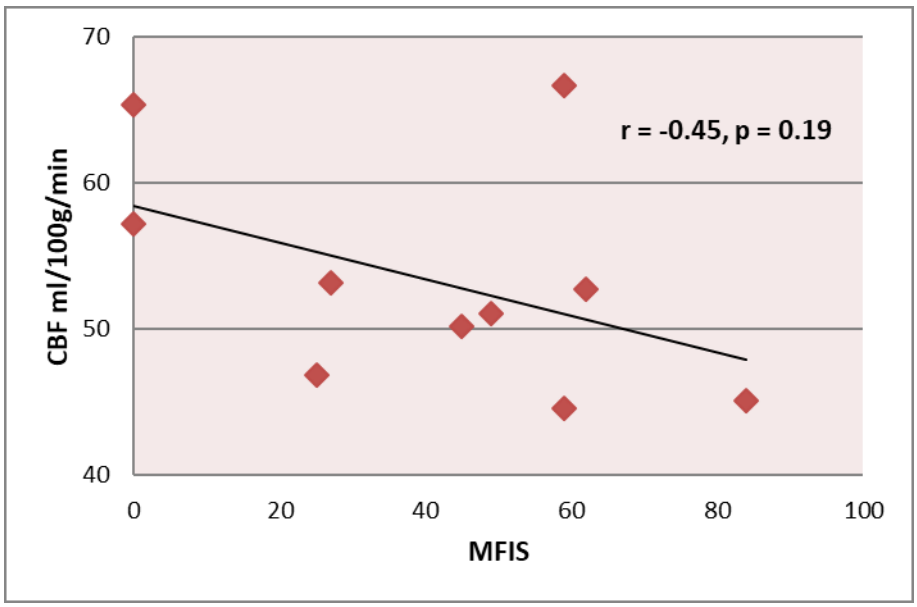


Figure 13 Correlation between MFIS and global cortical GM CBF

2.5 Discussion

To our knowledge, this is the first study measuring CL perfusion in MS using ASL at 7T. The majority of CLs showed hypoperfusion compared to NAGM, in line with the previous study by Peruzzo et al using DSC MRI at 1.5T (Peruzzo et al. 2013), demonstrating that this optimised ultra-high-field ASL-MRI technique is sensitive to the expected pathological hypoperfusion. In the DSC report, only pure intracortical lesions were studied; it was likely difficult to delineate the lesion accurately due to the reduced resolution at lower MRI field-strength ($0.9x0.9x6mm^3$). We included leuco-cortical lesions which are considered a type of CLs (Bø et al. 2003), and believed to be more inflammatory than intracortical and subpial lesions. We

compared CLs mean CBF with global cortical GM, not done in the DSC study.

Based on the findings of Moll et al. showing increasing tissue damage proximal to WMLs (Moll et al. 2011), we hypothesised that hypoperfusion is dependent on proximity from CLs. We were unable to demonstrate the presence of such gradient between zones. Our ability to discern subtle gradients of perfusion pathology near CLs may be limited by the low SNR inherent to ASL imaging.

This was an exploratory study aimed at using an ASL with a bSSFP acquisition scheme to collect high spatial resolution data and minimal distortions, following on from its development in healthy subjects (Hall et al. 2010). However, this restricted the acquisition to single-slice coverage, limiting our ability to robustly compare widespread cortical perfusion differences in patients compared to controls, and the clinical applicability of our technique. The next step is to assess the reproducibility of 7T FAIR ASL with increased brain coverage using an alternative 3D echo-planar imaging (EPI) acquisition scheme, for the comparison of perfusion measures in MS patients with controls. In order to assess the repeatability of focal perfusion values (e.g. the spatial scale of CLs) in different control and patient cohorts, further technical development is needed to simultaneously achieve high-resolution data with whole-

brain coverage by combining the bSSFP acquisition with simultaneous multi-slice methods.

The ASL PLDs used in this study were optimised for quantifying perfusion in cortical GM, hence we were unable to measure WM perfusion. Both PLDs and spatial resolution would need to be adjusted to achieve sufficient contrast-to-noise ratio for robust quantification of WM perfusion, which is significantly lower than NAGM and has been shown to be of the order of 16 ml/100g/min (Gardener and Jezzard 2015). Further generalisability of our observations is limited by the small sample size and heterogeneous disease course within our cohort. Future work needs to investigate applying this new imaging protocol to study CL perfusion across the distinct MS subtypes to better understand variations in lesion development in this diverse patient group. Finally, previous work has reported poor agreement between ASL and DSC perfusion estimates in CLs at 3T (D'Ortenzio et al. 2016), and we are seeking to validate our perfusion results derived from ASL in MS patients with results obtained using DSC-MRI, the clinical gold-standard technique (Dury et al. 2018).

Unlike DSC, ASL requires no exogenous contrast agent, making it an appropriate tool to study dynamic perfusion changes in MS. ASL-MRI may facilitate the study of CL formation and development, to test new therapeutic strategies and better understand the heterogeneous disease course in MS.

Chapter 3: 7T Arterial Spin Labeling MRI in Multiple Sclerosis: Reproducibility and Comparison with Dynamic Susceptibility Contrast

3.1 Introduction

MS is an immune mediated inflammatory disorder of the CNS. Perfusion is a physiological process which reflects the metabolic activity of the tissue (Steen et al. 2013). GM lesions in MS were shown to have reduced perfusion compared to NAGM using ASL-MRI (Dury et al. 2019) and DSC (Peruzzo et al. 2013). Widespread cerebral hypoperfusion in MS may contribute to focal lesion formation and diffuse axonal degeneration (Haselhorst et al. 2000).

Perfusion studies to date have described haemodynamic properties in MS showing differences among WMLs according to their chronicity; acute lesions have higher relative perfusion compared to chronic ones (Haselhorst et al. 2000) and this is observed in various MS disease subtypes, relapsing and progressive (Narayana et al. 2014). However, a contrast MRI study which compared MS patients and HCs, using DCE, demonstrated no NAWM perfusion difference between the two groups (Ingrisch et al. 2012). The

discrepancy in the literature regarding haemodynamic changes in MS is likely to be due to the differences between the methods and techniques used.

The gold standard MRI technique to measure cerebral perfusion is DSC-MRI which relies on use of contrast agent. The growing evidence of contrast media accumulation in the body and its unknown potential long-term risk (Kanda et al. 2015, Murata, Murata, et al. 2016) limits its use in longitudinal studies needed to measure dynamic changes in chronic conditions like MS. ASL-MRI requires no contrast and relies on magnetically labeling water in blood to measure perfusion in the tissue of interest. Benefits of such techniques are more important in people with renal disease where Gd-based contrast agents are contraindicated, children, and those needing scans at multiple time points. ASL benefits from using ultra-high field MRI scanners due to increased SNR (Gardener and Jezzard 2015), and we have demonstrated that ASL-MRI at 7T can measure hypoperfusion in small CLs in MS (Dury et al. 2019). Similar image acquisition techniques may be adapted to study widespread cortical perfusion across GM in clinical studies of MS.

To establish ASL as a reliable technique, it is important to assess its reproducibility as well as its ability to measure perfusion with comparable accuracy to DSC.

Chen et al studied the reproducibility of different ASL techniques in healthy individuals using 3T scanner, and demonstrated 8-10% variance in perfusion measurements, concluding that this variation is likely due to physiological fluctuations (Chen, Wang, and Detre 2011). Previous work reported moderate correlation between ASL and DSC at 3T in measuring cortical GM, WM, and WMLs perfusion in MS patients and HCs, cortical GM, WM, and WMLs; r = 0.51, 0.53, 0.54 respectively (D'Ortenzio et al. 2016). To date, there has been no study assessing the reproducibility of ASL or comparing it to DSC in MS at 7T.

In this study we investigate whether ASL at 7T can produce reliable, reproducible data when performed at two separate time points in MS patients and age-matched controls. We also compare 7T ASL and DSC, performed during the same scanning session, in MS patients.

Perfusion can vary across brain regions, and the two techniques may be differentially affected by transit delays or signal noise across brain regions. Therefore, we performed analysis of vascular territories regional GM perfusion. In addition, we analysed whether ASL is reproducible in measuring GM and regional perfusion.

3.2 Objectives

- Primary objectives:

- Assess the reproducibility of ASL in measuring GM CBF in MS patients and HCs
- Compare ASL with DSC GM CBF in MS patients

➢ Secondary objectives:

- Assess the reproducibility of ASL in measuring vascular territories GM CBF in MS patients and HCs
- Compare ASL with DSC in different vascular territories GM CBF in MS patients
- Compare ASL with DSC WM CBF in MS patients
- Compare ASL with DSC in white matter lesions CBF in MS patients
- Explore if there is a correlation between perfusion indices and clinical data

3.3 End points

- Primary endpoint: CBF (ml blood /100g tissue /min)
- Secondary endpoints:

  EDSS

  Fatigue scores

3.4 Methods

20 RRMS (12 women, 8 men (F/M 3:2); mean age: 39.5 years, range 25 to 49; median EDSS: 3.0, range 1.5 to 5.5; median

disease duration 5 years, range 0.5 to 15 years) and 19 age-matched healthy participants (12 women, 7 men; mean age: 39.5 years, range 25 to 50) were recruited from Nottingham University Hospitals and the University of Nottingham.

The scanning protocol included two visits, approximately 3 weeks apart. ASL was performed in both visits for all participants, while DSC was performed in MS patients at the first visit in the same scanning session as ASL. Inclusion and exclusion criteria are detailed in Table 7. Written informed consent was obtained from all participants and the study was approved by the West Midlands–South Birmingham Research Ethics Committee.

Table 7 Inclusion and exclusion criteria for MSGadASL study

Inclusion criteria for Healthy Controls:	*Inclusion criteria for Patients:*
• Male or female volunteers who are between the ages of 21 and 80. • Able to give voluntary written informed consent to participate in the study. • Able to understand the requirements of the study, including anonymous	• Diagnosed with MS. • Male or female volunteers who are between the ages of 21 and 80. • Able to give voluntary written informed consent to participate in the study. • Able to understand the requirements of the study,

publication, and agree to co-operate with the study procedures.	including anonymous publication, and agree to co-operate with the study procedures.

Exclusion criteria:

- Any history of neurological illness other than MS.
- MRI contraindications as screened on safety questionnaire (e.g. metal implants or pacemaker).
- Contrast agent contraindications as screened on the safety questionnaire.
- Known hypersensitivity to any MR or X-Ray contrast agent.
- Any history of renal failure or disease indicated by the patient's eGFR measured using the i-Stat blood testing equipment at the Sir Peter Mansfield Imaging Centre (SPMIC) prior to scanning.
- Any history of previous serious allergic reaction.
- Any history of circulation problems (vascular disease).
- Pregnancy or breastfeeding.
- Have taken part in any other clinical study within the previous 3 months. This involves taking a drug, being paid a disturbance allowance, having an invasive procedure or exposure to ionising radiation.

MRI acquisition:

MRI was performed using a 7T Phillips Achieva system with a 32-channel receive coil. FAIR ASL data were acquired using a single-shot 3D-EPI readout (spatial resolution=2×2×3mm^3, 18 slices, Echo time (TE)/Repetition time (TR)=15/42ms, flip angle=14°, SENSE=2 (in FH and AP), selective/non-selective width=50/300mm). Five ASL scans were acquired at PLDs of 700 and 1000ms (21 label-control repeats each), and 1300, 1600 and 1900ms. An M_0 map using the same imaging parameters was acquired for perfusion quantification. DSC data were acquired using a 2D-EPI readout (spatial resolution=2×2×3mm^3, TE=30ms, TR=1.5s, SENSE=2 in AP, 120 volumes, contrast administered at volume 20, Contrast used: ProHance (0.1mmol/kg) in two stacks; 4 slices placed below the cortex to image in inflowing arteries (with a 1mm slice gap) and 18 slices to image the cortex (contiguous slices).

Data analysis:

PSIR images were segmented to obtain GM and WM masks using FSL FAST (Smith 2002) and registering the masks into ASL and DSC space using FSL FLIRT (Jenkinson et al. 2002). Vascular territories masks were made by applying the GM masks to an atlas image which contains individual vascular territories (Mutsaerts et al. 2015). The territories studied were anterior cerebral artery

(ACA), MCA, and posterior cerebral artery (PCA) in each hemisphere.

Perfusion data were pre-processed by Dr Richard Dury (University of Nottingham). Perfusion-weighted images were produced by subtracting label-control image pairs. Images were motion corrected and co-registered using FSL FLIRT (Jenkinson et al. 2002). Partial volume correction was performed based on the algorithm described by Asllani et al. (Asllani, Borogovac, and Brown 2008) using the known proportions of GM and WM in each voxel (found using FSL FAST on the T1 map) in conjunction with the perfusion map; we can estimate the individual contributions to perfusion from each tissue type. Perfusion values were calculated by combining ASL data from all PLDs and calibrated using the M_0 image to yield quantitative perfusion maps in ml/100g/min using FSL BASIL (Chappell et al. 2009). CBF levels were obtained for global WM, global GM, and GM in each vascular territory using MATLAB (The MathWorks, Inc., Natick, MA, USA). The CBF histograms for GM contained few voxels with extremely high levels, caused by vascular contamination, potentially affecting the mean CBF. To find the peak perfusion we extracted all CBF values, fitted a double Gaussian, and extracted the peak of the first Gaussian. Perfusion maps were calculated from the DSC data using the central volume theorem with the block-circular deconvolution approach (Knutsson et al. 2017), and AIF was chosen by selecting

4-8 voxels from the inflowing arteries and averaging the time series.

Statistical analysis: Paired two-sample t-tests examined differences in CBF between different regions (significance threshold $p<0.05$). The coefficient of variation (CoV) for the mean GM CBF between scanning sessions (ASL visit 1 vs visit 2) and between ASL visit 1 vs DSC, was calculated. Pearson's correlation coefficient (r) was used to assess relationships between global and regional perfusion values achieved using ASL and DSC. In comparing GM vascular territories, the p value was corrected for multiple comparisons using Bonferroni correction; since 6 regions were analysed the corrected p value indicating significance was 0.0083).

3.5 Results

3.5.1 Global grey matter perfusion

3.5.1.1 ASL reproducibility

17 MS patients and 19 HCs were scanned twice with a median of 23 days apart. 2 MS patients and 2 HCs were deemed outliers (perfusion difference fell outside the 95% confidence interval) and data from 1 HC were discarded due to severe head motion (Figure 14, Figure 15). After removing outliers data, significant correlation

was observed between the GM perfusion values across visits in MS patients; r=0.57, p=0.027 (CoV=17.04±9.84%) (Figure 16) and in HCs; r=0.75, p=0.0008 (CoV=8.66±6.96%) (Figure 17). This in agreement with the perfusion study by Chen et al. in healthy individuals (Chen, Wang, and Detre 2011)

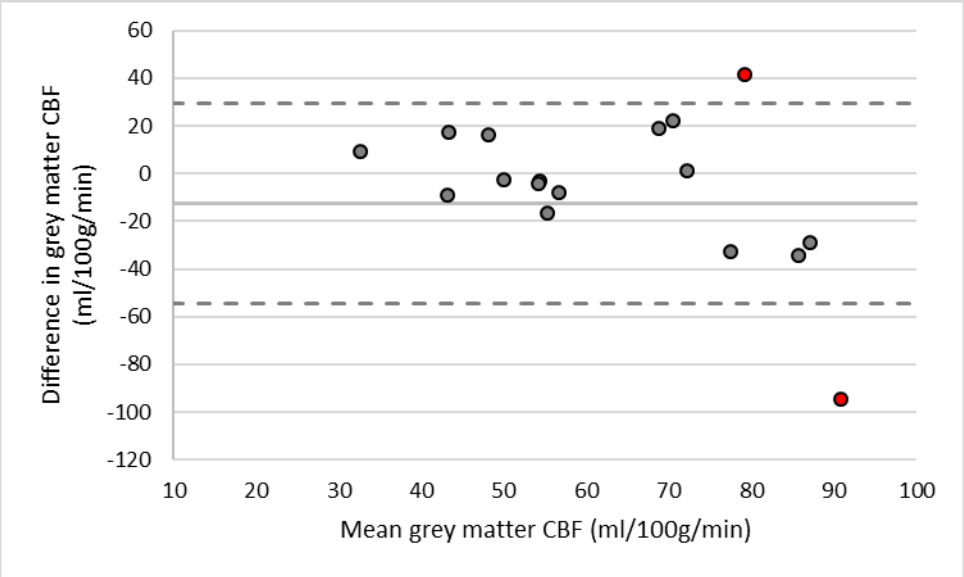


Figure 14 Bland-Altman plot for ASL in MS patients

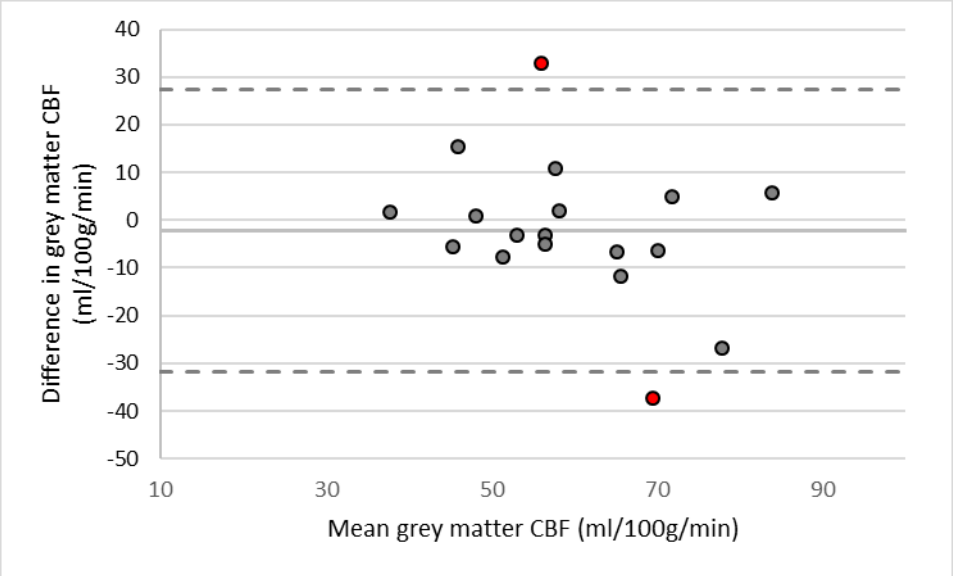


Figure 15 Bland-Altman plot for ASL in healthy controls

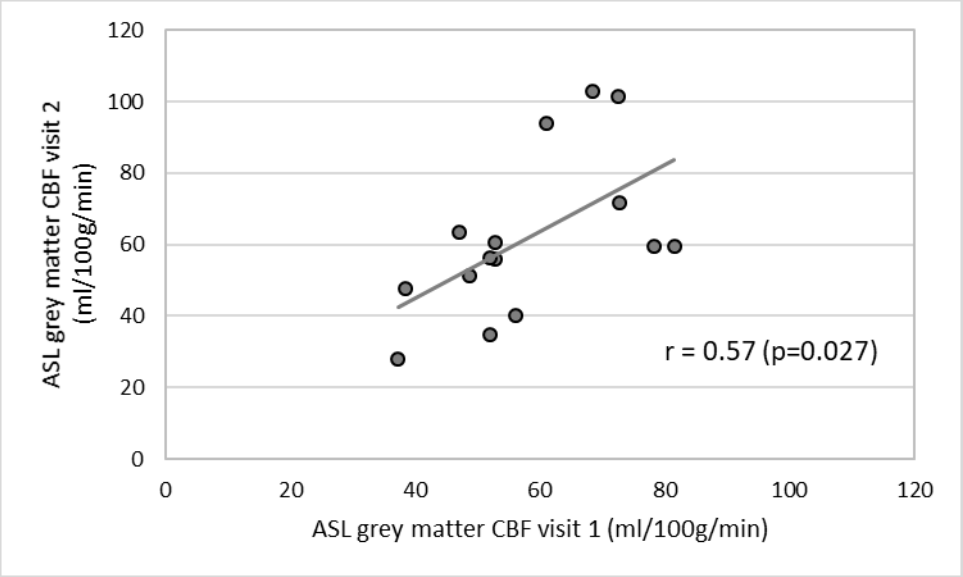


Figure 16 Correlation between ASL GM CBF data in MS patients

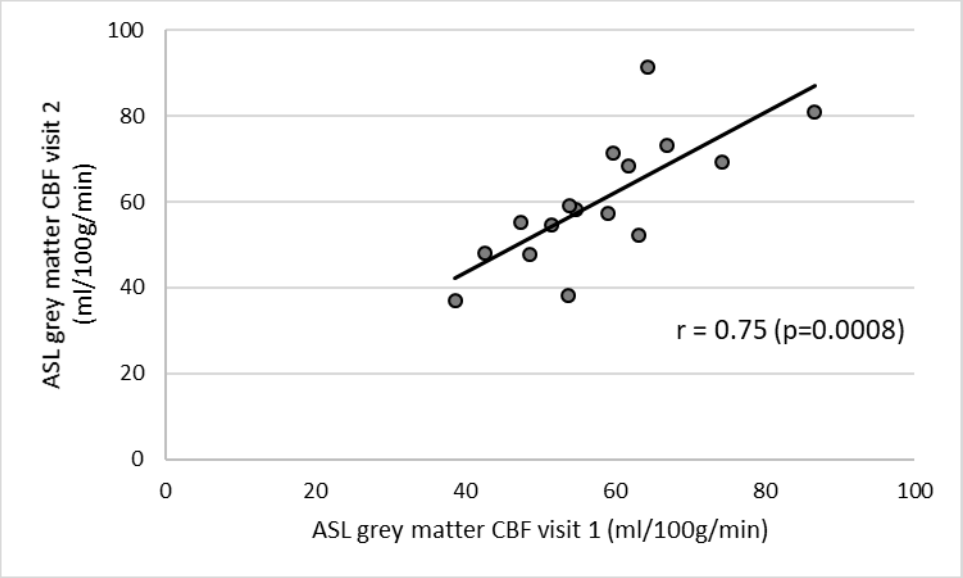


Figure 17 Correlation between ASL GM CBF data in healthy controls

3.5.1.2 ASL v DSC correlation

20 MS patients had both ASL and DSC scans performed in the same scanning session. Two patients were deemed outliers (mean GM perfusion difference between ASL and DSC fell outside the 95%

confidence interval) (Figure 18). After removing the outliers, there was significant correlation between the two techniques; r=0.51, p=0.031 (Figure 19).

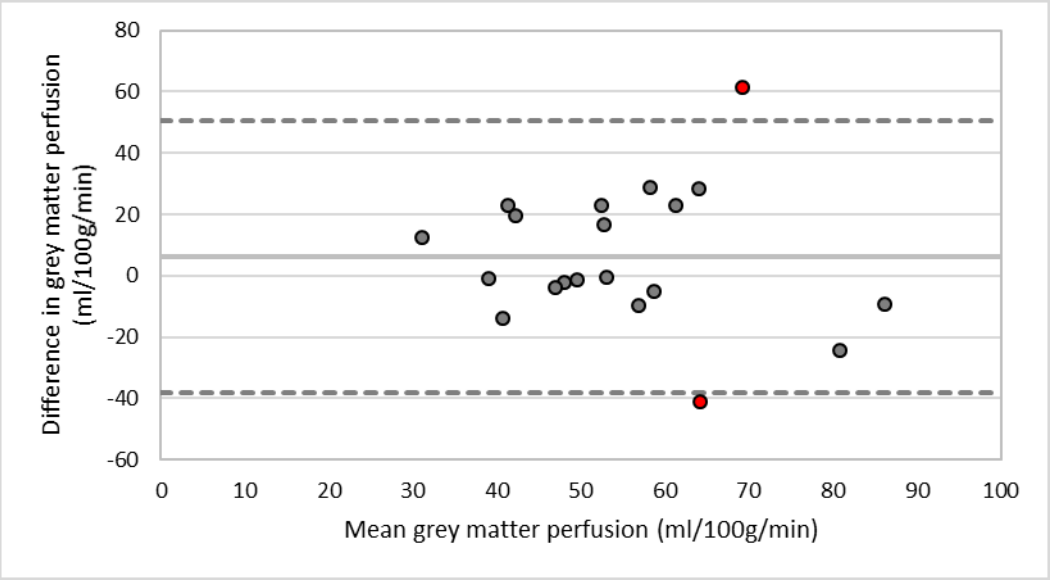


Figure 18 Bland-Altman plot for ASL and DSC in MS patients

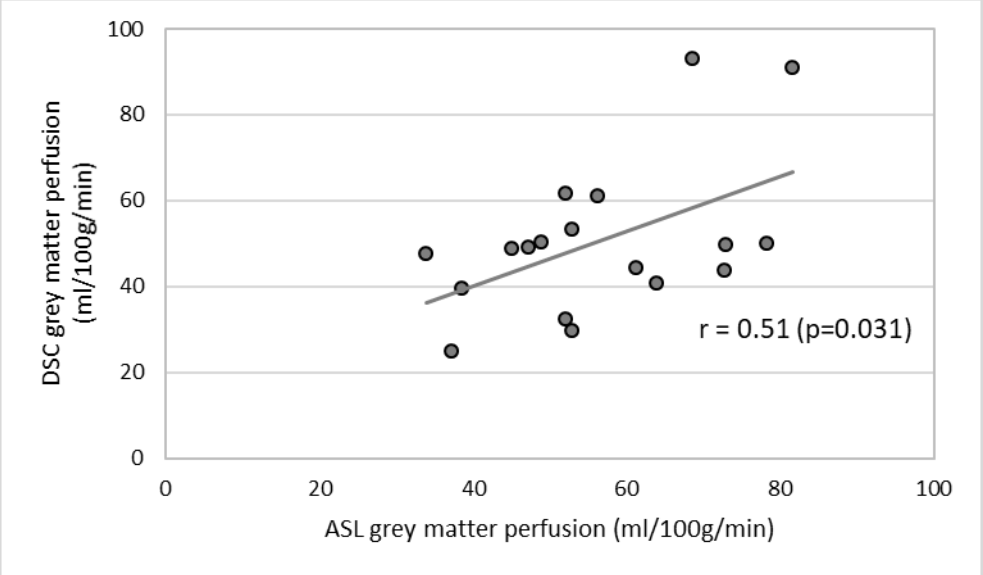


Figure 19 Correlation between mean GM CBF measurements using ASL and DSC in MS patients

3.5.2 Regional grey matter perfusion

3.5.2.1 ASL reproducibility in MS group

In MS patients (n=16), the total GM CBF data between the two visits showed no significant difference (Figure 20). The corrected p value for multiple correlation comparisons indicating significance was <0.0083. The correlations were not so strong when regions were compared. There was no significant correlation between the two visits in all regions; right ACA (r=0.37, p=0.158), left ACA region (r=0.56, p=0.024), right MCA (r=0.36, p=0.171), left MCA (r=0.4, p=0.125), right PCA (r=0.16, p=0.554), and left PCA (r=0.44, p=0.088) (Figure 20 to Figure 26).

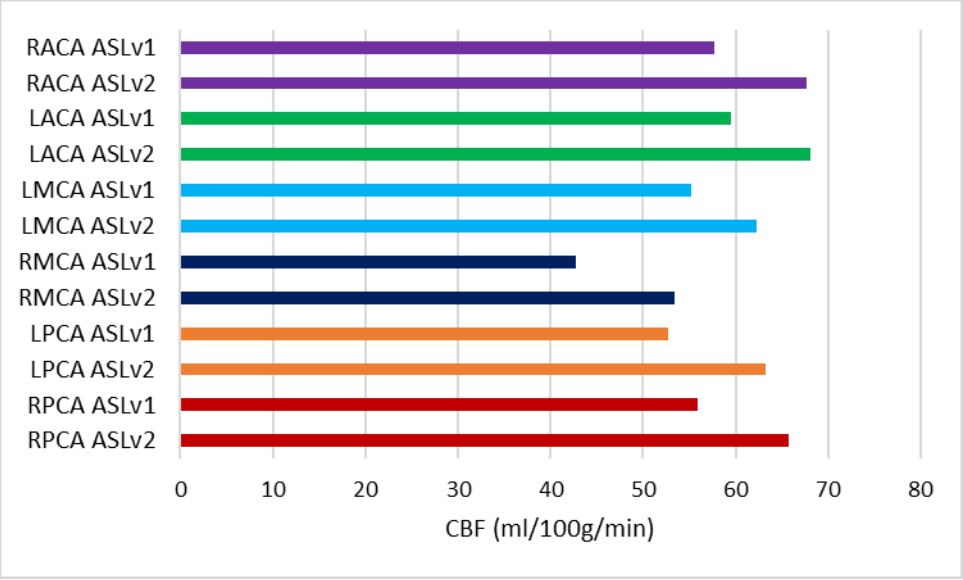


Figure 20 Comparison of regional GM CBF between ASL visit 1 and 2 in MS patients

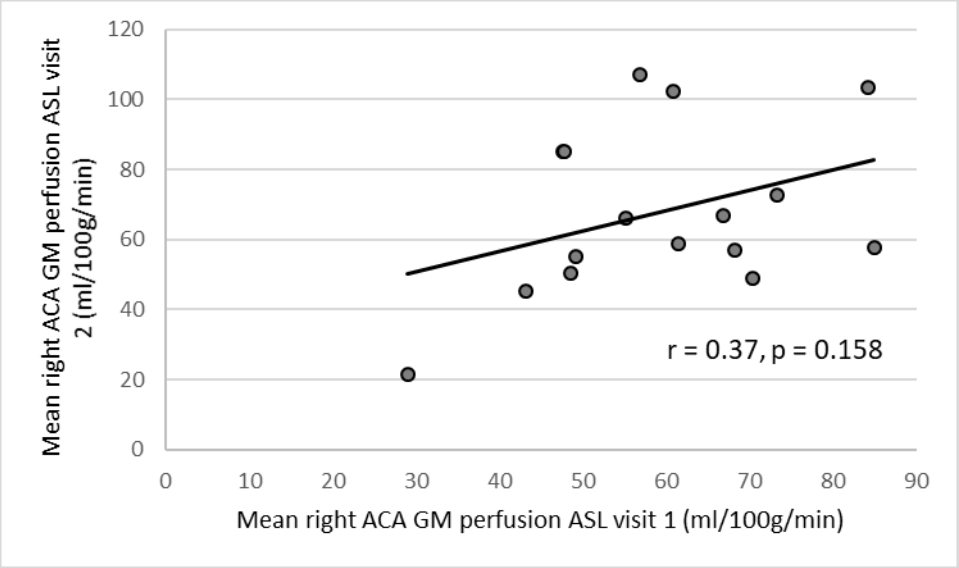


Figure 21 Correlation between right ACA ASL GM CBF data in MS patients

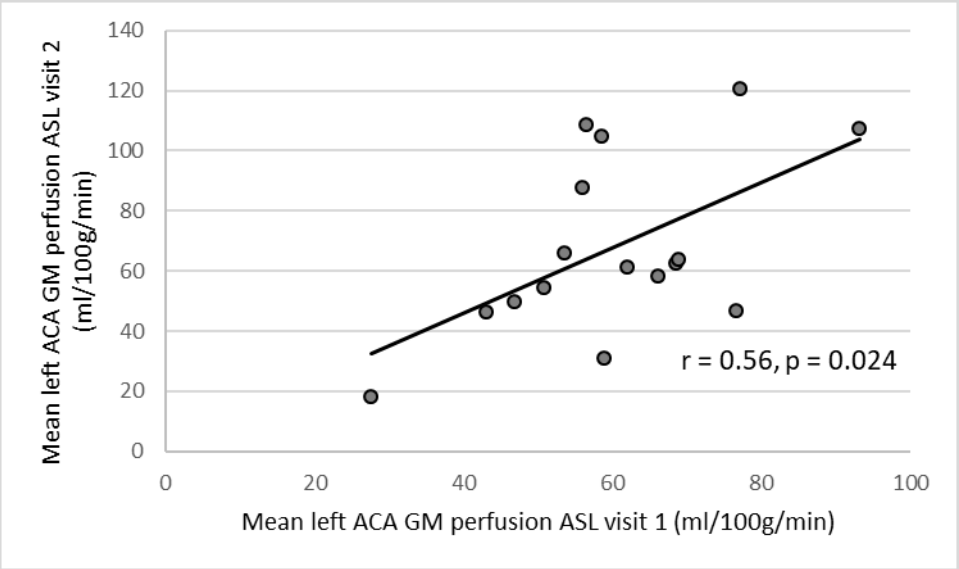


Figure 22 Correlation between left ACA ASL GM CBF data in MS patients

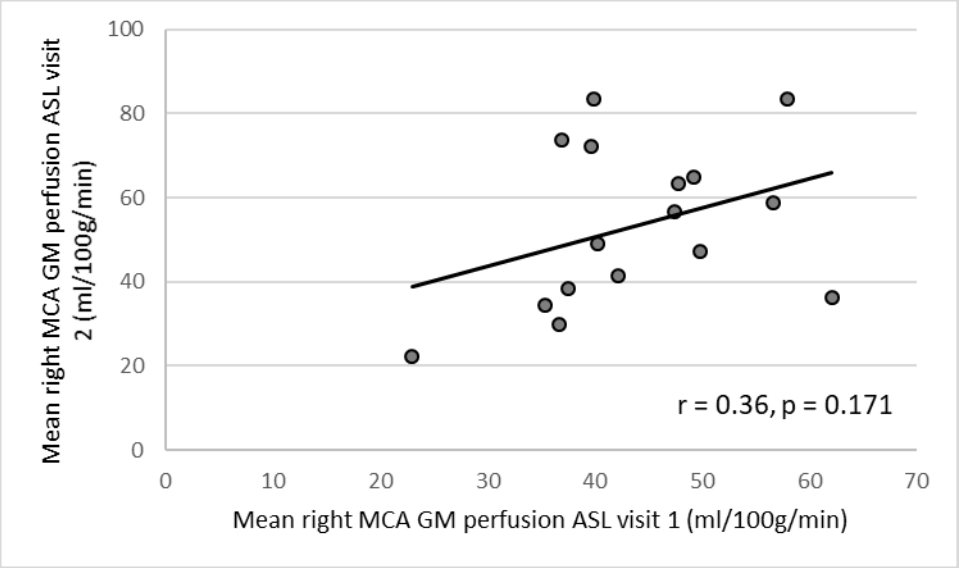


Figure 23 Correlation between right MCA ASL GM CBF data in MS patients

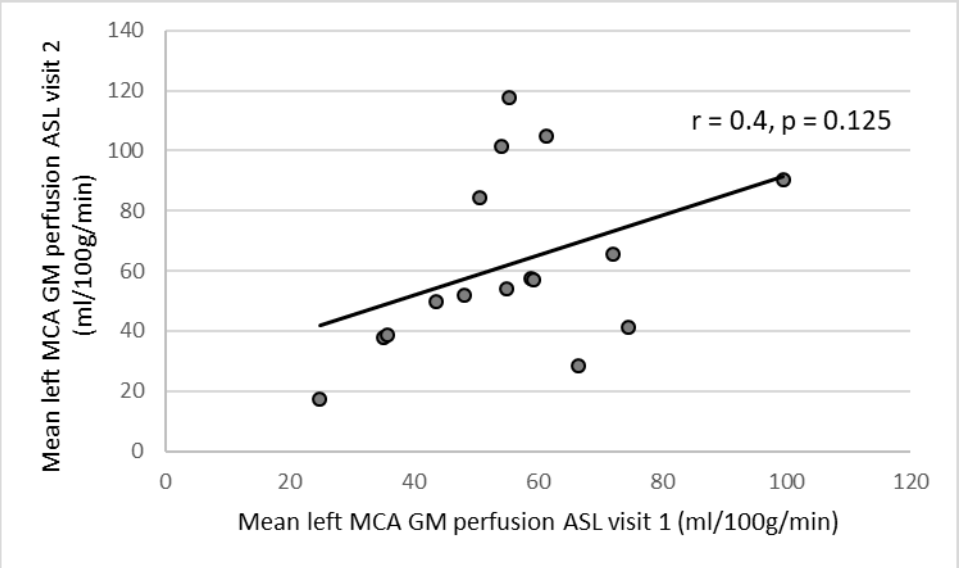


Figure 24 Correlation between left MCA ASL GM CBF data in MS patients

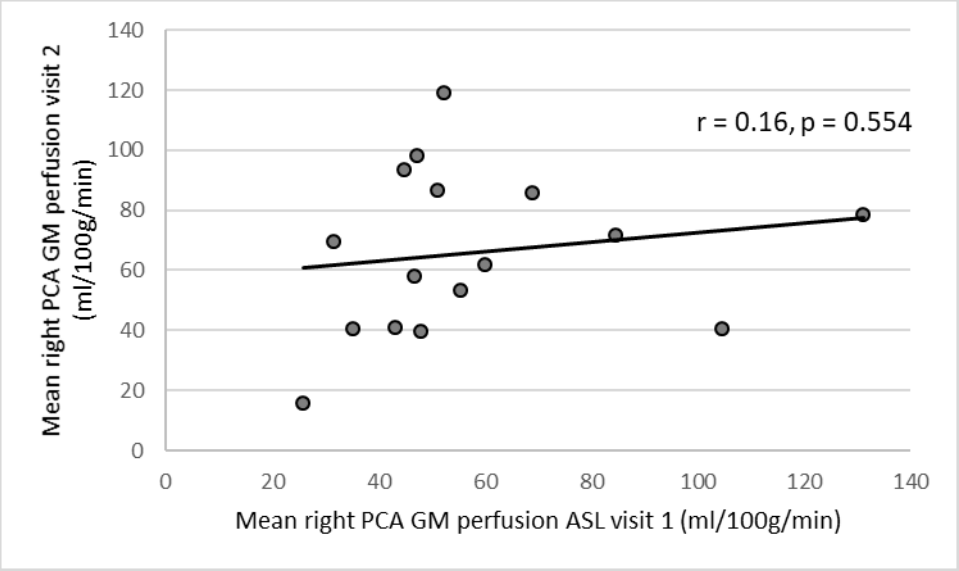


Figure 25 Correlation between right PCA ASL GM CBF data in MS patients

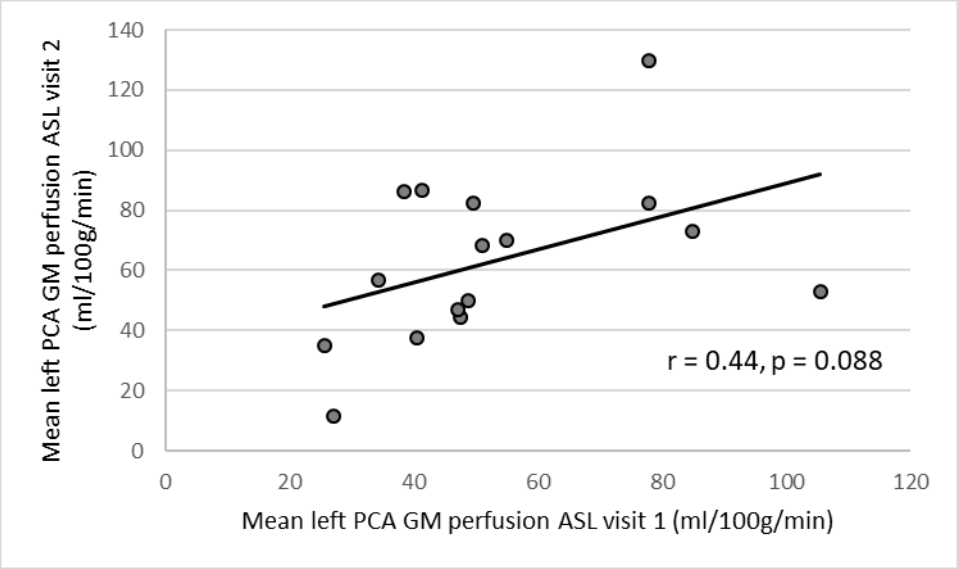


Figure 26 Correlation between left PCA ASL GM CBF data in MS patients

3.5.2.2 ASL reproducibility in HCs

In HCs (n=18), GM CBF data between the two visits showed no significant difference in all regions (Figure 27). The corrected p value for multiple correlation comparisons indicating significance was <0.0083. There was significant correlation between the two visits in: right ACA (r=0.61, p=0.007), left ACA (r=0.69, p=0.002), left MCA (r=0.67, p=0.002), right PCA (r=0.7, p=0.001), and left PCA (r=0.77, p=0.0002). No significant correlation was seen in right MCA (r=0.51, p=0.031) (Figure 28 to Figure 33).

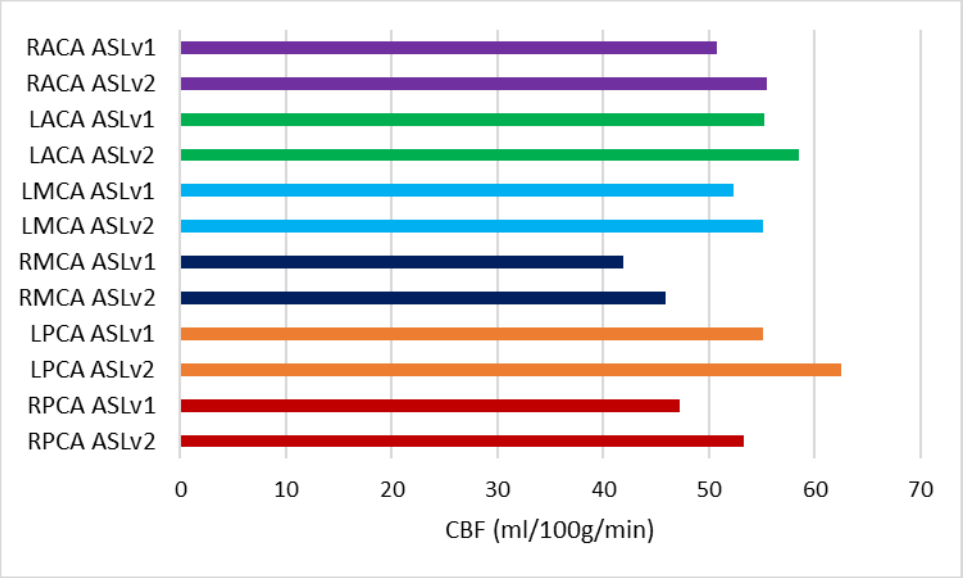


Figure 27 Comparison of regional GM CBF between ASL visit 1 and 2 in healthy controls

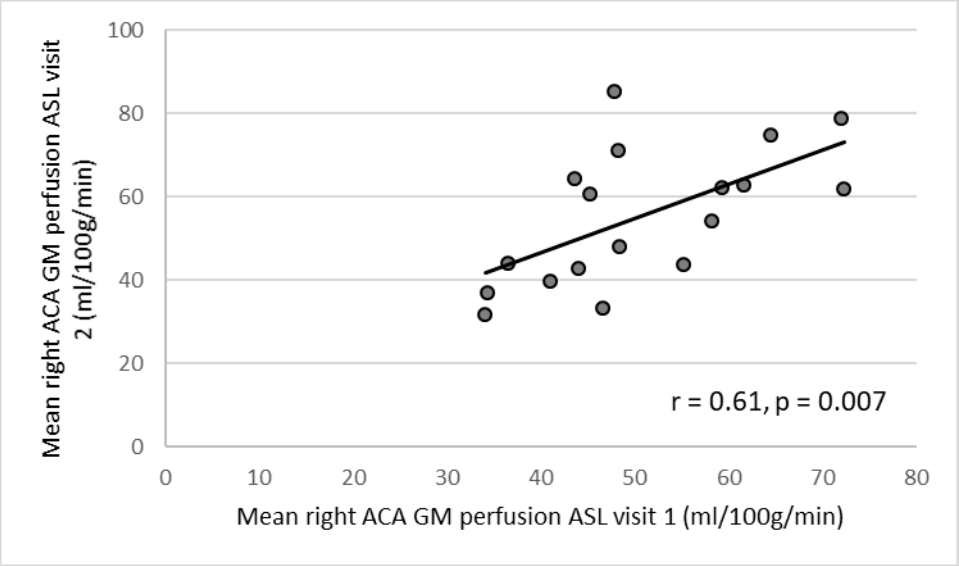


Figure 28 Correlation between right ACA ASL GM CBF data in healthy controls

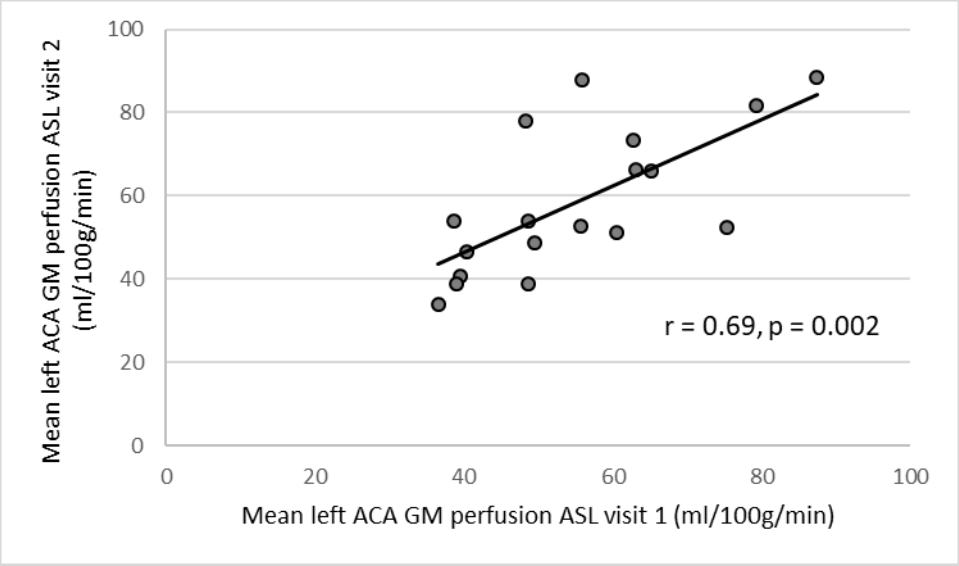


Figure 29 Correlation between left ACA ASL GM CBF data in healthy controls

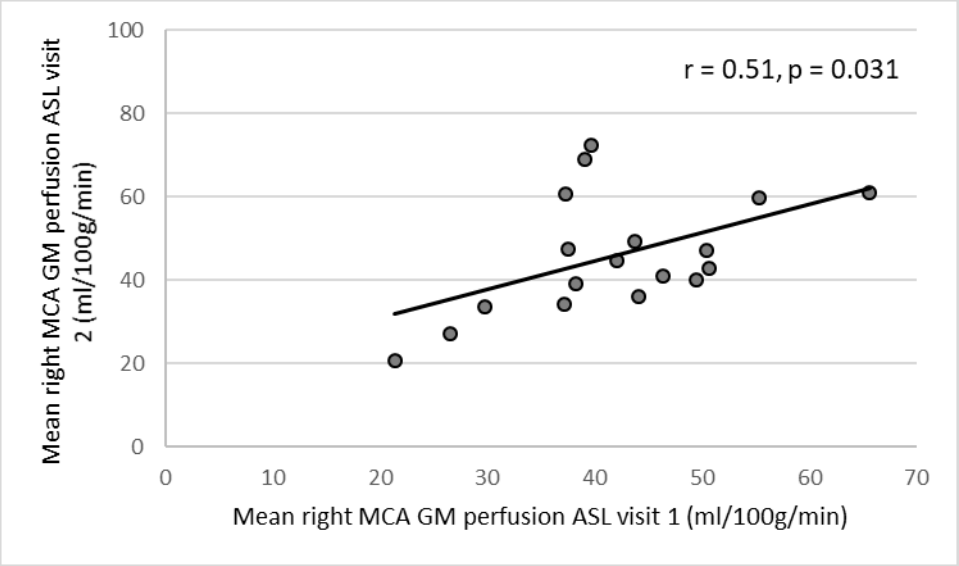


Figure 30 Correlation between right MCA ASL GM CBF data in healthy controls

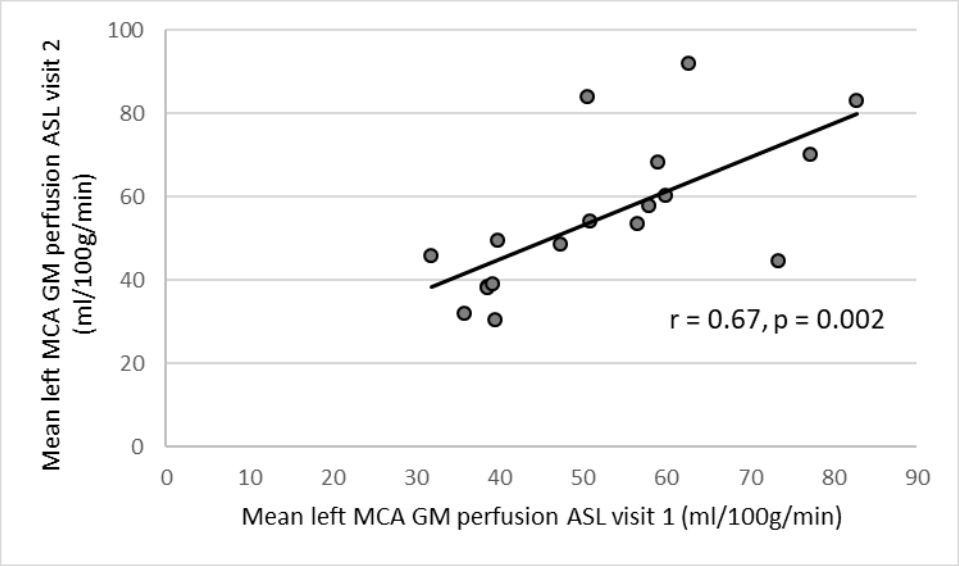


Figure 31 Correlation between left MCA ASL GM CBF data in healthy controls

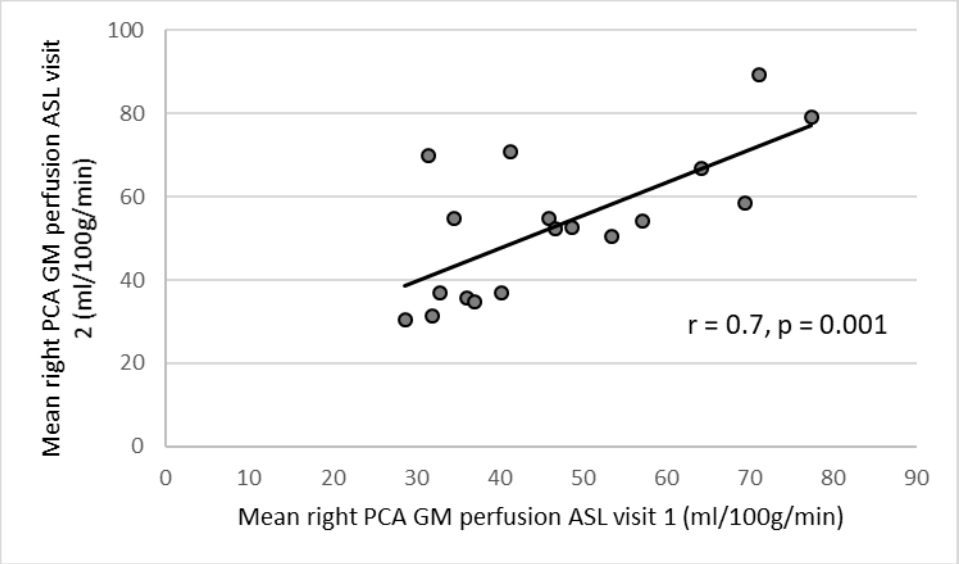


Figure 32 Correlation between right PCA ASL GM CBF data in healthy controls

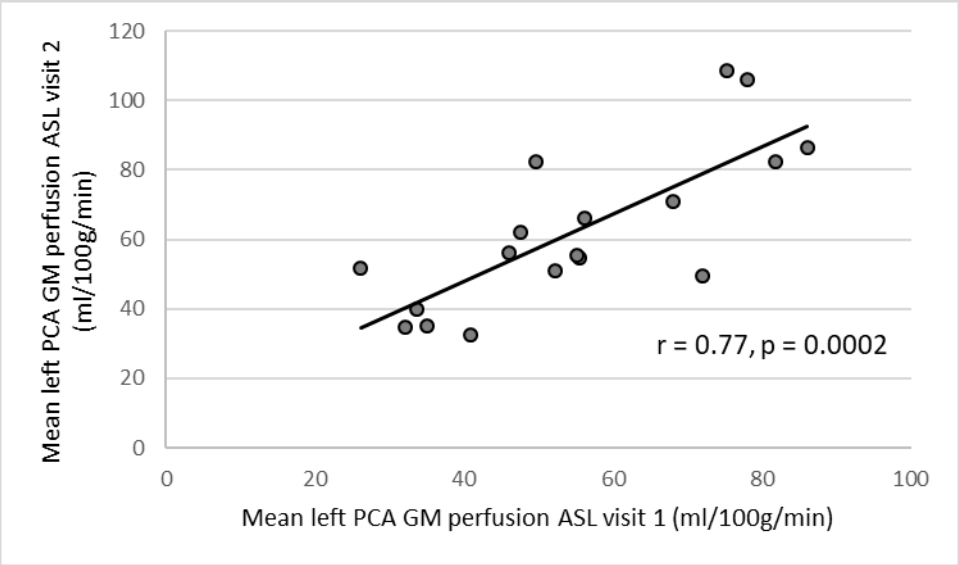


Figure 33 Correlation between left PCA ASL GM CBF data in healthy controls

3.5.2.3 ASL vs DSC correlation

In MS patients (n=18), ASL (visit 1) and DSC GM CBF data showed no significant difference apart from right MCA region (p=0.05) (Figure 34). The corrected p value for multiple correlation comparisons indicating significance was <0.0083. There was significant correlation in the left MCA territory (r=0.61, p=0.007). No significant correlation was seen in the other territories; right ACA (r=0.57, p=0.014), left ACA (r=0.57, p=0.014), right MCA (r=0.48, p=0.044), right PCA (r=0.14, p=0.58) and left PCA (r=0.16, p=0.526) (Figure 35 to Figure 40).

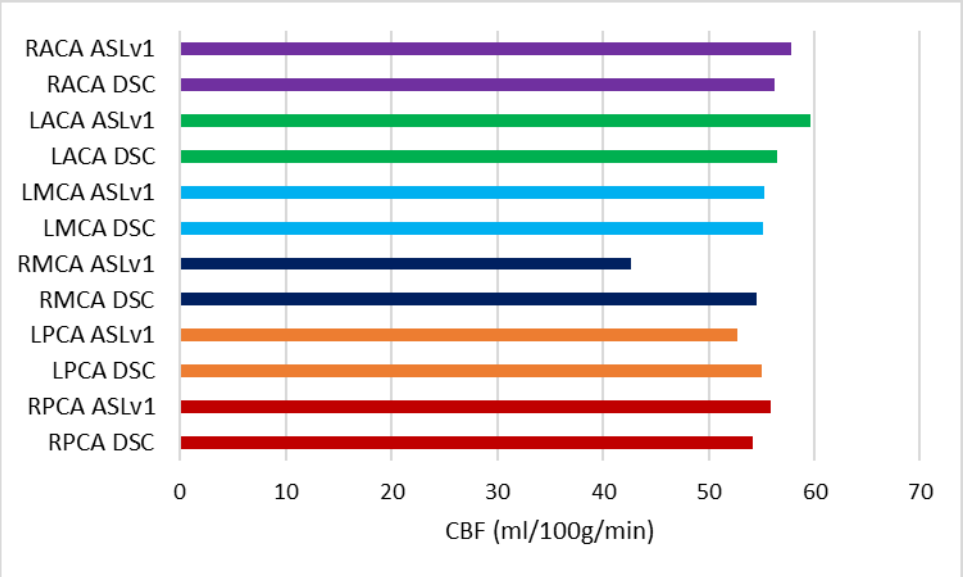


Figure 34 Comparison of regional GM CBF between ASL visit 1 and DSC in MS patients

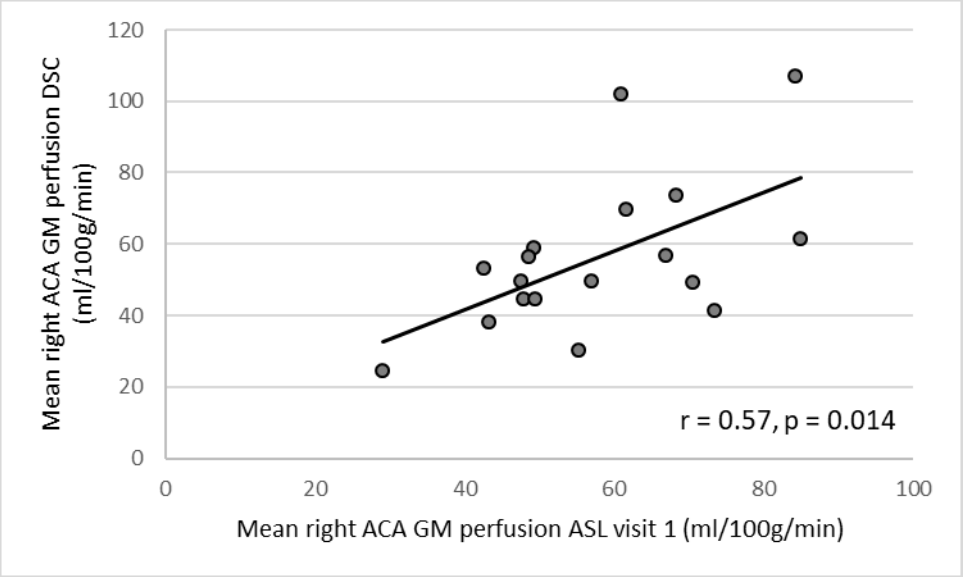


Figure 35 Correlation between right ACA GM CBF data in MS patients

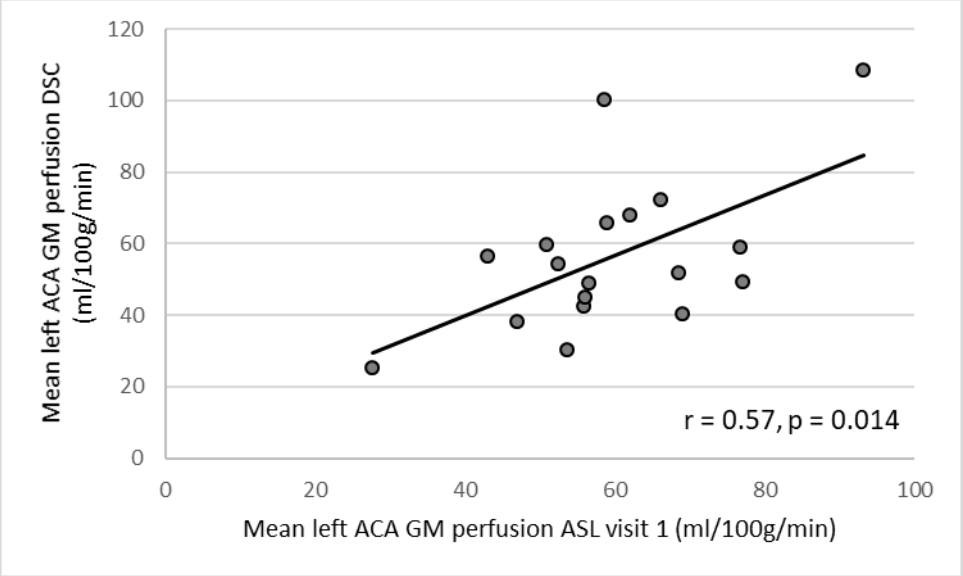


Figure 36 Correlation between left ACA GM CBF data in MS patients

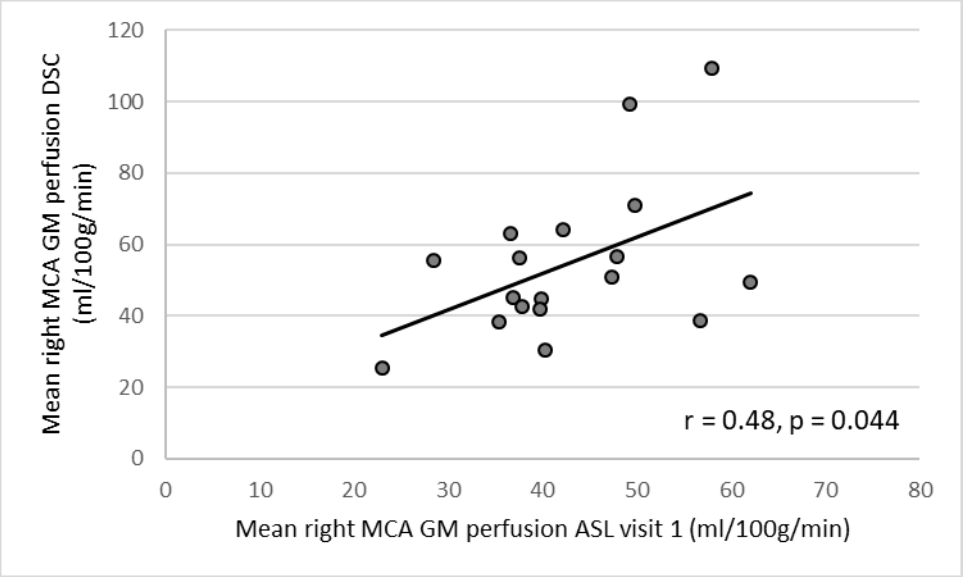


Figure 37 Correlation between right MCA GM CBF data in MS patients

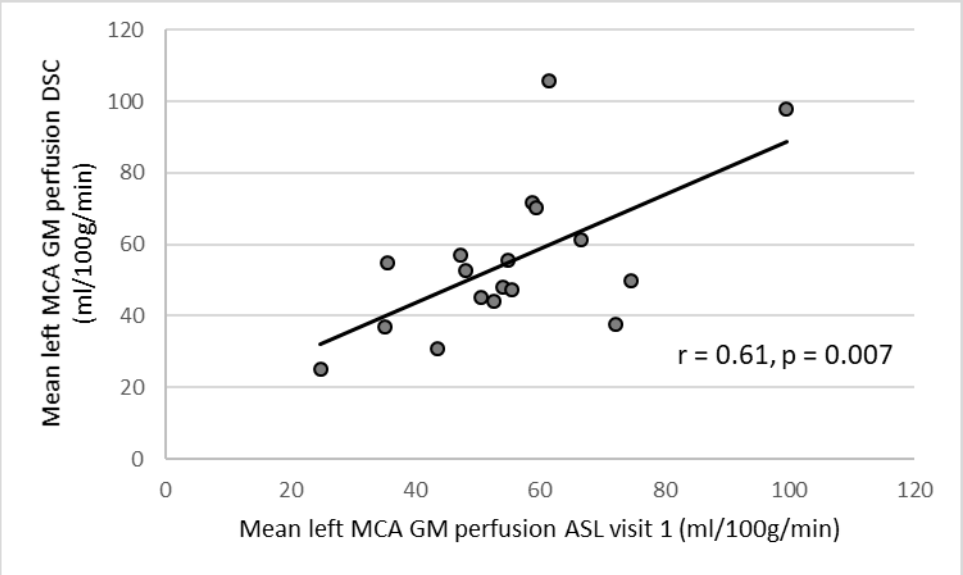


Figure 38 Correlation between left MCA GM CBF data in MS patients

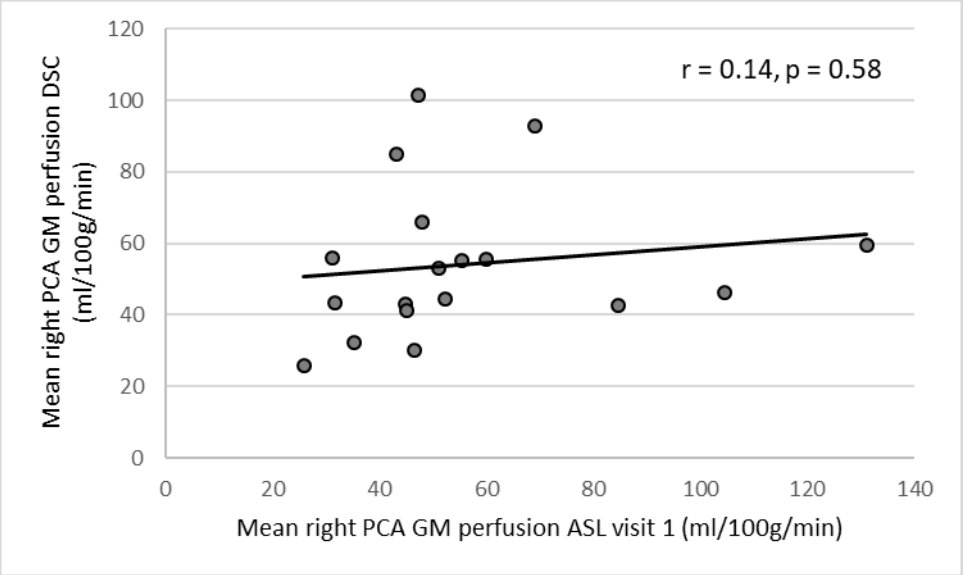


Figure 39 Correlation between right PCA GM CBF data in MS patients

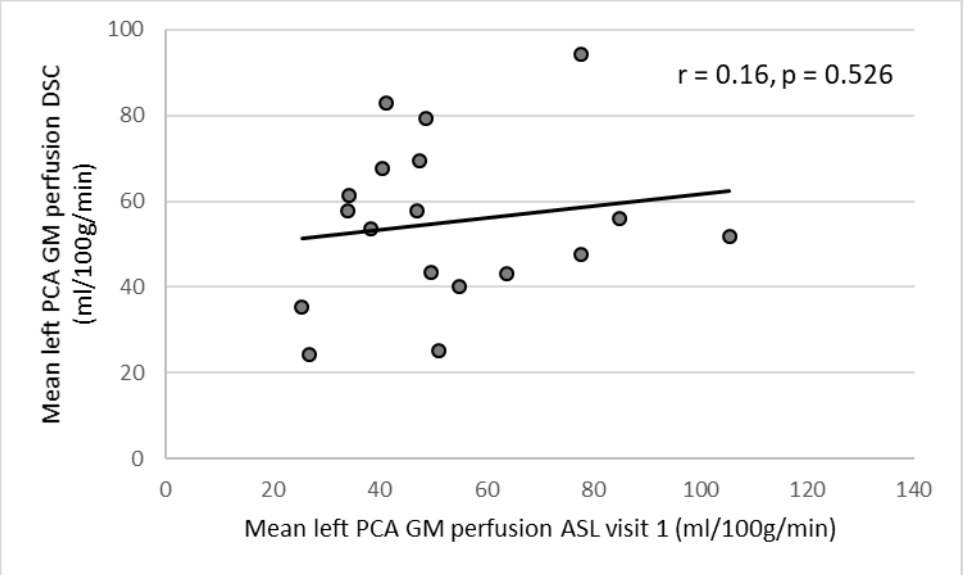


Figure 40 Correlation between left PCA GM CBF data in MS patients

3.5.3 Global white matter perfusion

3.5.3.1 ASL vs DSC correlation

WM perfusion analysis was performed on the MS patients' data (n=20) comparing ASL and DSC. A paired t-test showed significant difference in mean WM CBF between the two techniques (ASL mean = 41.48 ml/100g/min, DSC mean = 23.87, $p<0.0001$). The correlation between the two techniques was not significant; $r = 0.42$, $p = 0.065$ (Figure 41).

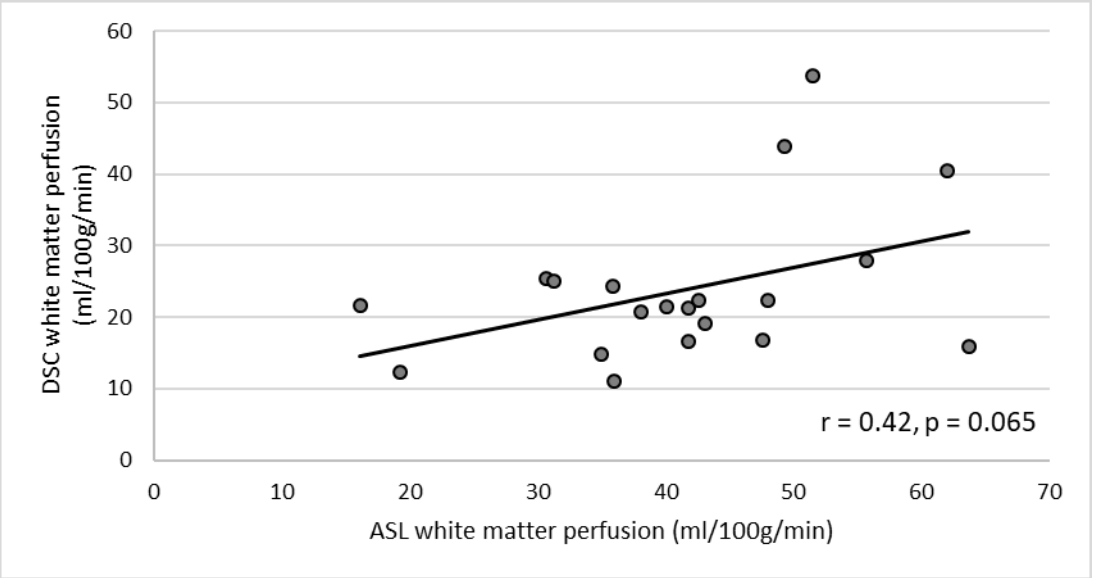


Figure 41 Correlation between mean WM CBF measurements using ASL and DSC in MS patients

3.5.4 White matter lesion perfusion

3.5.4.1 ASL vs DSC correlation

WMLs perfusion analysis was performed on the MS patients' data (n=19) comparing ASL and DSC. There was significant difference between the two techniques (ASL mean = 14.66 ml/100g/min (35% of mean WM CBF), DSC mean = 24.35 ml/100g/min (higher than mean WM CBF), p=0.011). There was negative correlation between the two techniques (r = -0.46). This finding confirms that ASL is not sensitive to measuring WM pathology.

3.5.5 Clinical data

3.5.5.1 ASL

In both MS group (n=20) and HCs (n=18) we observed a trend for old age to be associated with reduced perfusion (r=-0.18 and -0.37 respectively) but this lacked statistical significance (p=0.448 and 0.131 respectively) (Figure 42, Figure 43).

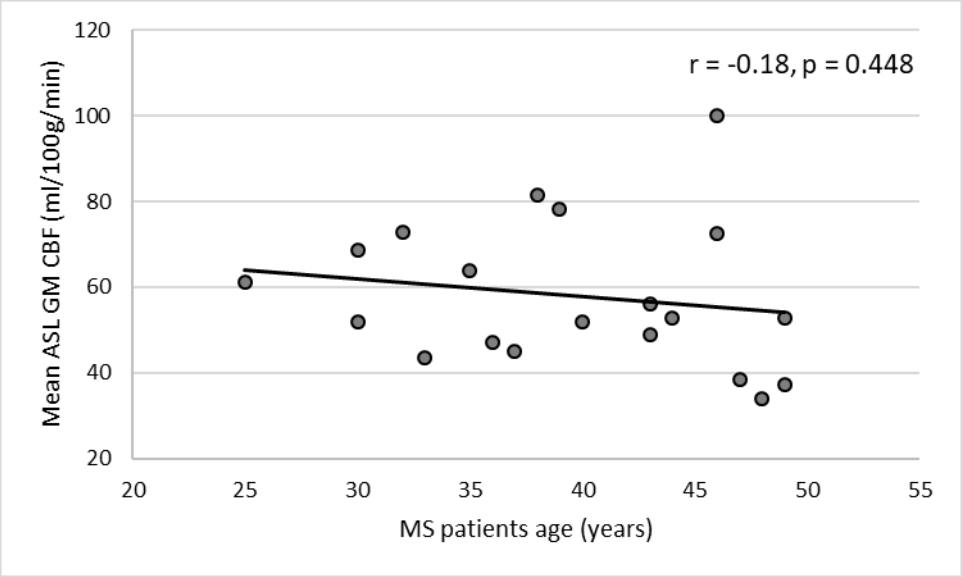


Figure 42 Correlation between age and ASL GM CBF in MS patients

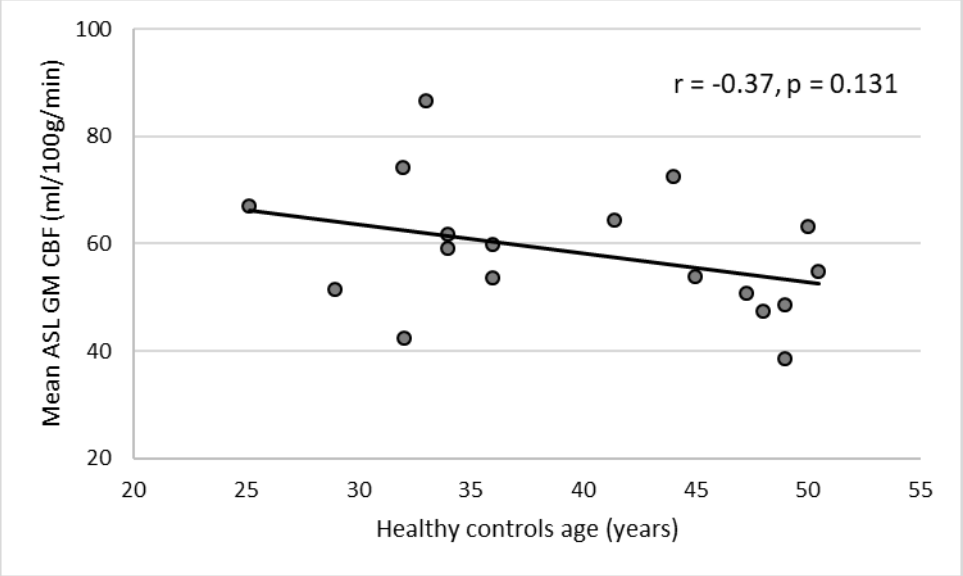


Figure 43 Correlation between age and ASL GM CBF in healthy controls

MS patients with longer disease duration (Figure 44) and higher EDSS (Figure 45) had more reduced GM CBF (r=-0.09 and -0.04 respectively) but this lacked statistical significance (p=0.706 and

0.867 respectively). Similarly, we couldn't find a correlation between fatigue scores (FSS and MFIS) and GM CBF; r=0.12 (p=0.614) and 0.2 (p=0.398) respectively.

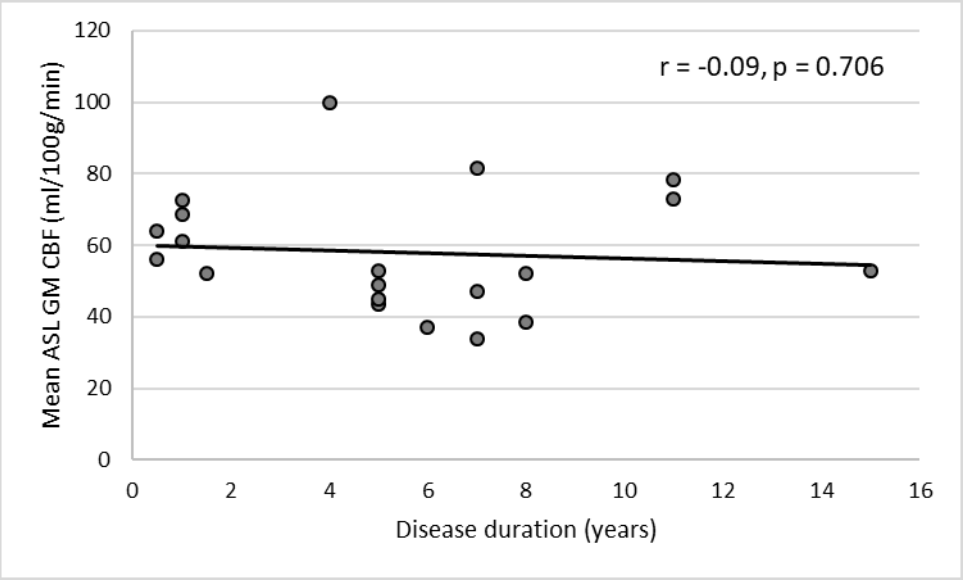


Figure 44 Correlation between disease duration and ASL GM CBF in MS patients

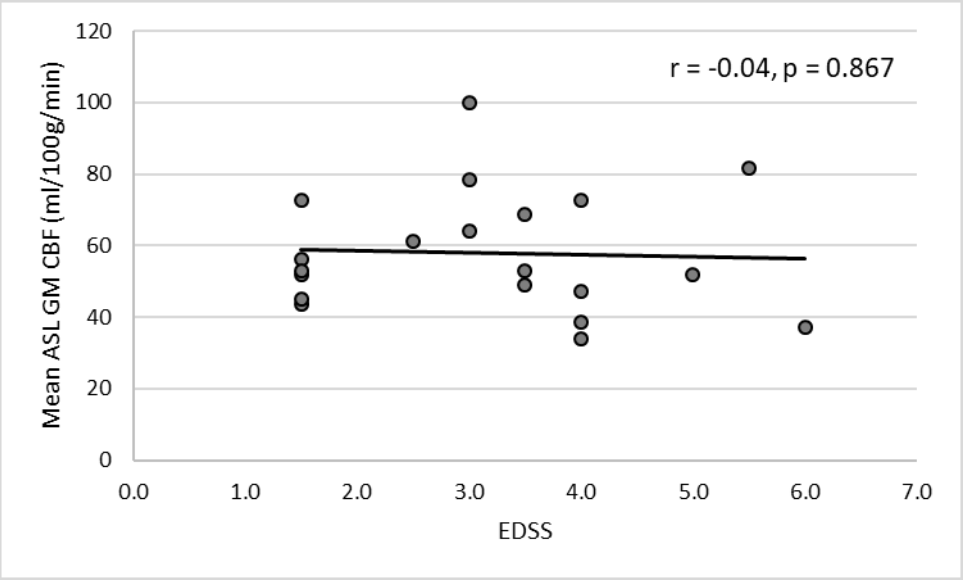


Figure 45 Correlation between EDSS and ASL GM CBF in MS patients

3.5.5.2 DSC

Significant correlation was found between patient's age and GM CBF (r=-0.45, p=0.046) (Figure 46). There was a trend for patients with longer disease duration (Figure 47) and higher EDSS (Figure 48) to have reduced GM CBF (r=-0.13 and -0.12 respectively) but this lacked statistical significance (p=0.585 and 0.614 respectively). There was a non-significant correlation between fatigue scores (FSS and MFIS) and GM CBF; r=-0.12 (p=0.614) and -0.07 (p=0.77) respectively.

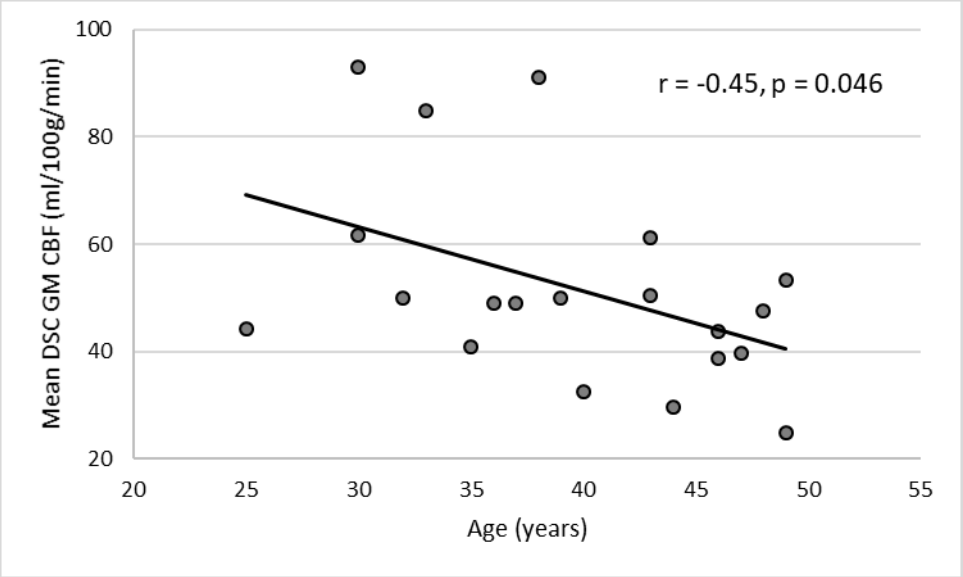


Figure 46 Correlation between age and DSC GM CBF in MS patients

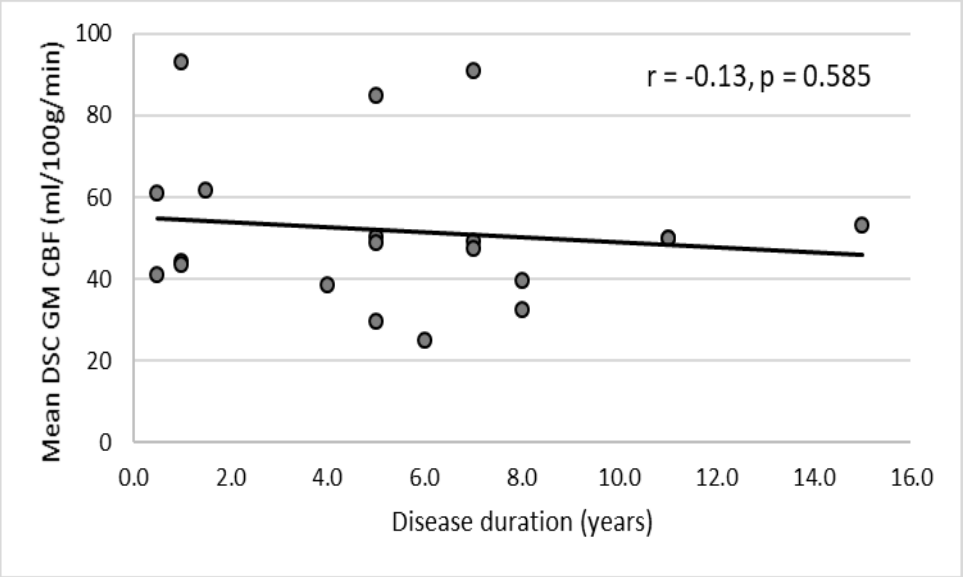


Figure 47 Correlation between disease duration and DSC GM CBF in MS patients

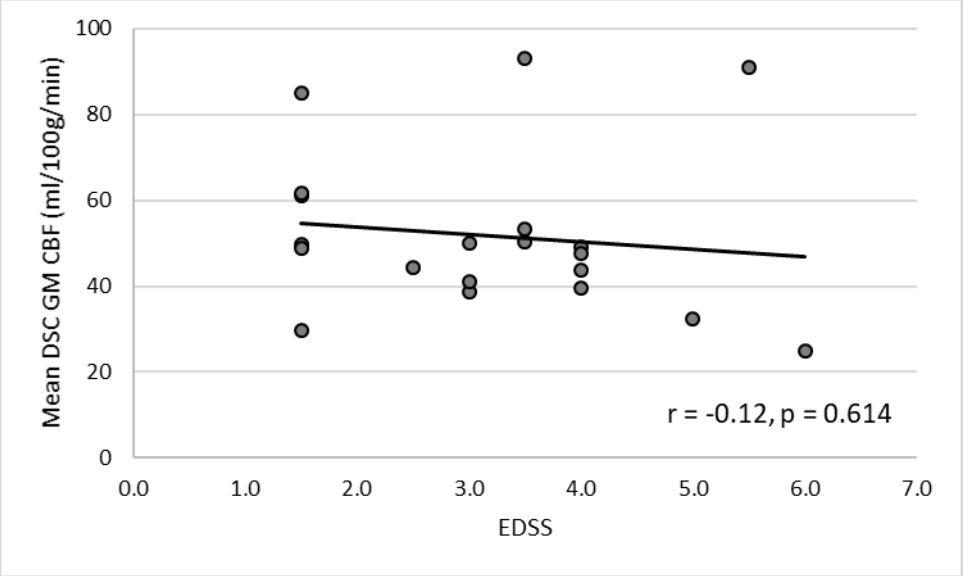


Figure 48 Correlation between EDSS and DSC GM CBF in MS patients

3.6 Discussion

GM perfusion can be quantified reproducibly using ASL at 7T in HCs and MS patients. The observed CoV for both cohorts (17.04% in MS group and 8.66% in HCs) is comparable with the variability reported in between-session whole brain perfusion (12.5-44.4%) using different ASL acquisitions; including PASL, pCASL, and CASL, at the lower field strength of 3T (Gevers et al. 2011).

We found significant correlation between ASL and DSC in measuring GM perfusion in MS patients ($r = 0.51$, $p = 0.031$). This indicates that ASL can play an important role in the future in studying and monitoring GM involvement in MS without need for contrast with all the known drawbacks related to long term use.

Studying vascular territories perfusion in MS is a new concept which we explored in this study. There is evidence of vascular reactivity changes in MS and we wanted to measure GM perfusion in the main vascular territories and assess the reproducibility of ASL in measuring individual vascular territories. The regional perfusion correlation was significant in HCs but not in MS patients. This is an interesting finding which needs to be considered in future studies looking into longitudinal regional changes in MS and how that correlate to clinical outcomes such as fatigue and cognition.

We assessed the correlation between ASL and DSC in measuring the mean CBF in each vascular territory. Majority of the

correlations observed were not significant. Further work is needed to investigate the reasons behind this difference.

WM perfusion, including WMLs, is low compared to GM, we confirmed in this study that ASL is less reliable in studying WM CBF compared to DSC due to low SNR and long transit time within WM (van Gelderen, de Zwart, and Duyn 2008).

We found no conclusive results when assessing the correlation between GM perfusion and clinical outcomes. To investigate this, a study involving a bigger cohort and more extensive cognitive assessments is needed.

The study has number of limitations which could be contributing to some of the results. Theoretically, MS as a disease affects brain blood flow in different ways; it is an immune mediated condition with cellular and vascular pathophysiological consequences that are dynamic and sometimes progressive. These factors are difficult to account for when studying perfusion longitudinally; it is impossible to disentangle perfusion measurement variability from disease induced variability. This may explain the higher CoV in the MS group compared to HCs.

Our study, similar to the available literature, did not account for age effect on perfusion data variability. It is known that global GM CBF declines by about 7-9% per decade of age (Liu et al. 2012).

The effect of MS treatments on perfusion is unknown; most of the MS patients in our study were taking different DMT drugs for

variable duration. This can be addressed by studying groups of treated and untreated cohorts.

Measuring fatigue using questionnaires as a marker of cognition carries risk of subjectivity as patients report fatigue and its effect on their life differently. More robust and formal cognitive assessments are required to assess correlation between cerebral perfusion and cognition. One study found that Multidimensional Fatigue Inventory reduced motivation score was significantly correlated with deep GM CBF in 22 MS patients; $r=0.4$, $p<0.001$ (Inglese et al. 2007).

ASL and DSC differ in the way perfusion is measured using both methods, this could limit the ability to do direct comparisons using absolute CBF values. Using relative CBF between region of interest and global brain perfusion could be tried as an alternative approach (not addressed in this study). We identified few outliers when we did our correlation measurements, these were removed from the analysis due to the significant impact on the results (the small number of participants was another factor that contributed to this impact). Further work is in progress to clarify the reason behind the results of the outliers.

GM perfusion maps contained some voxels with very high values likely caused by vascular contamination; we have not found a reliable answer in literature on how to account for this. We used a method of plotting two Gaussian curves on the histograms and

used the lower mean as a comparable parameter between scanning sessions and techniques. Interestingly, there is no clear unified method in the literature on how to address this issue.

Clinical scanners in daily practice use field strength of 1.5T and 3T, translating what we learn from using ultra-high-field ASL-MRI by developing the technique to be applied at lower field strength or direct comparison between the 3T and 7T would be very beneficial for transforming ASL into a clinically useful imaging method.

Chapter 4: Arterial Spin Labeling MRI in Reversible Cerebral Vasoconstriction Syndrome: Longitudinal perfusion study

4.1 Introduction

Thunderclap headache is one of the most common emergency neurological presentations in secondary care settings (Mortimer et al. 2013) with the majority of patients requiring urgent investigations to rule out secondary headache causes such as SAH. Recurrent thunderclap headache is a less common presentation; one study reported recurrence in 24% of patients with non-SAH thunderclap headache (Landtblom et al. 2002). Even though headache recurrence usually indicates a more benign cause, healthcare professionals' vigilance often leads to an extensive investigative approach which commonly results in prolonged hospital stay.

Cheng et al. reported that nearly half of thunderclap headache cases are diagnosed with RCVS (Cheng, Kuo, and Lai 2014). RCVS is a group of conditions characterised by prolonged but reversible multifocal narrowing of the cerebral arteries (Calabrese, Dodick, et al. 2007). It presents typically as acute severe headache, usually recurrent and thunderclap in character, with or without additional symptoms and signs (Ducros et al. 2007). The prognosis of RCVS

is fortunately good; it follows a monophasic self-limiting course in majority of cases (Miller et al. 2015a).

Minority of patients develop adverse complications associated with RCVS, these have been reported more frequently in the postpartum period and can lead to devastating consequences especially if not recognised early. Depending on the degree of vasoconstriction, RCVS may be associated with cortical SAH (in one third of patients), ischaemic infarction (6-39% of patients), concomitant PRES (9-38% of patients), and up to 10% risk of death (Miller et al. 2015a). RCVS may also present as parenchymal brain haemorrhage in 20% of cases (Bernard and Rivera 2015). The data on complication rates highlight the uncertainty about the condition and indicate a need for more research to better characterise the evolution of the pathology. In this chapter, we seek to address this need in a prospective, longitudinal imaging study.

The hallmark of RCVS is vasoconstriction seen on vascular imaging scans, which typically reverses within 3 months. Prevalence of radiological vasoconstriction seen on MRA in RCVS is reported to be between 60-90% and typically appears as diffuse segmental constriction of large and medium sized vessels lasting 4-12 weeks (Sattar, Manousakis, and Jensen 2010, Lee, Ramadan, and Bamford 2013, Calic, Cappelen-Smith, and Zagami 2015). The main advantage of MRA is that it can be performed without the use

of a radioactive tracer, thus providing a safe method for repeat observations of vascular pathology. Imaging is often negative in first 4-5 days following the onset of headache (Mortimer et al. 2013); the mean time to detect abnormality on vascular imaging has been reported as 8 days after headache onset (Bernard and Rivera 2015). RCVS symptoms usually resolve by 1 month after presentation (Ducros et al. 2007), however the adverse complications associated with RCVS may have lasting consequences as described above. In addition to identifying and monitoring vasoconstriction using MRA acquisitions, MRI is an excellent tool for characterising brain changes during the progression and resolution of RCVS. Standard structural images can identify complications of RCVS, such as bleeding, ischaemia, and PRES (Lee, Ramadan, and Bamford 2013, Dilli 2014).

ASL MRI can be used to non-invasively quantify perfusion of brain tissue, providing a measure of the impact of upstream arterial vasoconstriction on local cortical regions (Miller et al. 2015b).

Cortical perfusion has not yet been extensively studied in RCVS; at time of writing, only two case reports have been published. Rosenbloom and Singhal reported a case of RCVS induced by carotid endarterectomy following a frontal lobe ischaemic stroke. Perfusion MRI showed unilateral hypo-perfusion, mainly affecting internal watershed areas with superficial cortical regions being relatively spared (Rosenbloom and Singhal 2007). In a second

study, ASL-MRI was performed on a 50-year-old man with RCVS who presented with severe recurrent headaches and neurological deficits (localising to the right hemisphere). ASL-MRI demonstrated significant hypo-perfusion in the right parieto-occipital lobe, but no infarct was seen on diffusion imaging. At 12 weeks, there was complete resolution of cerebral vasoconstriction on angiography and normal perfusion findings on ASL-MRI (Komatsu et al. 2014). These case studies suggest that perfusion MRI can offer an additional tool to confirm and understand RCVS. ASL-MRI is a non-invasive, radiation and contrast-free technique that can be performed at multiple time points to monitor changes in perfusion over the time period of RCVS resolution and assess response to potential therapeutics.

One of the disadvantages of ASL-MRI is low SNR, this can be improved by using high-field MRI at 3T. In addition, 3T MRI can facilitate improved spatial resolution. Applying advanced non-invasive MRI techniques in this study will be a significant advantage as we investigate RCVS, understand the pathophysiology, and assess brain perfusion in multiple time points.

This a pilot feasibility study aims to quantify perfusion, assess arterial vasoconstriction, and confirm reversibility using 3T ASL-MRI and MRA in 4 patients with suspected RCVS. Acquiring these data at multiple time points during RCVS progression, we will

assess the relationship between vasoconstriction and downstream perfusion and determine the role of these imaging techniques in early and accurate diagnosis of RCVS. We also aim to investigate whether early imaging abnormalities can predict RCVS complications and clinical outcomes.

4.2 Objectives

Primary objective: Is perfusion MRI abnormal in suspected RCVS cases (target recruitment number = 10) and does it correlate with vascular changes on MRA?

Secondary objectives:

1- Does early imaging (within a few days of headache onset) detect perfusion deficits in the absence of vasoconstriction?

2- Can RCVS patients with complications be predicted based on early MRA and perfusion studies?

3- Does headache severity, frequency, and duration correlate with imaging changes?

4.3 Endpoints

Primary endpoint

Regional brain blood flow changes at three time points as measured by perfusion MRI and degree of blood vessel constriction on MRA

Secondary endpoints

1- Longitudinal correlation between blood flow changes and arterial vasoconstriction

2- Correlation between initial radiological observations and development of complications due to RCVS

4.4 Eligibility criteria

Inclusion criteria:

1- Male or female patients aged 18-60 years old

2- Able to give informed written consent

3- Clinical presentation suggestive of RCVS

4- Able to understand the requirements of the study, including anonymous publication, and agree to co-operate with the study procedures

Exclusion criteria:

1- Evidence of brain haemorrhage or significant brain pathology on CT scan

2- Any history of significant cerebrovascular disease

3- Pregnancy or breastfeeding

4- MRI contraindications (e.g. metal implants or pacemaker)

5- Significant claustrophobia

4.5 Methods

A prospective, longitudinal, observational, pilot study on 4 patients with suspected RCVS recruited from acute medical unit and neurology clinics at Queen's Medical Centre. Written informed consent was obtained from all patients and the study was approved by the West Midlands–Solihull Research Ethics Committee.

All patients were men, aged 22-51 years, presented with recurrent thunderclap headache, frequency of 2-5 attacks within 1-2 weeks, triggered by coitus or exercise. None of the patients were on medications or recreational drugs. Two patients were regular smokers. All patients underwent investigations to rule out significant intracranial events such as intracranial haemorrhage or ischaemia. Patients characteristics and clinical data is summarised in

Table 8.

Table 8 RCVS study patients' clinical data

	Participant 1	Participant 2	Participant 3	Participant 4
Age (years)	24	36	22	51
Sex	Male	Male	Male	Male
Smoking history	No	No	Yes	Yes
Drugs	No	No	No	No
Headache history	No	No	No	No
Headache trigger	Coital	Coital and exercise induced	Coital	Coital
Attacks frequency	2	3	5	2
Significant CT findings	No	No	No	No
Lumbar puncture	Normal	Mildly raised protein	Normal	Normal
Headache at 1 month (trigger)	Episodic mild dull headache (none)	Episodic mild dull headache (none)	Unknown	No
Headache at 3 months	No	No	Unknown	No

MRI acquisition:

Patients were scanned during the acute phase and at two follow-up timepoints using the 3T Philips Ingenia MRI scanner and 32-channel head-coil at SPMIC, University of Nottingham. The "acute" scan was performed between day 6 and day 14 after the headache onset, we expected this to be the best window to identify RCVS related vascular changes (Mortimer et al. 2013). To assess progression and reversibility, two further scans were performed at two later time-points: between weeks 4 and 5 after onset and between weeks 13 and 14 (Figure 49).

All MRI sessions included high-resolution time-of-flight MRA scan to characterize potential vasoconstriction (TR=23 ms; TE=3.5 ms; flip angle = 18°; Field of View (FOV) = 200 x 200 x 140 mm^3; resolution = 0.39 x 0.39 x 0.6 mm^3; SENSE (RL) = 2.5; 6 chunks, descending, 23.4 mm thick). Additional clinical scans were

collected to identify bleeding or tissue damage, as well as facilitate image co-registration across the multiple sessions:

- Magnetization Prepared Rapid Acquisition Gradient Echo (MPRAGE) - High-resolution T1-weighted scan to facilitate co-registration of images across sessions and with atlas templates of vascular territory locations
    - FOV: 256 x 256 x 162 mm^3
    - Resolution: 1.0 x 1.0 x 1.0 mm^3
    - Acquisition time: 3 min 44 sec
- FLAIR - improved visualization of brain tissue integrity due to nulling of signal from CSF
    - 3D acquisition
    - FOV: 250 x 229 x 165 mm^3
    - Resolution: 0.7 x 0.7 x 3 mm^3
    - Acquisition time: 5 min 2 sec
- DWI (Diffusion weighted imaging) - assessing diffusion of protons in 3 directions to characterize tissue microstructure
    - b-value = 0, 1000 s/mm^2
    - FOV: 230 x 230 x 119 mm^3
    - Resolution: 1.2 x 1.2 x 5.0 mm^3
    - Acquisition time: 46 sec
- SWI - a T2*-weighted image to highlight venous structures and microbleeds
    - TE = 52.7 ms

- FOV: 230 x 180 x 100 mm^3
- Resolution: 0.53 x 0.53 x 1.0 mm^3
- Acquisition time: 4 min 22 sec

To measure perfusion, a multi-PLD ASL-MRI acquisition was performed. By acquiring ASL MRI data at multiple PLDs, a kinetic model can be applied to measure changes in both vascular transit times and tissue perfusion. Although this approach requires much longer scan times due to repeating the ASL acquisition at each PLD, it is important to differentiate these two effects which may both contribute to RCVS pathology. Using the Philips product sequence, a pCASL labeling strategy was combined with a gradient-echo EPI image read-out approach (TR = 4500 ms; TE = 16 ms; flip angle = 90°; FOV = 240 x 240 x 80 mm^3; 16 ascending slices, image resolution = 1.88 x 1.88 x 5.0 mm^3; no background suppression; SENSE (AP) = 2.3). The labeling plane was positioned to orthogonally transect the carotid and vertebral arteries, and the positioning was carefully recorded in the first scan session to guide the accurate reproduction of this placement in the follow-up scans. The labeling duration was set to 1800 ms, in line with the ASL white-paper recommendations (Alsop et al. 2015). Seven pCASL scans were acquired at PLD = 300, 600, 900, 1200, 1500, 1800, and 2000 ms. Each scan contained 12 control-label image pairs, except for the PLD=1800 ms acquisition which contained 24 image

pairs to improve SNR. An M_0 calibration image was also acquired using identical acquisition parameters but a prolonged TR=8 s.

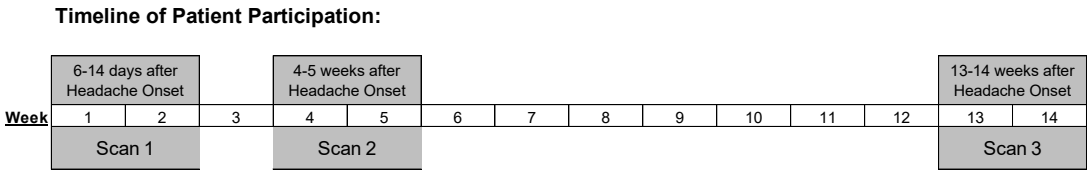


Figure 49 RCVS study participation timeline

Data analysis:

Data were pre-processed by Prof. Molly Bright (Northwestern University). Clinical scans were assessed by Dr Robert Dineen, an expert radiologist and Clinical Associate Professor of Neuroimaging at the University of Nottingham.

Each image of each ASL MRI scan (acquired at different PLDs) were aligned to the M_0 calibration scan, correcting for head movement during and between scans. Perfusion-weighted data were calculated by performing surround-subtraction of the control-label image pairs. Outliers were rejected using the algorithm of Tan et al. (Tan et al. 2009) and the mean perfusion-weighted image was calculated for each PLD. Brain extraction was performed, and the results were input into the Oxford ASL software package (FSL, Oxford, UK; (Chappell et al. 2009). This software invokes a

Variational Bayes method for estimating arterial arrival time and tissue perfusion from the multi-PLD perfusion-weighted images.

The MPRAGE images were analysed using FSL BET to remove the skull from the brain image (Smith 2002) and FSL FAST to segment the brain and extract the GM mask (Zhang, Brady, and Smith 2001). An image representing the cortical vascular territories was adopted from Mutsaerts et al. study (Mutsaerts et al., 2015). Each vascular territory image and the GM masks were registered into ASL space using FSL FLIRT (Jenkinson et al. 2002) and the images were multiplied by each other to produce cortical GM vascular territory masks for each individual and scan session.

4.6 Results

Recruitment for the study took place between March and November 2017. Despite best efforts we were only able to recruit four participants (six patients were approached in total). Participant 3 attended only the first visit and was not keen to attend further visits. Unfortunately, we experienced problems with the signal intensity scaling due to a scanner software upgrade during the study period; it was not possible to compare absolute CBF measures across scan sessions.

4.6.1 Anatomical data

Standard MRI sequences showed no significant abnormality apart from a small incidental arachnoid cyst in one participant and few non-specific WM hyperintensities in another. Table 9 summarises the MRA scans findings. Examples of the MRA results are shown in Figure 50 to Figure 54 (all were approved by an experienced radiologist).

Table 9 MRA scans findings

Patient	*Visit 1*	*Visit 2*	*Visit 3*
01	Narrowing of left ACA at A1 and A4, and right ACA at A3 and A4 segments	Normal	Normal
02	Narrowing of right MCA at distal M1 segment and in the basilar artery	Normal	Normal
03	Normal	NA	NA
04	Normal	Normal	Normal

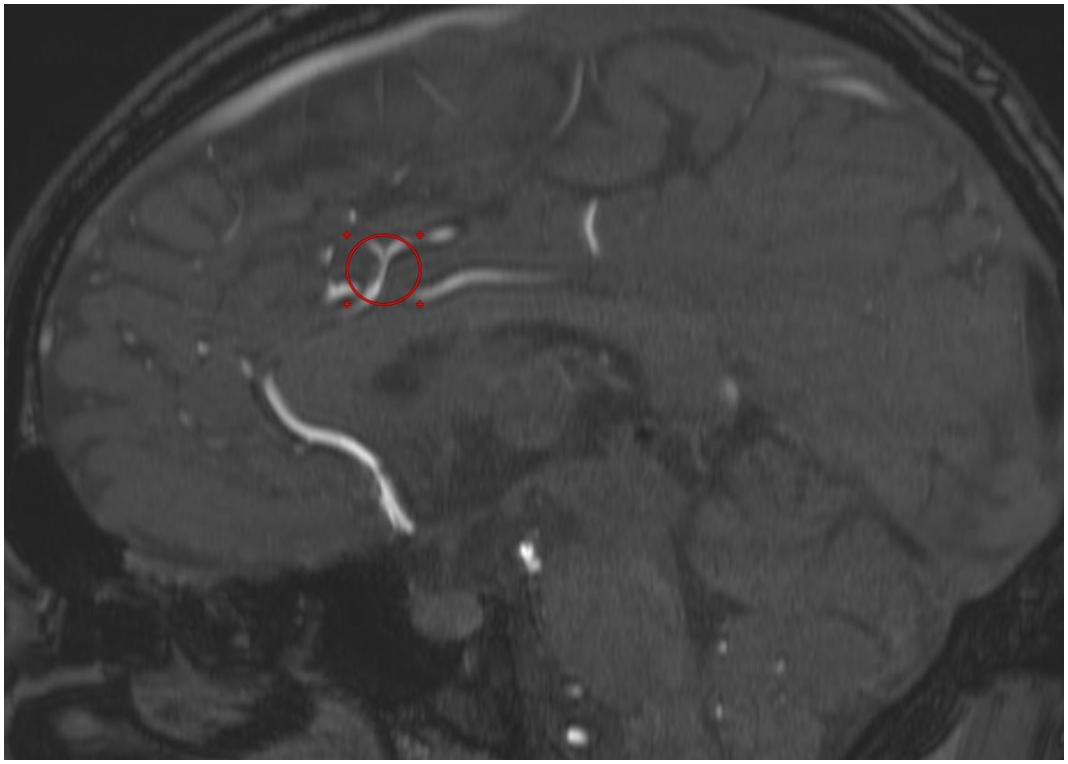


Figure 50 Distal narrowing in the left anterior cerebral artery (participant 1, visit 1)

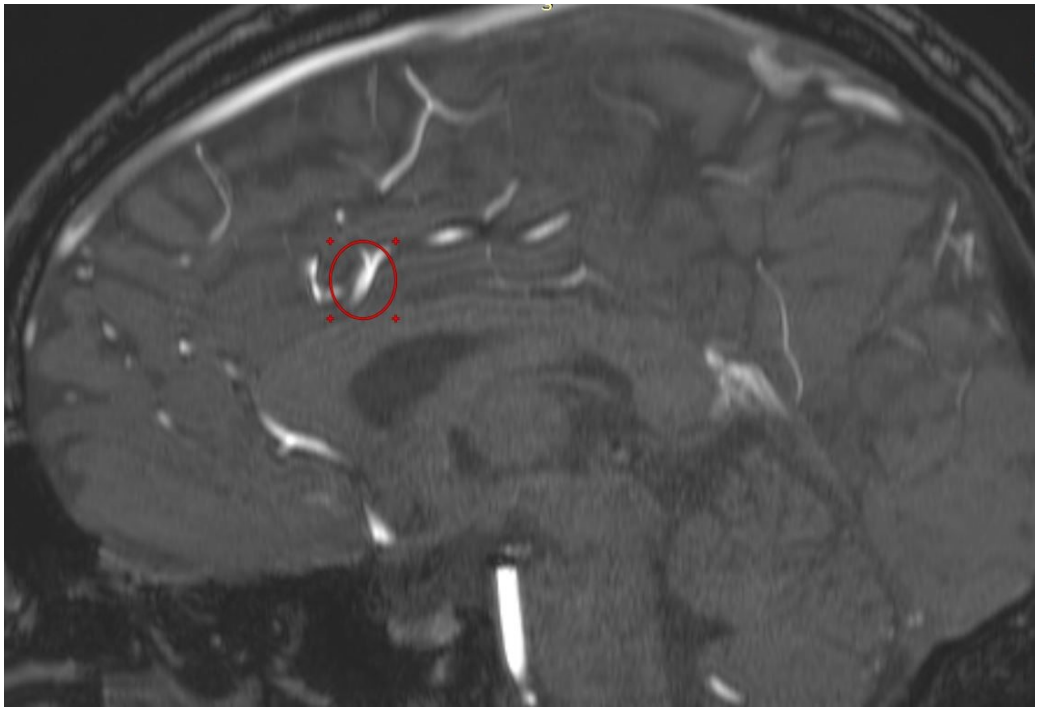


Figure 51 Resolution of the left anterior cerebral artery narrowing (participant 1, visit 2)

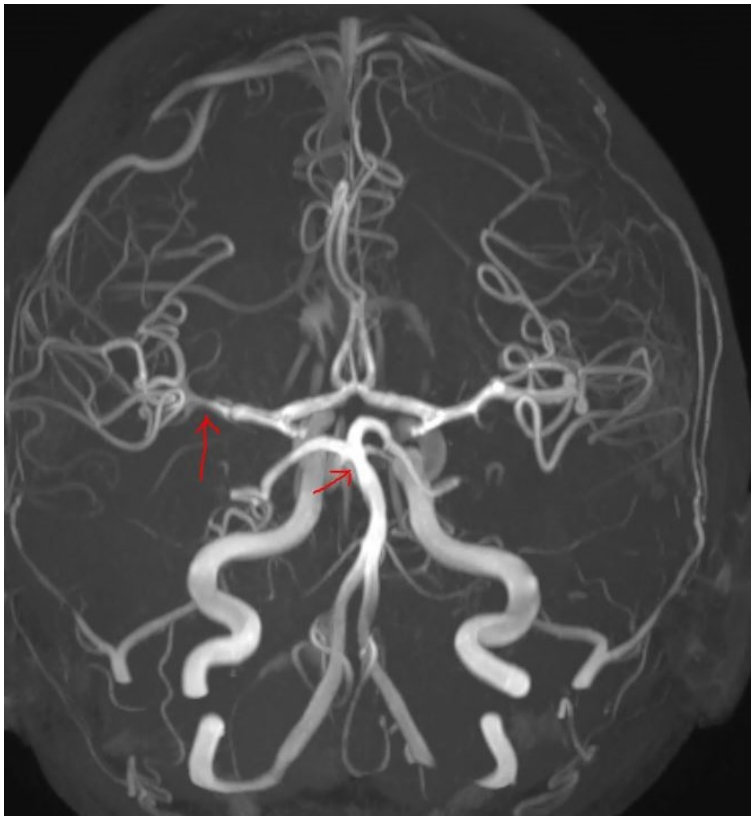


Figure 52 Narrowing of the right middle cerebral and basilar arteries (participant 2, visit 1)

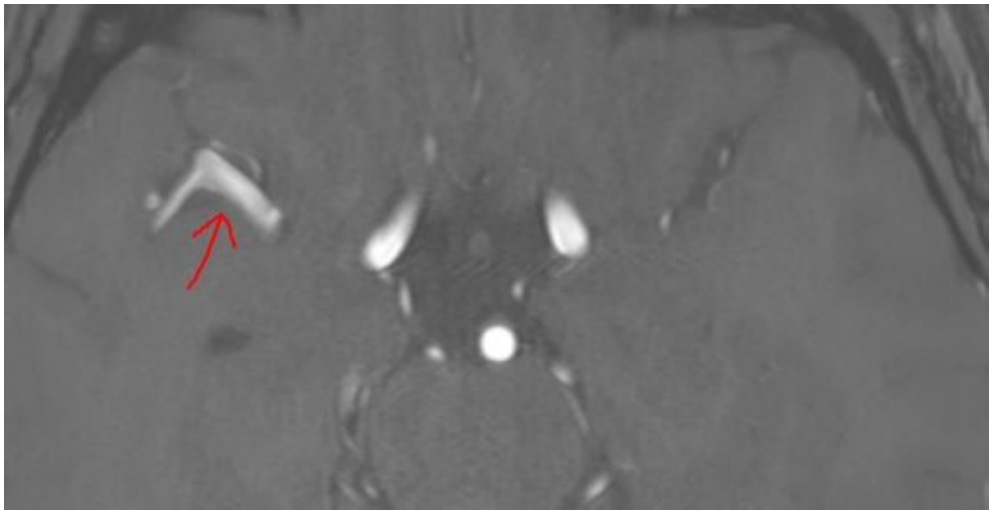


Figure 53 Resolution of the right middle cerebral artery narrowing (participant 2, visit 2)

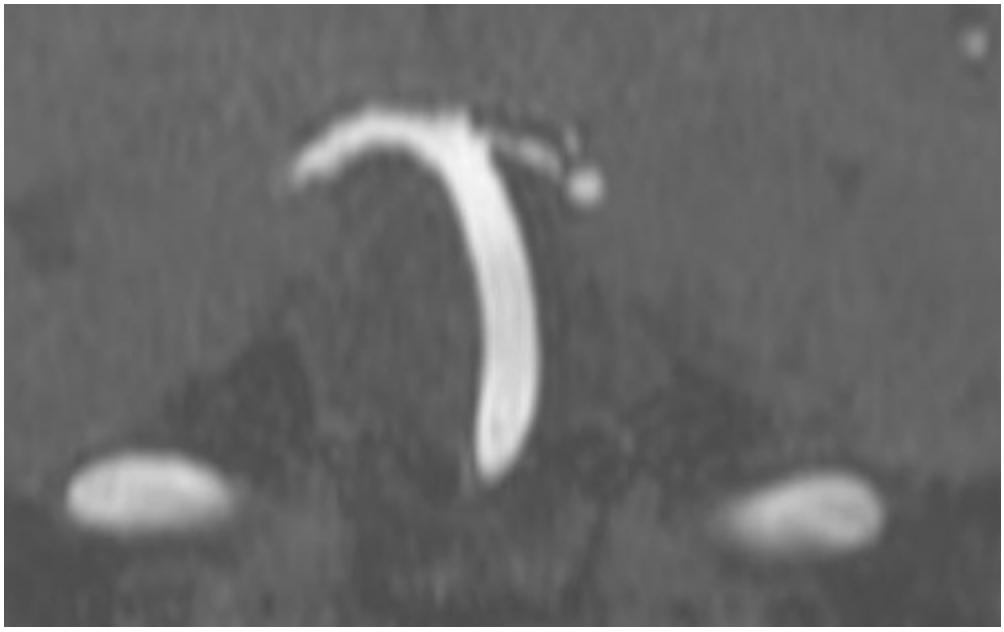


Figure 54 Resolution of the basilar artery narrowing (participant 2, visit 2)

4.6.2 Perfusion data

Data from the only visit of participant 3 were not analysed given that the MRA was normal and we had no longitudinal data. Perfusion data from the last visit of participant 4 was not suitable for analysis due to the scanner upgrade that altered the ASL scan sequence and changed how data were saved, so it was not possible to analyse the data in the same way.

Absolute CBF is the ideal parameter to measure regional differences in perfusion between sessions. Unfortunately, during the study there was an upgrade in the scanner software which resulted in non-comparable results between scanning sessions. We used relative cerebral blood flow (rCBF) to measure regional perfusion differences. Two approaches were considered for

calculating rCBF, using the global GM perfusion value or a specific vascular territory GM perfusion value to normalize the whole-brain maps. Global GM perfusion is a common reference for calculating rCBF maps, but it will be inherently influenced by the presence or absence of vasoconstriction in any of the arterial vessels. This may make it less suitable for assessing changes in areas of expected pathology. Alternatively, no vasoconstriction was observed in the left MCA territory in any of our patient data, and therefore the perfusion of this region should be minimally affected by any RCVS pathology. Although this approach is not seen directly in the literature, it may be a more appropriate method for estimating rCBF in our cohort. Both methods for extracting rCBF maps from the multi-PLD ASL MRI data were considered.

When using global GM perfusion values to normalize the data, the affected vascular territories in participant 1 (defined by vasoconstriction on the MRA) showed marginally higher average rCBF, and this did increase by 5-10% in subsequent visits (Figure 55). Left MCA was not shown to be abnormal on MRA, however the territory changes were similar to affected regions. Similarly, in participant 2 no specific pattern was seen in affected regions compared to normal ones (Figure 56). Results of Participant 4 with normal MRA are shown in Figure 57.

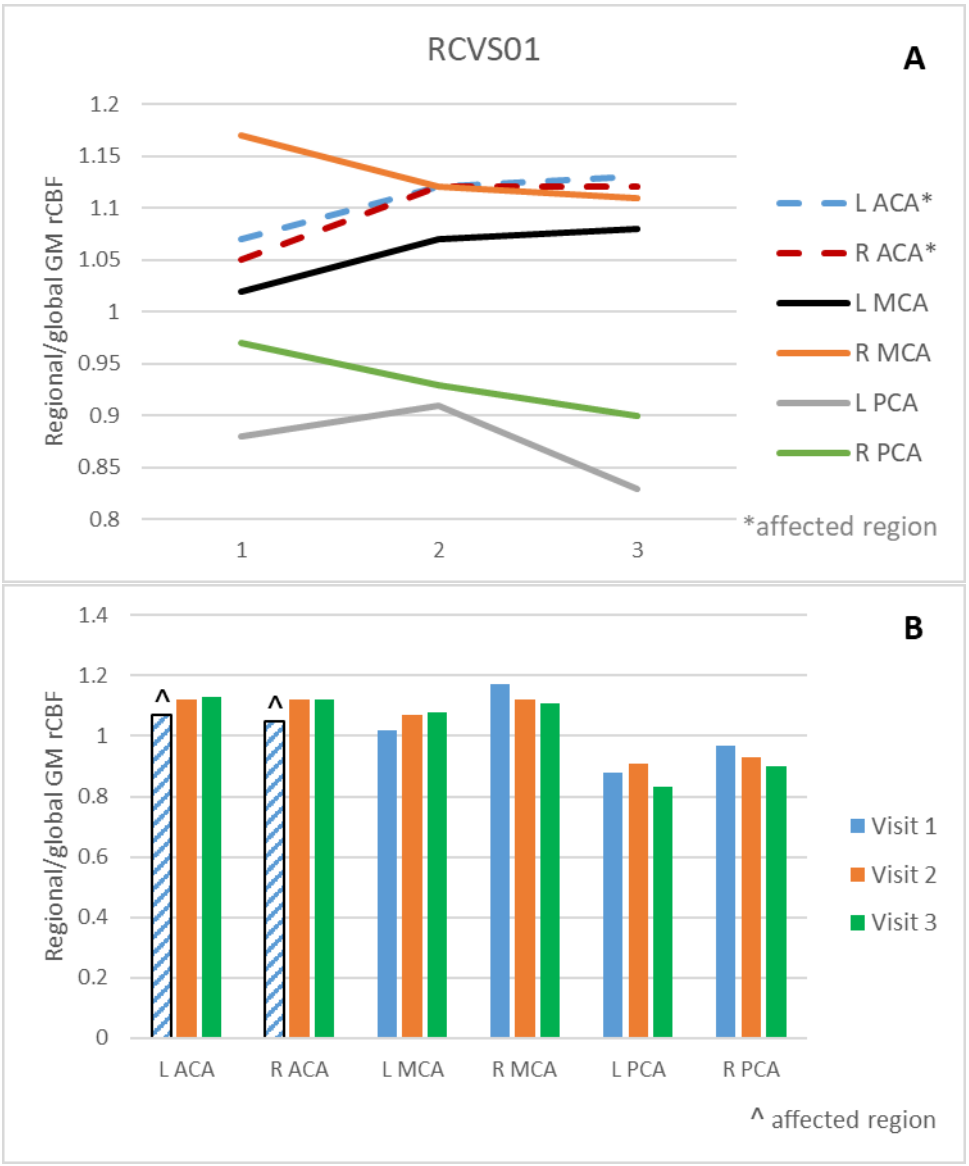


Figure 55 Participant 1 regional/global GM rCBF across visits

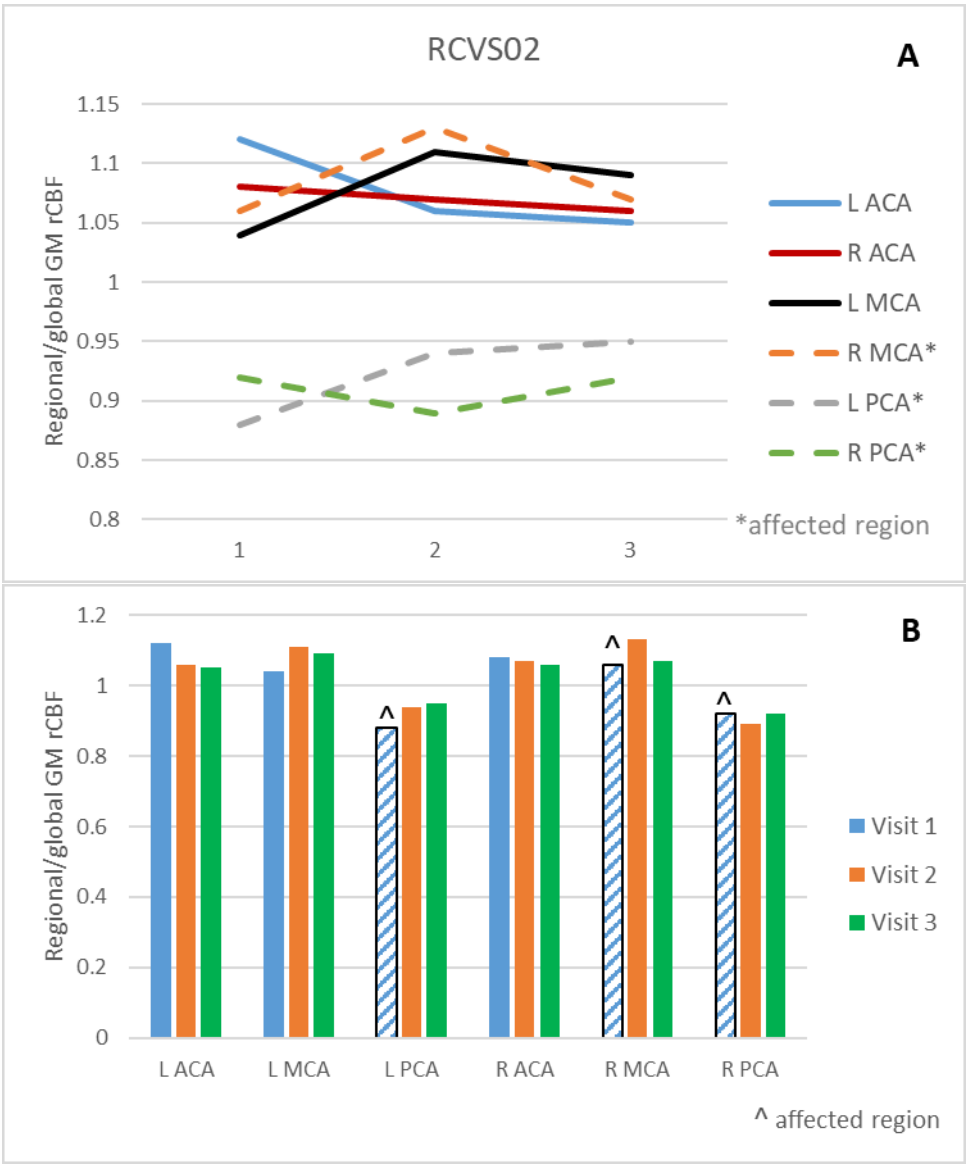


Figure 56 Participant 2 regional/global GM rCBF across visits

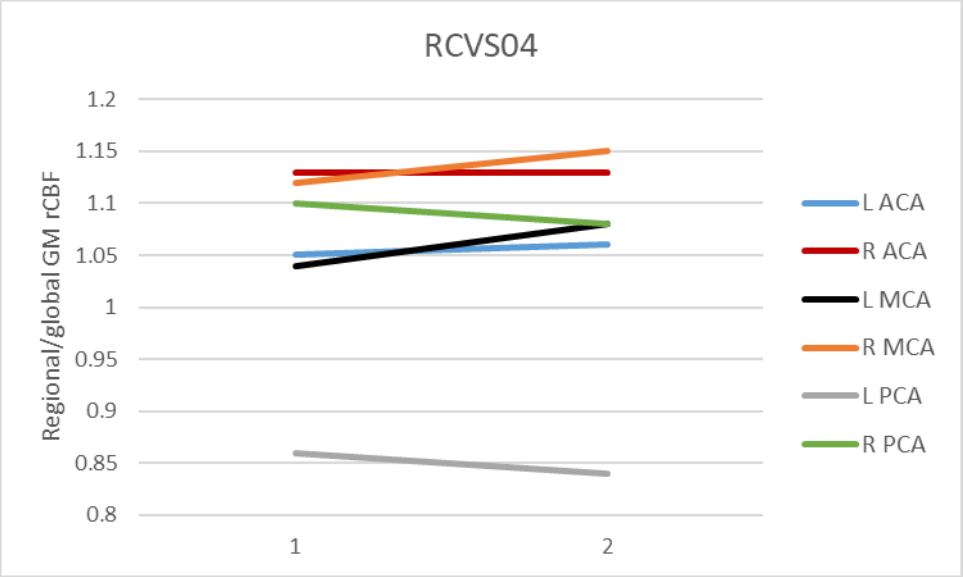


Figure 57 Participant 4 regional/global GM rCBF across visits

When the perfusion within the left MCA territory was used as a reference region to calculate rCBF, participant 1 (Figure 58) and 2 (Figure 59) results did not show a specific pattern apart from less fluctuation between visits compared to the first analysis. Participant 4 data are shown in (Figure 60).

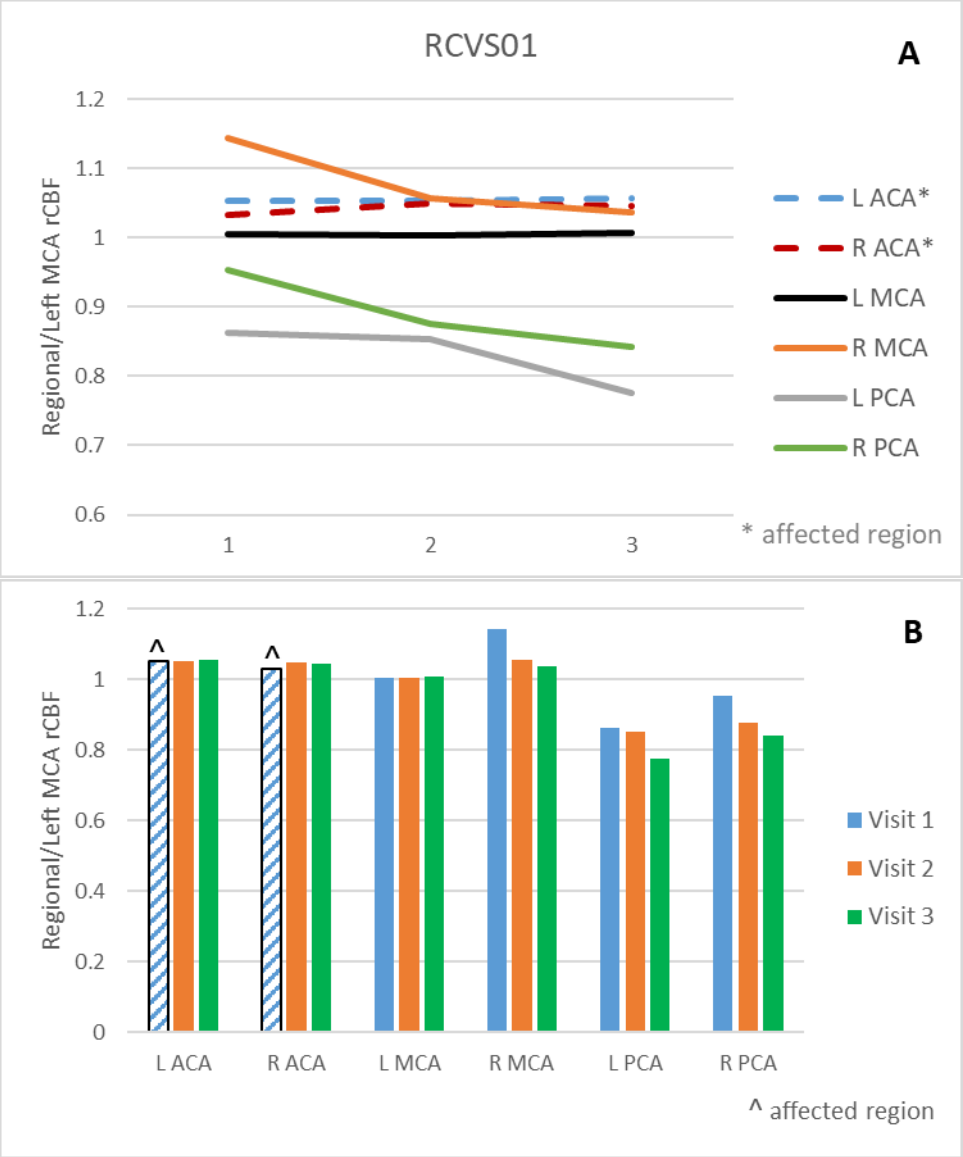


Figure 58 Participant 1 regional/left MCA rCBF across visits

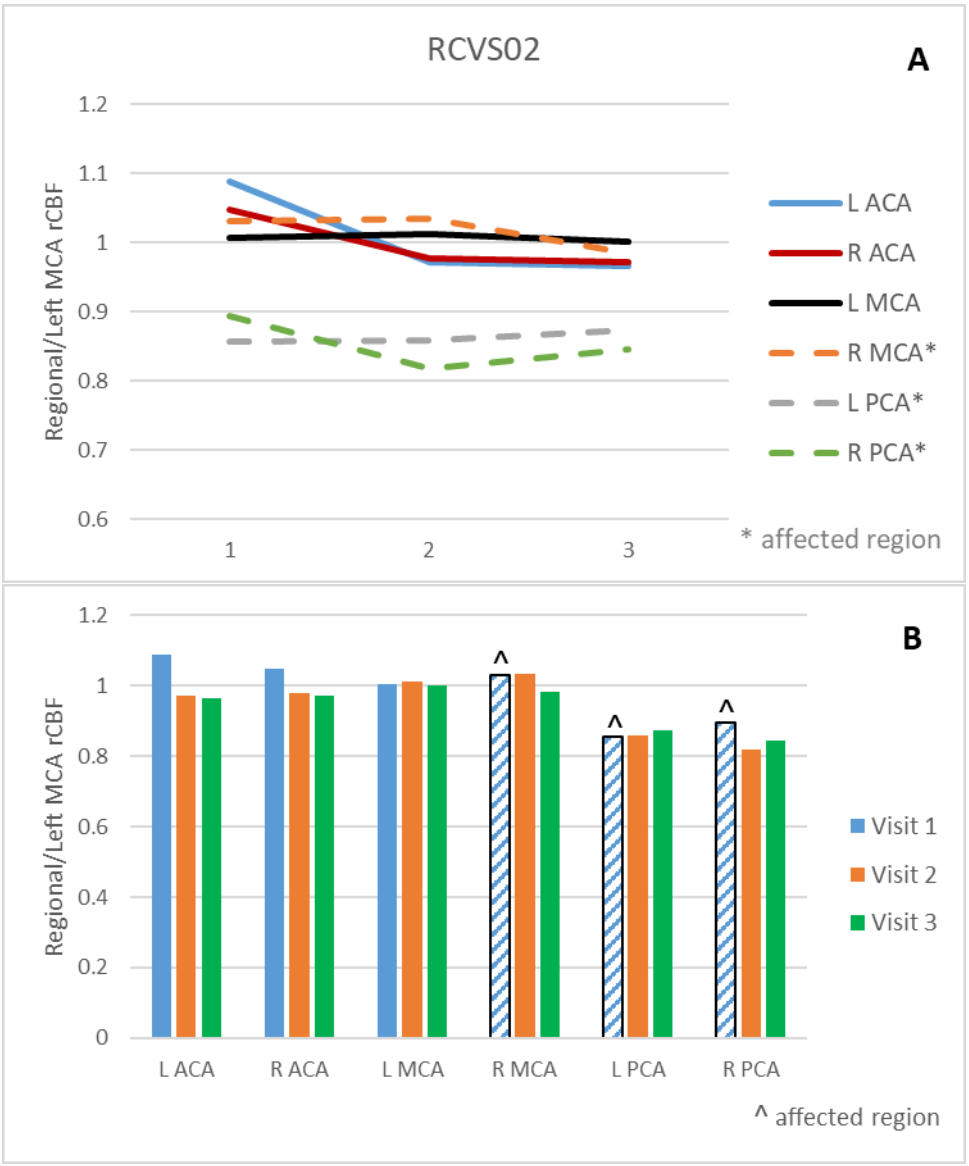


Figure 59 Participant 2 regional/left MCA rCBF across visits

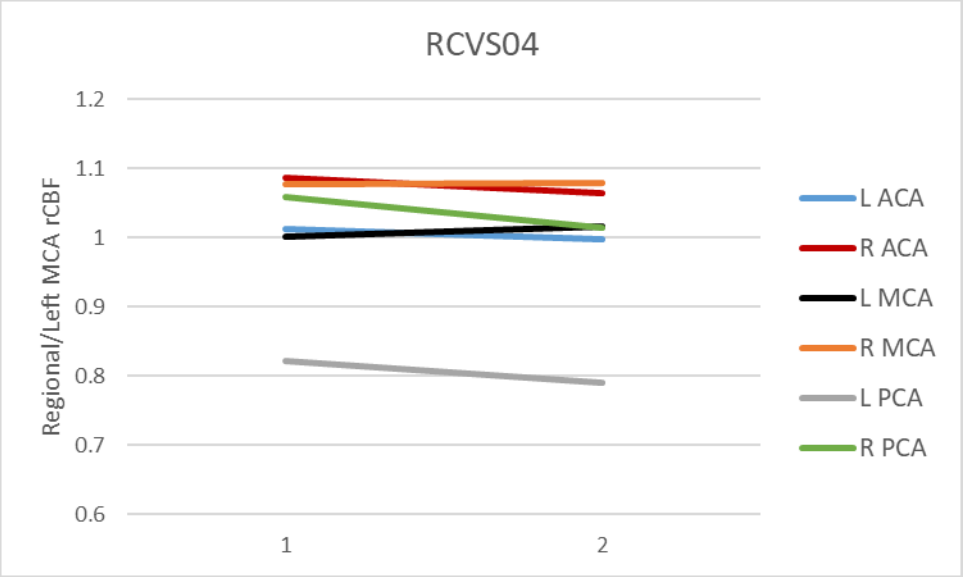


Figure 60 Participant 4 regional/left MCA rCBF across visits

4.7 Discussion

This is the first study to date looking into the longitudinal use of perfusion MRI in monitoring patients with suspected RCVS. Furthermore, the use of ASL MRI to characterize perfusion is an optimal choice for longitudinal studies, due to the lack of injected intravascular contrast agent.

The four participants recruited to this study presented with typical history of RCVS. Two out of four patients had changes on MRA suggestive of vasoconstriction. All participants had a benign course and developed no complications. The MRA changes seen in the two confirmed cases were reversible as confirmed by month 1 scans. However, the perfusion data did not correlate well with the anatomical scans' findings, irrespective of our choice of reference region for calculating rCBF maps.

The study has significant limitations which could be contributing to the negative perfusion results. The scanner software upgrade during the study affected the image quality and consistency across scan sessions, and ultimately lead to inconsistencies in the perfusion data across visits. I believe this demonstrated well the challenges with collecting longitudinal data. Absolute CBF quantification is the parameter of choice to compare regional differences, however due to the upgrade issue we had to use rCBF between affected territories and a normal appearing region. The global GM CBF can be affected by extreme values in different regions hence the choice of using left MCA territory as a reference region in the second analysis. This approach did not alter the study findings and could well cause confusion if used as a routine method in clinical practice. RCVS changes on MRA were not widespread and given that we measured average CBF in each territory, it is plausible that the perfusion changes were not significant enough to affect the mean CBF in the corresponding territory. Using qualitative ASL data in the form of scaled coloured maps can be helpful to visualise the abnormal areas in patients with significant ischaemia secondary to RCVS, however our participants showed no obvious reduced perfusion caused by the observed vasoconstriction.

There are potential errors related to the MRA figures (50-54); flow may alter the sequence depending on the readout direction relative to the flow which in turn could result in artificial signal loss.

Further work needs to look into addressing the limitations and difficulties we faced in our study. ASL-MRI has advantages, being a contrast free technique, can be added to standard MRI sequences to aid diagnosis, monitoring, and prognosis in suspected RCVS cases. However, for the technique to be reliable, there is need to ensure a more stable MRI scanner system. Considering the time scale of RCVS symptoms, it is important to establish the 1-month and 3-month reproducibility or variation of normal human perfusion values, so we can better gauge if the changes seen are related to RCVS or just normal variation. Variability of repeated cerebral perfusion measurements using ASL of up to 20% is considered normal in healthy individuals (Gevers et al. 2011). Considering the possibility that majority of suspected RCVS patients have normal perfusion, as in our cohort, future studies will need to be larger than this study to potentially detect subclinical reduced perfusion with or without complications. Recruitment for a future study can be improved by longer recruitment duration and potentially a multi-centre collaboration.

Chapter 5: Conclusion

This thesis has examined the use of ASL as an evolving MRI technique to measure cerebral perfusion. Although contrast-MRI remains the gold standard method, it is not feasible to perform longitudinal studies in view of the risk of contrast accumulation in the brain and other parts of the body. ASL does not require exogenous contrast and instead uses tagged blood as an endogenous tracer.

5.1 ASL in MS

ASL use in MS research studies started around two decades ago but due to technical difficulties and incomplete understanding of disease pathogenesis, it remained an underdeveloped technique despite its huge potential.

Reviewing the MS literature, I found that the results from different perfusion MRI studies were contradictive. This stimulated my interest in addressing the fundamental issues behind the limited development in ASL. 7T MRI scanning was performed to increase the SNR and to improve the detection of CLs on PSIR images.

Chapter 2 details the study I did to measure perfusion in CLs in a cohort of 12 MS patients with different disease stages. At the time the study was carried out I was not aware of another study looking

into the use of ASL in assessing CLs perfusion. I recruited patients who were known to have CLs from previous studies within our research unit. Using 7T MRI, I assessed perfusion in 40 CLs, the surrounding NAGM, and global cortical GM. The reason behind the relatively small number of lesions is that I had to identify CLs in a selected number of slices with maximum number of lesions (single slice ASL technique was used). The results of the study are in line with the single previous study which assessed CLs perfusion using DSC (Peruzzo et al. 2013). Majority of CLs are hypo-perfused compared to local and global cortical GM.

A crucial step in validating ASL required comparing it to the gold standard MRI method, DSC; Chapter 3 details the study that addresses this issue; ASL and DSC were performed in the same session on MS patients to measure global GM perfusion and concluded that there is moderate correlation between the two techniques. At the time of writing, this comparison has never been done before in MS studies.

For a technique to be reliable in measuring a physiological change, it needs to be reproducible. I performed ASL imaging on MS and HCs in two separate visits and found that the perfusion maps were not significantly different. This is an indication that ASL can reliably be performed at multiple time-points to measure changes in perfusion.

Future work is needed to validate the use of the 7T ASL protocol, we tested, on 3T scanners. This would transform the technique from a research tool to an imaging method which can be potentially used in clinical practice in the future.

Clinicians use MRI to assess MS disease activity by demonstrating WM changes as those are easier to see on standard MRI images. WM perfusion is not reliably measured using ASL as shown in our studies even at 7T; this could be a limiting factor to future clinical application of non-contrast perfusion MRI. However, ASL can be used to differentiate large demyelinating WMLs from other space occupying lesions (Tourdias et al. 2008, Yeo, Hutton, and Fung 2018), this can help avoid unnecessary invasive procedures such as brain biopsy.

CLs are seen in all MS stages including CIS; a study looking at perfusion changes in CIS compared to established MS cases would be helpful to further understand the role of CLs in different disease stages. Using PSIR or DIR can help detect CLs although many of these lesions remain undetected. Possibly with refinement of the techniques, adding a perfusion sequence such as ASL to clinical scanners can increase the lesions detection rate and probably help with the diagnostic and monitoring process of patients with MS (suspected and definite cases). It can also help with the understanding of the CLs role in disease progression by comparing their evolution compared to WMLs.

GM involvement in MS is an exciting field which has attracted interest in the research community. Measuring perfusion in GM and monitoring its change overtime can help further understand the disease progression in MS and how that affects both cognitive and physical disability long-term. Studies with larger number of participants are needed to measure the correlation between cerebral perfusion and clinical outcomes.

To further understand the significance of perfusion abnormalities in MS, comparison with other neuroinflammatory conditions is warranted.

In conclusion, ASL is a contrast free perfusion MRI technique with promising potential, but its use in the MS field will likely remain in the research setting for the foreseeable future.

5.2 ASL in RCVS

In the RCVS study (chapter 4), I used ASL to measure cerebral perfusion in patients who presented with suspected RCVS and assess the correlation between perfusion imaging and MRA. There was no noticeable association between perfusion and angiogram changes. The study included only 4 patients; future work will be needed to assess a bigger cohort to validate the technique use. Adding ASL sequence to routine clinical scans, as done in space occupying lesions assessment, for patients with suspected RCVS

can potentially help in the diagnostic and monitoring process especially with the known fact that MRA can be initially normal in many cases (Sattar, Manousakis, and Jensen 2010).

A comparison study between people with RCVS and those with other headache disorders such as migraine is needed to confirm the specificity of ASL changes seen in the former group.

Chapter 6: Bibliography

(IHS), Headache Classification Committee of the International Headache Society. 2013. "The International Classification of Headache Disorders, 3rd edition (beta version)." *Cephalalgia* 33 (9):629-808. doi: 10.1177/0333102413485658.

Adhya, S., G. Johnson, J. Herbert, H. Jaggi, J. S. Babb, R. I. Grossman, and M. Inglese. 2006. "Pattern of hemodynamic impairment in multiple sclerosis: dynamic susceptibility contrast perfusion MR imaging at 3.0 T." *Neuroimage* 33 (4):1029-35. doi: 10.1016/j.neuroimage.2006.08.008.

Alsop, D. C., J. A. Detre, X. Golay, M. Günther, J. Hendrikse, L. Hernandez-Garcia, H. Lu, B. J. MacIntosh, L. M. Parkes, M. Smits, M. J. van Osch, D. J. Wang, E. C. Wong, and G. Zaharchuk. 2015. "Recommended implementation of arterial spin-labeled perfusion MRI for clinical applications: A consensus of the ISMRM perfusion study group and the European consortium for ASL in dementia." *Magn Reson Med* 73 (1):102-16. doi: 10.1002/mrm.25197.

Amann, M., L. Achtnichts, J. G. Hirsch, Y. Naegelin, J. Gregori, K. Weier, A. Thöni, N. Mueller-Lenke, E. W. Radue, M. Günther, L. Kappos, and A. Gass. 2012. "3D GRASE arterial spin labelling reveals an inverse correlation of cortical perfusion with the white matter lesion volume in MS." *Mult Scler* 18 (11):1570-6. doi: 10.1177/1352458512441984.

Anderson, J. M., D. W. Hampton, R. Patani, G. Pryce, R. A. Crowther, R. Reynolds, R. J. Franklin, G. Giovannoni, D. A. Compston, D. Baker, M. G. Spillantini, and S. Chandran. 2008. "Abnormally phosphorylated tau is associated with neuronal and axonal loss in experimental autoimmune encephalomyelitis and multiple sclerosis." *Brain* 131 (Pt 7):1736-48. doi: 10.1093/brain/awn119.

Asllani, I., A. Borogovac, and T. R. Brown. 2008. "Regression algorithm correcting for partial volume effects in arterial spin labeling MRI." *Magn Reson Med* 60 (6):1362-71. doi: 10.1002/mrm.21670.

Aviv, R. I., P. L. Francis, R. Tenenbein, P. O'Connor, L. Zhang, A. Eilaghi, L. Lee, T. J. Carroll, J. Mouannes-Srour, and A. Feinstein. 2012. "Decreased frontal lobe gray matter perfusion in cognitively impaired patients with secondary-progressive multiple sclerosis detected by the bookend

technique." *AJNR Am J Neuroradiol* 33 (9):1779-85. doi: 10.3174/ajnr.A3060.

Bagnato, F., J. A. Butman, S. Gupta, M. Calabrese, L. Pezawas, J. M. Ohayon, F. Tovar-Moll, M. Riva, M. M. Cao, S. L. Talagala, and H. F. McFarland. 2006. "In vivo detection of cortical plaques by MR imaging in patients with multiple sclerosis." *AJNR Am J Neuroradiol* 27 (10):2161-7.

Barkhof, F., W. Bruck, C. J. De Groot, E. Bergers, S. Hulshof, J. Geurts, C. H. Polman, and P. van der Valk. 2003. "Remyelinated lesions in multiple sclerosis: magnetic resonance image appearance." *Arch Neurol* 60 (8):1073-81. doi: 10.1001/archneur.60.8.1073.

Belbasis, L., V. Bellou, E. Evangelou, J. P. Ioannidis, and I. Tzoulaki. 2015. "Environmental risk factors and multiple sclerosis: an umbrella review of systematic reviews and meta-analyses." *Lancet Neurol* 14 (3):263-73. doi: 10.1016/S1474-4422(14)70267-4.

Bernard, K. R., and M. Rivera. 2015. "Reversible Cerebral Vasoconstriction Syndrome." *J Emerg Med*. doi: 10.1016/j.jemermed.2015.01.012.

Bester, M., N. D. Forkert, J. P. Stellmann, L. Aly, A. Drabik, K. L. Young, C. Heesen, J. Fiehler, and S. Siemonsen. 2015. "Increased perfusion in normal appearing white matter in high inflammatory multiple sclerosis patients." *PLoS One* 10 (3):e0119356. doi: 10.1371/journal.pone.0119356.

Binnewijzend, M. A., J. P. Kuijer, W. M. van der Flier, M. R. Benedictus, C. M. Möller, Y. A. Pijnenburg, A. W. Lemstra, N. D. Prins, M. P. Wattjes, B. N. van Berckel, P. Scheltens, and F. Barkhof. 2014. "Distinct perfusion patterns in Alzheimer's disease, frontotemporal dementia and dementia with Lewy bodies." *Eur Radiol* 24 (9):2326-33. doi: 10.1007/s00330-014-3172-3.

Blockley, N. P., L. Jiang, A. G. Gardener, C. N. Ludman, S. T. Francis, and P. A. Gowland. 2008. "Field strength dependence of R1 and R2* relaxivities of human whole blood to ProHance, Vasovist, and deoxyhemoglobin." *Magn Reson Med* 60 (6):1313-20. doi: 10.1002/mrm.21792.

Bogousslavsky, J., P. A. Despland, F. Regli, and P. Y. Dubuis. 1989. "Postpartum cerebral angiopathy: reversible vasoconstriction assessed by transcranial Doppler ultrasounds." *Eur Neurol* 29 (2):102-5.

Brooks, D. J., K. L. Leenders, G. Head, J. Marshall, N. J. Legg, and T. Jones. 1984. "Studies on regional cerebral oxygen utilisation and cognitive function in multiple sclerosis." *J Neurol Neurosurg Psychiatry* 47 (11):1182-91.

Bø, L., C. A. Vedeler, H. I. Nyland, B. D. Trapp, and S. J. Mørk. 2003. "Subpial demyelination in the cerebral cortex of multiple sclerosis patients." *J Neuropathol Exp Neurol* 62 (7):723-32.

Calabrese, L. H., D. W. Dodick, T. J. Schwedt, and A. B. Singhal. 2007. "Narrative review: reversible cerebral vasoconstriction syndromes." *Ann Intern Med* 146 (1):34-44.

Calabrese, M., F. Agosta, F. Rinaldi, I. Mattisi, P. Grossi, A. Favaretto, M. Atzori, V. Bernardi, L. Barachino, L. Rinaldi, P. Perini, P. Gallo, and M. Filippi. 2009. "Cortical lesions and atrophy associated with cognitive impairment in relapsing-remitting multiple sclerosis." *Arch Neurol* 66 (9):1144-50. doi: 10.1001/archneurol.2009.174.

Calabrese, M., M. Atzori, V. Bernardi, A. Morra, C. Romualdi, L. Rinaldi, M. J. McAuliffe, L. Barachino, P. Perini, B. Fischl, L. Battistin, and P. Gallo. 2007. "Cortical atrophy is relevant in

multiple sclerosis at clinical onset." *J Neurol* 254 (9):1212-20. doi: 10.1007/s00415-006-0503-6.

Calabrese, M., M. Filippi, M. Rovaris, I. Mattisi, V. Bernardi, M. Atzori, A. Favaretto, L. Barachino, L. Rinaldi, C. Romualdi, P. Perini, and P. Gallo. 2008. "Morphology and evolution of cortical lesions in multiple sclerosis. A longitudinal MRI study." *Neuroimage* 42 (4):1324-8. doi: 10.1016/j.neuroimage.2008.06.028.

Calabrese, M., V. Poretto, A. Favaretto, S. Alessio, V. Bernardi, C. Romualdi, F. Rinaldi, P. Perini, and P. Gallo. 2012. "Cortical lesion load associates with progression of disability in multiple sclerosis." *Brain* 135 (Pt 10):2952-61. doi: 10.1093/brain/aws246.

Calabrese, M., R. Reynolds, R. Magliozzi, M. Castellaro, A. Morra, A. Scalfari, G. Farina, C. Romualdi, A. Gajofatto, M. Pitteri, M. D. Benedetti, and S. Monaco. 2015. "Regional Distribution and Evolution of Gray Matter Damage in Different Populations of Multiple Sclerosis Patients." *PLoS One* 10 (8):e0135428. doi: 10.1371/journal.pone.0135428.

Calabrese, M., M. A. Rocca, M. Atzori, I. Mattisi, A. Favaretto, P. Perini, P. Gallo, and M. Filippi. 2010. "A 3-year magnetic

resonance imaging study of cortical lesions in relapse-onset multiple sclerosis." *Ann Neurol* 67 (3):376-83. doi: 10.1002/ana.21906.

Calabrese, M., C. Romualdi, V. Poretto, A. Favaretto, A. Morra, F. Rinaldi, P. Perini, and P. Gallo. 2013. "The changing clinical course of multiple sclerosis: a matter of gray matter." *Ann Neurol* 74 (1):76-83. doi: 10.1002/ana.23882.

Calic, Z., C. Cappelen-Smith, and A. S. Zagami. 2015. "Reversible cerebral vasoconstriction syndrome." *Intern Med J* 45 (6):599-608. doi: 10.1111/imj.12669.

Call, G. K., M. C. Fleming, S. Sealfon, H. Levine, J. P. Kistler, and C. M. Fisher. 1988. "Reversible cerebral segmental vasoconstriction." *Stroke* 19 (9):1159-70.

Cha, S., S. Pierce, E. A. Knopp, G. Johnson, C. Yang, A. Ton, A. W. Litt, and D. Zagzag. 2001. "Dynamic contrast-enhanced T2*-weighted MR imaging of tumefactive demyelinating lesions." *AJNR Am J Neuroradiol* 22 (6):1109-16.

Chappell, MA, AR Groves, B Whitcher, and MW Woolrich. 2009. Variational Bayesian inference for a non-linear forward model. IEEE Transactions on Signal Processing 57(1):223-236.

Chavhan, G. B., P. S. Babyn, B. Thomas, M. M. Shroff, and E. M. Haacke. 2009. "Principles, techniques, and applications of T2*-based MR imaging and its special applications." *Radiographics* 29 (5):1433-49. doi: 10.1148/rg.295095034.

Chen, S. P., Y. T. Chung, T. Y. Liu, Y. F. Wang, J. L. Fuh, and S. J. Wang. 2013. "Oxidative stress and increased formation of vasoconstricting F2-isoprostanes in patients with reversible cerebral vasoconstriction syndrome." *Free Radic Biol Med* 61:243-8. doi: 10.1016/j.freeradbiomed.2013.04.022.

Chen, S. P., J. L. Fuh, J. F. Lirng, F. C. Chang, and S. J. Wang. 2006. "Recurrent primary thunderclap headache and benign CNS angiopathy: spectra of the same disorder?" *Neurology* 67 (12):2164-9. doi: 10.1212/01.wnl.0000249115.63436.6d.

Chen, S. P., J. L. Fuh, and S. J. Wang. 2010. "Reversible cerebral vasoconstriction syndrome: an under-recognized clinical emergency." *Ther Adv Neurol Disord* 3 (3):161-71. doi: 10.1177/1756285610361795.

Chen, S. P., J. L. Fuh, S. J. Wang, S. J. Tsai, C. J. Hong, and A. C. Yang. 2011. "Brain-derived neurotrophic factor gene Val66Met polymorphism modulates reversible cerebral

vasoconstriction syndromes." *PLoS One* 6 (3):e18024. doi: 10.1371/journal.pone.0018024.

Chen, S. P., Y. F. Wang, P. H. Huang, C. W. Chi, J. L. Fuh, and S. J. Wang. 2014. "Reduced circulating endothelial progenitor cells in reversible cerebral vasoconstriction syndrome." *J Headache Pain* 15:82. doi: 10.1186/1129-2377-15-82.

Chen, S. P., A. C. Yang, J. L. Fuh, and S. J. Wang. 2013. "Autonomic dysfunction in reversible cerebral vasoconstriction syndromes." *J Headache Pain* 14:94. doi: 10.1186/1129-2377-14-94.

Chen, Y., D. J. Wang, and J. A. Detre. 2011. "Test-retest reliability of arterial spin labeling with common labeling strategies." *J Magn Reson Imaging* 33 (4):940-9. doi: 10.1002/jmri.22345.

Cheng, Y. C., K. H. Kuo, and T. H. Lai. 2014. "A common cause of sudden and thunderclap headaches: reversible cerebral vasoconstriction syndrome." *J Headache Pain* 15:13. doi: 10.1186/1129-2377-15-13.

Christoforidis, G. A., E. M. Spickler, M. V. Recio, and B. M. Mehta. 1999. "MR of CNS sarcoidosis: correlation of imaging features to clinical symptoms and response to treatment." *AJNR Am J Neuroradiol* 20 (4):655-69.

Coles, A. 2009. "Multiple sclerosis." *Pract Neurol* 9 (2):118-26. doi: 10.1136/jnnp.2008.171132.

Compston, A., and A. Coles. 2008. "Multiple sclerosis." *Lancet* 372 (9648):1502-17. doi: 10.1016/S0140-6736(08)61620-7.

Compston, D. A., J. R. Batchelor, and W. I. McDonald. 1976. "B-lymphocyte alloantigens associated with multiple sclerosis." *Lancet* 2 (7998):1261-5.

Currie, S., N. Hoggard, I. J. Craven, M. Hadjivassiliou, and I. D. Wilkinson. 2013. "Understanding MRI: basic MR physics for physicians." *Postgrad Med J* 89 (1050):209-23. doi: 10.1136/postgradmedj-2012-131342.

D'haeseleer, M., R. Beelen, Y. Fierens, M. Cambron, A. M. Vanbinst, C. Verborgh, J. Demey, and J. De Keyser. 2013. "Cerebral hypoperfusion in multiple sclerosis is reversible and mediated by endothelin-1." *Proc Natl Acad Sci U S A* 110 (14):5654-8. doi: 10.1073/pnas.1222560110.

D'haeseleer, M., S. Hostenbach, I. Peeters, S. E. Sankari, G. Nagels, J. De Keyser, and M. B. D'hooghe. 2015. "Cerebral hypoperfusion: a new pathophysiologic concept in multiple sclerosis?" *J Cereb Blood Flow Metab*. doi: 10.1038/jcbfm.2015.131.

D'Ortenzio, R. M., S. P. Hojjat, R. Vitorino, C. G. Cantrell, L. Lee, A. Feinstein, P. O'Connor, T. J. Carroll, and R. I. Aviv. 2016. "Comparison of Quantitative Cerebral Blood Flow Measurements Performed by Bookend Dynamic Susceptibility Contrast and Arterial Spin-Labeling MRI in Relapsing-Remitting Multiple Sclerosis." *AJNR Am J Neuroradiol* 37 (12):2265-2272. doi: 10.3174/ajnr.A4939.

De Keyser, J., C. Steen, J. P. Mostert, and M. W. Koch. 2008. "Hypoperfusion of the cerebral white matter in multiple sclerosis: possible mechanisms and pathophysiological significance." *J Cereb Blood Flow Metab* 28 (10):1645-51. doi: 10.1038/jcbfm.2008.72.

Debernard, L., T. R. Melzer, S. Van Stockum, C. Graham, C. A. Wheeler-Kingshott, J. C. Dalrymple-Alford, D. H. Miller, and D. F. Mason. 2014. "Reduced grey matter perfusion without volume loss in early relapsing-remitting multiple sclerosis." *J Neurol Neurosurg Psychiatry* 85 (5):544-51. doi: 10.1136/jnnp-2013-305612.

Dilli, E. 2014. "Thunderclap headache." *Curr Neurol Neurosci Rep* 14 (4):437. doi: 10.1007/s11910-014-0437-9.

Doche, E., A. Lecocq, A. Maarouf, G. Duhamel, E. Soulier, S. Confort-Gouny, A. Rico, M. Guye, B. Audoin, J. Pelletier, J. P. Ranjeva, and W. Zaaraoui. 2017. "Hypoperfusion of the thalamus is associated with disability in relapsing remitting multiple sclerosis." *J Neuroradiol* 44 (2):158-164. doi: 10.1016/j.neurad.2016.10.001.

Dodick, D. W. 2002. "Thunderclap headache." *J Neurol Neurosurg Psychiatry* 72 (1):6-11.

Dodick, D. W., R. D. Brown, J. W. Britton, and J. Huston. 1999. "Nonaneurysmal thunderclap headache with diffuse, multifocal, segmental, and reversible vasospasm." *Cephalalgia* 19 (2):118-23.

Ducros, A. 2013. "L37. Reversible cerebral vasoconstriction syndrome: distinction from CNS vasculitis." *Presse Med* 42 (4 Pt 2):602-4. doi: 10.1016/j.lpm.2013.01.037.

Ducros, A., M. Boukobza, R. Porcher, M. Sarov, D. Valade, and M. G. Bousser. 2007. "The clinical and radiological spectrum of reversible cerebral vasoconstriction syndrome. A prospective series of 67 patients." *Brain* 130 (Pt 12):3091-101. doi: 10.1093/brain/awm256.

Dury, R. J., Y. Falah, P. A. Gowland, N. Evangelou, M. G. Bright, and S. T. Francis. 2019. "Ultra-high-field arterial spin labelling MRI for non-contrast assessment of cortical lesion perfusion in multiple sclerosis." *Eur Radiol* 29 (4):2027-2033. doi: 10.1007/s00330-018-5707-5.

Dury, RJ, Y Falah, PA Gowland, N Evangelou, ST Francis, and MG Bright. 2018. Reproducibility and quality assessment of a 3D-EPI pulsed arterial spin labelling scheme at 7 T in a clinical cohort. Proc Intl Soc Magn Reson Med Ann Mtg Paris, France.

Duyn, J. H. 2012. "The future of ultra-high field MRI and fMRI for study of the human brain." *Neuroimage* 62 (2):1241-8. doi: 10.1016/j.neuroimage.2011.10.065.

ElSankari, S., O. Balédent, V. van Pesch, C. Sindic, Q. de Broqueville, and T. Duprez. 2013. "Concomitant analysis of arterial, venous, and CSF flows using phase-contrast MRI: a quantitative comparison between MS patients and healthy controls." *J Cereb Blood Flow Metab* 33 (9):1314-21. doi: 10.1038/jcbfm.2013.95.

Elster, M. J. 2013. "Natalizumab (tysabri)-associated progressive multifocal leukoencephalopathy: insights from perfusion

magnetic resonance imaging." *J Comput Assist Tomogr* 37 (5):694-7. doi: 10.1097/RCT.0b013e318298aa0d.

Essig, M., T. B. Nguyen, M. S. Shiroishi, M. Saake, J. M. Provenzale, D. S. Enterline, N. Anzalone, A. Dörfler, À Rovira, M. Wintermark, and M. Law. 2013. "Perfusion MRI: the five most frequently asked clinical questions." *AJR Am J Roentgenol* 201 (3):W495-510. doi: 10.2214/AJR.12.9544.

Filippi, M., P. Preziosa, E. Pagani, M. Copetti, S. Mesaros, B. Colombo, M. A. Horsfield, A. Falini, G. Comi, H. Lassmann, and M. A. Rocca. 2013. "Microstructural magnetic resonance imaging of cortical lesions in multiple sclerosis." *Mult Scler* 19 (4):418-26. doi: 10.1177/1352458512457842.

Filippi, M., M. A. Rocca, M. Calabrese, M. P. Sormani, F. Rinaldi, P. Perini, G. Comi, and P. Gallo. 2010. "Intracortical lesions: relevance for new MRI diagnostic criteria for multiple sclerosis." *Neurology* 75 (22):1988-94. doi: 10.1212/WNL.0b013e3181ff96f6.

Firbank, M. J., S. J. Colloby, D. J. Burn, I. G. McKeith, and J. T. O'Brien. 2003. "Regional cerebral blood flow in Parkinson's disease with and without dementia." *Neuroimage* 20 (2):1309-19. doi: 10.1016/S1053-8119(03)00364-1.

Francis, P. L., R. Jakubovic, P. O'Connor, L. Zhang, A. Eilaghi, L. Lee, T. J. Carroll, J. Mouannes-Srour, A. Feinstein, and R. I. Aviv. 2013. "Robust perfusion deficits in cognitively impaired patients with secondary-progressive multiple sclerosis." *AJNR Am J Neuroradiol* 34 (1):62-7. doi: 10.3174/ajnr.A3148.

Francis, S. T., R. Bowtell, and P. A. Gowland. 2008. "Modeling and optimization of Look-Locker spin labeling for measuring perfusion and transit time changes in activation studies taking into account arterial blood volume." *Magn Reson Med* 59 (2):316-25. doi: 10.1002/mrm.21442.

Gardener, A. G., P. A. Gowland, and S. T. Francis. 2009. "Implementation of quantitative perfusion imaging using pulsed arterial spin labeling at ultra-high field." *Magn Reson Med* 61 (4):874-82. doi: 10.1002/mrm.21796.

Gardener, A. G., and P. Jezzard. 2015. "Investigating white matter perfusion using optimal sampling strategy arterial spin labeling at 7 Tesla." *Magn Reson Med* 73 (6):2243-8. doi: 10.1002/mrm.25333.

Ge, Y. 2006. "Multiple sclerosis: the role of MR imaging." *AJNR Am J Neuroradiol* 27 (6):1165-76.

Ge, Y., M. Law, G. Johnson, J. Herbert, J. S. Babb, L. J. Mannon, and R. I. Grossman. 2005. "Dynamic susceptibility contrast perfusion MR imaging of multiple sclerosis lesions: characterizing hemodynamic impairment and inflammatory activity." *AJNR Am J Neuroradiol* 26 (6):1539-47.

Ge, Y., V. M. Zohrabian, E. O. Osa, J. Xu, H. Jaggi, J. Herbert, E. M. Haacke, and R. I. Grossman. 2009. "Diminished visibility of cerebral venous vasculature in multiple sclerosis by susceptibility-weighted imaging at 3.0 Tesla." *J Magn Reson Imaging* 29 (5):1190-4. doi: 10.1002/jmri.21758.

Geurts, J. J., P. J. Pouwels, B. M. Uitdehaag, C. H. Polman, F. Barkhof, and J. A. Castelijns. 2005. "Intracortical lesions in multiple sclerosis: improved detection with 3D double inversion-recovery MR imaging." *Radiology* 236 (1):254-60. doi: 10.1148/radiol.2361040450.

Gevers, S., M. J. van Osch, R. P. Bokkers, D. A. Kies, W. M. Teeuwisse, C. B. Majoie, J. Hendrikse, and A. J. Nederveen. 2011. "Intra- and multicenter reproducibility of pulsed, continuous and pseudo-continuous arterial spin labeling methods for measuring cerebral perfusion." *J Cereb Blood Flow Metab* 31 (8):1706-15. doi: 10.1038/jcbfm.2011.10.

Giovannoni, G., B. Turner, S. Gnanapavan, C. Offiah, K. Schmierer, and M. Marta. 2015. "Is it time to target no evident disease activity (NEDA) in multiple sclerosis?" *Mult Scler Relat Disord* 4 (4):329-33. doi: 10.1016/j.msard.2015.04.006.

Gore, J. C., E. W. Emery, J. S. Orr, and F. H. Doyle. 1981. "Medical nuclear magnetic resonance imaging: I. Physical principles." *Invest Radiol* 16 (4):269-74.

Hajj-Ali, R. A., A. Furlan, A. Abou-Chebel, and L. H. Calabrese. 2002. "Benign angiopathy of the central nervous system: cohort of 16 patients with clinical course and long-term followup." *Arthritis Rheum* 47 (6):662-9. doi: 10.1002/art.10797.

Hall, EL, R Wesolowski, PA Gowland, and ST Francis. 2010. Optimising image readout for perfusion imaging at 7T. Proc Intl Soc Magn Reson Med Ann Mtg Stockholm, Sweden.

Hammad, Tariq, Leonard H. Calabrese, Ken Uchino, Seby John, Mark Stillman, Stewart Tepper, and Colin O'Rourke. 2013. Enothelin-1 plays a role in the pathogenesis of reversible cerebral vasoconstriction syndrome. [abstract]. *Arthritis Rheum*, 65 Suppl 10, 1657.

Haselhorst, R., L. Kappos, D. Bilecen, K. Scheffler, D. Möri, E. W. Radü, and J. Seelig. 2000. "Dynamic susceptibility contrast MR imaging of plaque development in multiple sclerosis: application of an extended blood-brain barrier leakage correction." *J Magn Reson Imaging* 11 (5):495-505.

Hashemi, R. H., W. G. Bradley, D. Y. Chen, J. E. Jordan, J. A. Queralt, A. E. Cheng, and J. N. Henrie. 1995. "Suspected multiple sclerosis: MR imaging with a thin-section fast FLAIR pulse sequence." *Radiology* 196 (2):505-10. doi: 10.1148/radiology.196.2.7617868.

Haufschild, T., S. G. Shaw, J. Kesselring, and J. Flammer. 2001. "Increased endothelin-1 plasma levels in patients with multiple sclerosis." *J Neuroophthalmol* 21 (1):37-8.

Hill, J. M., G. Zalos, J. P. Halcox, W. H. Schenke, M. A. Waclawiw, A. A. Quyyumi, and T. Finkel. 2003. "Circulating endothelial progenitor cells, vascular function, and cardiovascular risk." *N Engl J Med* 348 (7):593-600. doi: 10.1056/NEJMoa022287.

Hojjat, S. P., C. G. Cantrell, R. Vitorino, A. Feinstein, Z. Shirzadi, B. J. MacIntosh, D. E. Crane, L. Zhang, S. A. Morrow, L. Lee, P. O'Connor, T. J. Carroll, and R. I. Aviv. 2016. "Regional reduction in cortical blood flow among cognitively impaired

adults with relapsing-remitting multiple sclerosis patients." *Mult Scler* 22 (11):1421-1428. doi: 10.1177/1352458515622696.

Hojjat, S. P., M. Kincal, R. Vitorino, C. G. Cantrell, A. Feinstein, L. Zhang, L. Lee, P. O'Connor, T. J. Carroll, and R. I. Aviv. 2016. "Cortical Perfusion Alteration in Normal-Appearing Gray Matter Is Most Sensitive to Disease Progression in Relapsing-Remitting Multiple Sclerosis." *AJNR Am J Neuroradiol* 37 (8):1454-61. doi: 10.3174/ajnr.A4737.

Holland, C. M., A. Charil, I. Csapo, Z. Liptak, M. Ichise, S. J. Khoury, R. Bakshi, H. L. Weiner, and C. R. Guttmann. 2012. "The relationship between normal cerebral perfusion patterns and white matter lesion distribution in 1,249 patients with multiple sclerosis." *J Neuroimaging* 22 (2):129-36. doi: 10.1111/j.1552-6569.2011.00585.x.

Honce, J. M., L. Nagae, and E. Nyberg. 2015. "Neuroimaging of Natalizumab Complications in Multiple Sclerosis: PML and Other Associated Entities." *Mult Scler Int* 2015:809252. doi: 10.1155/2015/809252.

Hoppenbrouwers, I. A., and R. Q. Hintzen. 2011. "Genetics of multiple sclerosis." *Biochim Biophys Acta* 1812 (2):194-201. doi: 10.1016/j.bbadis.2010.09.017.

Huang, Y. C., H. L. Liu, J. D. Lee, J. T. Yang, H. H. Weng, M. Lee, M. Y. Yeh, and Y. H. Tsai. 2013. "Comparison of arterial spin labeling and dynamic susceptibility contrast perfusion MRI in patients with acute stroke." *PLoS One* 8 (7):e69085. doi: 10.1371/journal.pone.0069085.

Hurley, A. C., A. Al-Radaideh, L. Bai, U. Aickelin, R. Coxon, P. Glover, and P. A. Gowland. 2010. "Tailored RF pulse for magnetization inversion at ultrahigh field." *Magn Reson Med* 63 (1):51-8. doi: 10.1002/mrm.22167.

Inglese, M., S. Adhya, G. Johnson, J. S. Babb, L. Miles, H. Jaggi, J. Herbert, and R. I. Grossman. 2008. "Perfusion magnetic resonance imaging correlates of neuropsychological impairment in multiple sclerosis." *J Cereb Blood Flow Metab* 28 (1):164-71. doi: 10.1038/sj.jcbfm.9600504.

Inglese, M., S. J. Park, G. Johnson, J. S. Babb, L. Miles, H. Jaggi, J. Herbert, and R. I. Grossman. 2007. "Deep gray matter perfusion in multiple sclerosis: dynamic susceptibility

contrast perfusion magnetic resonance imaging at 3 T." *Arch Neurol* 64 (2):196-202. doi: 10.1001/archneur.64.2.196.

Ingrisch, M., S. Sourbron, S. Herberich, M. J. Schneider, T. Kümpfel, R. Hohlfeld, M. F. Reiser, and B. Ertl-Wagner. 2017. "Dynamic Contrast-Enhanced Magnetic Resonance Imaging Suggests Normal Perfusion in Normal-Appearing White Matter in Multiple Sclerosis." *Invest Radiol* 52 (3):135-141. doi: 10.1097/RLI.0000000000000320.

Ingrisch, M., S. Sourbron, D. Morhard, B. Ertl-Wagner, T. Kümpfel, R. Hohlfeld, M. Reiser, and C. Glaser. 2012. "Quantification of perfusion and permeability in multiple sclerosis: dynamic contrast-enhanced MRI in 3D at 3T." *Invest Radiol* 47 (4):252-8. doi: 10.1097/RLI.0b013e31823bfc97.

Jahng, G. H., K. L. Li, L. Ostergaard, and F. Calamante. 2014. "Perfusion magnetic resonance imaging: a comprehensive update on principles and techniques." *Korean J Radiol* 15 (5):554-77. doi: 10.3348/kjr.2014.15.5.554.

Jankowska-Lech, I., B. Terelak-Borys, I. Grabska-Liberek, W. Palasik, W. Bik, and E. Wolińska-Witort. 2015. "Decreased endothelin-1 plasma levels in multiple sclerosis patients: a

possible factor of vascular dysregulation?" *Med Sci Monit* 21:1066-71. doi: 10.12659/MSM.890899.

Jenkinson, M., P. Bannister, J. M. Brady, and S. M. Smith. 2002. "Improved Optimisation for the Robust and Accurate Linear Registration and Motion Correction of Brain Images." *NeuroImage* 17 (2):825-841.

Juurlink, B. H. 2013. "The evidence for hypoperfusion as a factor in multiple sclerosis lesion development." *Mult Scler Int* 2013:598093. doi: 10.1155/2013/598093.

Kanda, T., T. Fukusato, M. Matsuda, K. Toyoda, H. Oba, J. Kotoku, T. Haruyama, K. Kitajima, and S. Furui. 2015. "Gadolinium-based Contrast Agent Accumulates in the Brain Even in Subjects without Severe Renal Dysfunction: Evaluation of Autopsy Brain Specimens with Inductively Coupled Plasma Mass Spectroscopy." *Radiology* 276 (1):228-32. doi: 10.1148/radiol.2015142690.

Kanda, T., K. Ishii, H. Kawaguchi, K. Kitajima, and D. Takenaka. 2014. "High signal intensity in the dentate nucleus and globus pallidus on unenhanced T1-weighted MR images: relationship with increasing cumulative dose of a gadolinium-

based contrast material." *Radiology* 270 (3):834-41. doi: 10.1148/radiol.13131669.

Kebir, H., K. Kreymborg, I. Ifergan, A. Dodelet-Devillers, R. Cayrol, M. Bernard, F. Giuliani, N. Arbour, B. Becher, and A. Prat. 2007. "Human TH17 lymphocytes promote blood-brain barrier disruption and central nervous system inflammation." *Nat Med* 13 (10):1173-5. doi: 10.1038/nm1651.

Keston, P., A. D. Murray, and A. Jackson. 2003. "Cerebral perfusion imaging using contrast-enhanced MRI." *Clin Radiol* 58 (7):505-13.

Khoury, M. N., S. Gheuens, L. Ngo, X. Wang, D. C. Alsop, and I. J. Koralnik. 2013. "Hyperperfusion in progressive multifocal leukoencephalopathy is associated with disease progression and absence of immune reconstitution inflammatory syndrome." *Brain* 136 (Pt 11):3441-50. doi: 10.1093/brain/awt268.

Kidd, D., F. Barkhof, R. McConnell, P. R. Algra, I. V. Allen, and T. Revesz. 1999. "Cortical lesions in multiple sclerosis." *Brain* 122 (Pt 1):17-26.

Kilsdonk, I. D., L. E. Jonkman, R. Klaver, S. J. van Veluw, J. J. Zwanenburg, J. P. Kuijer, P. J. Pouwels, J. W. Twisk, M. P.

Wattjes, P. R. Luijten, F. Barkhof, and J. J. Geurts. 2016. "Increased cortical grey matter lesion detection in multiple sclerosis with 7 T MRI: a post-mortem verification study." *Brain* 139 (Pt 5):1472-81. doi: 10.1093/brain/aww037.

Kim, S. G. 2012. "Perfusion MR imaging: evolution from initial development to functional studies." *Neuroimage* 62 (2):672-5. doi: 10.1016/j.neuroimage.2012.01.015.

Knutsson, L., X. Xu, F. Ståhlberg, P. B. Barker, E. Lind, P. C. Sundgren, P. C. M. van Zijl, and R. Wirestam. 2017. "Dynamic Susceptibility Contrast MRI at 7 T: Tail-Scaling Analysis and Inferences About Field Strength Dependence." *Tomography* 3 (2):74-78. doi: 10.18383/j.tom.2017.00001.

Komatsu, T., T. Kimura, A. Yagishita, K. Takahashi, and R. Koide. 2014. "A case of reversible cerebral vasoconstriction syndrome presenting with recurrent neurological deficits: Evaluation using noninvasive arterial spin labeling MRI." *Clin Neurol Neurosurg* 126:96-8. doi: 10.1016/j.clineuro.2014.08.023.

Kuhlmann, T., G. Lingfeld, A. Bitsch, J. Schuchardt, and W. Brück. 2002. "Acute axonal damage in multiple sclerosis is most

extensive in early disease stages and decreases over time." *Brain* 125 (Pt 10):2202-12.

Kutzelnigg, A., C. F. Lucchinetti, C. Stadelmann, W. Brück, H. Rauschka, M. Bergmann, M. Schmidbauer, J. E. Parisi, and H. Lassmann. 2005. "Cortical demyelination and diffuse white matter injury in multiple sclerosis." *Brain* 128 (Pt 11):2705-12. doi: 10.1093/brain/awh641.

Landtblom, A. M., S. Fridriksson, J. Boivie, J. Hillman, G. Johansson, and I. Johansson. 2002. "Sudden onset headache: a prospective study of features, incidence and causes." *Cephalalgia* 22 (5):354-60. doi: 10.1046/j.1468-2982.2002.00368.x.

Langrish, C. L., Y. Chen, W. M. Blumenschein, J. Mattson, B. Basham, J. D. Sedgwick, T. McClanahan, R. A. Kastelein, and D. J. Cua. 2005. "IL-23 drives a pathogenic T cell population that induces autoimmune inflammation." *J Exp Med* 201 (2):233-40. doi: 10.1084/jem.20041257.

Lassmann, H. 1998. "Neuropathology in multiple sclerosis: new concepts." *Mult Scler* 4 (3):93-8.

Law, M., A. M. Saindane, Y. Ge, J. S. Babb, G. Johnson, L. J. Mannon, J. Herbert, and R. I. Grossman. 2004.

"Microvascular abnormality in relapsing-remitting multiple sclerosis: perfusion MR imaging findings in normal-appearing white matter." *Radiology* 231 (3):645-52. doi: 10.1148/radiol.2313030996.

Lee, M. S., I. S. Choi, and T. S. Chung. 1989. "Thalamic syndrome and cortical hypoperfusion on technetium-99m HM-PAO brain SPECT." *Yonsei Med J* 30 (2):151-7. doi: 10.3349/ymj.1989.30.2.151.

Lee, R., H. Ramadan, and J. Bamford. 2013. "Reversible cerebral vasoconstriction syndrome." *J R Coll Physicians Edinb* 43 (3):225-8. doi: 10.4997/JRCPE.2013.307.

Leffers, A. M., and A. Wagner. 2000. "Neurologic complications of cerebral angiography. A retrospective study of complication rate and patient risk factors." *Acta Radiol* 41 (3):204-10.

Li, L., M. Chopp, S. P. Nejad-Davarani, K. Jafari-Khouzani, S. C. Patel, J. Budaj, M. Lu, S. B. Elias, M. Cerghet, and Q. Jiang. 2014. "Perfusion and Diffusion Abnormalities of Multiple Sclerosis Lesions and Relevance of Classified Lesions to Disease Status." *J Neurol Neurophysiol* 2014 (Suppl 12):12. doi: 10.4172/2155-9562.S12-012.

Liao, Y. C., J. L. Fuh, J. F. Lirng, S. R. Lu, Z. A. Wu, and S. J. Wang. 2003. "Bathing headache: a variant of idiopathic thunderclap headache." *Cephalalgia* 23 (9):854-9.

Liu, Y., X. Zhu, D. Feinberg, M. Guenther, J. Gregori, M. W. Weiner, and N. Schuff. 2012. "Arterial spin labeling MRI study of age and gender effects on brain perfusion hemodynamics." *Magn Reson Med* 68 (3):912-22. doi: 10.1002/mrm.23286.

Lycke, J., C. Wikkelsö, A. C. Bergh, L. Jacobsson, and O. Andersen. 1993. "Regional cerebral blood flow in multiple sclerosis measured by single photon emission tomography with technetium-99m hexamethylpropyleneamine oxime." *Eur Neurol* 33 (2):163-7.

Maderwald, S., S. C. Ladd, E. R. Gizewski, O. Kraff, J. M. Theysohn, K. Wicklow, C. Moenninghoff, I. Wanke, M. E. Ladd, and H. H. Quick. 2008. "To TOF or not to TOF: strategies for non-contrast-enhanced intracranial MRA at 7 T." *MAGMA* 21 (1-2):159-67. doi: 10.1007/s10334-007-0096-9.

Magliozzi, R., B. Serafini, B. Rosicarelli, G. Chiappetta, C. Veroni, R. Reynolds, and F. Aloisi. 2013. "B-cell enrichment and

Epstein-Barr virus infection in inflammatory cortical lesions in secondary progressive multiple sclerosis." *J Neuropathol Exp Neurol* 72 (1):29-41. doi: 10.1097/NEN.0b013e31827bfc62.

Mainero, C., T. Benner, A. Radding, A. van der Kouwe, R. Jensen, B. R. Rosen, and R. P. Kinkel. 2009. "In vivo imaging of cortical pathology in multiple sclerosis using ultra-high field MRI." *Neurology* 73 (12):941-8. doi: 10.1212/WNL.0b013e3181b64bf7.

Markus, H. S. 2004. "Cerebral perfusion and stroke." *J Neurol Neurosurg Psychiatry* 75 (3):353-61.

Marshall, O., H. Lu, J. C. Brisset, F. Xu, P. Liu, J. Herbert, R. I. Grossman, and Y. Ge. 2014. "Impaired cerebrovascular reactivity in multiple sclerosis." *JAMA Neurol* 71 (10):1275-81. doi: 10.1001/jamaneurol.2014.1668.

Martin, K., T. Rogers, and A. Kavanaugh. 1995. "Central nervous system angiopathy associated with cocaine abuse." *J Rheumatol* 22 (4):780-2.

Maumet, C., P. Maurel, J. C. Ferré, and C. Barillot. 2014. "Robust estimation of the cerebral blood flow in arterial spin labelling." *Magn Reson Imaging* 32 (5):497-504. doi: 10.1016/j.mri.2014.01.016.

McDonald, R. J., J. S. McDonald, D. F. Kallmes, M. E. Jentoft, D. L. Murray, K. R. Thielen, E. E. Williamson, and L. J. Eckel. 2015. "Intracranial Gadolinium Deposition after Contrast-enhanced MR Imaging." *Radiology* 275 (3):772-82. doi: 10.1148/radiol.15150025.

McDonald, W. I., A. Compston, G. Edan, D. Goodkin, H. P. Hartung, F. D. Lublin, H. F. McFarland, D. W. Paty, C. H. Polman, S. C. Reingold, M. Sandberg-Wollheim, W. Sibley, A. Thompson, S. van den Noort, B. Y. Weinshenker, and J. S. Wolinsky. 2001. "Recommended diagnostic criteria for multiple sclerosis: guidelines from the International Panel on the diagnosis of multiple sclerosis." *Ann Neurol* 50 (1):121-7.

Mehdi, A., and R. A. Hajj-Ali. 2014. "Reversible cerebral vasoconstriction syndrome: a comprehensive update." *Curr Pain Headache Rep* 18 (9):443. doi: 10.1007/s11916-014-0443-2.

Miller, D. H., P. Rudge, G. Johnson, B. E. Kendall, D. G. Macmanus, I. F. Moseley, D. Barnes, and W. I. McDonald. 1988. "Serial gadolinium enhanced magnetic resonance imaging in multiple sclerosis." *Brain* 111 (Pt 4):927-39.

Miller, T. R., R. Shivashankar, M. Mossa-Basha, and D. Gandhi. 2015a. "Reversible Cerebral Vasoconstriction Syndrome, Part 1: Epidemiology, Pathogenesis, and Clinical Course." *AJNR Am J Neuroradiol*. doi: 10.3174/ajnr.A4214.

Miller, T. R., R. Shivashankar, M. Mossa-Basha, and D. Gandhi. 2015b. "Reversible Cerebral Vasoconstriction Syndrome, Part 2: Diagnostic Work-Up, Imaging Evaluation, and Differential Diagnosis." *AJNR Am J Neuroradiol*. doi: 10.3174/ajnr.A4215.

Moll, N. M., A. M. Rietsch, S. Thomas, A. J. Ransohoff, J. C. Lee, R. Fox, A. Chang, R. M. Ransohoff, and E. Fisher. 2011. "Multiple sclerosis normal-appearing white matter: pathology-imaging correlations." *Ann Neurol* 70 (5):764-73. doi: 10.1002/ana.22521.

Morse, O. C., and J. R. Singer. 1970. "Blood velocity measurements in intact subjects." *Science* 170 (3956):440-1.

Mortimer, A. M., M. D. Bradley, N. G. Stoodley, and S. A. Renowden. 2013. "Thunderclap headache: diagnostic considerations and neuroimaging features." *Clin Radiol* 68 (3):e101-13. doi: 10.1016/j.crad.2012.08.032.

Mougin, O., R. Abdel-Fahim, R. Dineen, A. Pitiot, N. Evangelou, and P. Gowland. 2016. "Imaging gray matter with concomitant null point imaging from the phase sensitive inversion recovery sequence." *Magn Reson Med* 76 (5):1512-1516. doi: 10.1002/mrm.26061.

Munger, K. L., L. I. Levin, B. W. Hollis, N. S. Howard, and A. Ascherio. 2006. "Serum 25-hydroxyvitamin D levels and risk of multiple sclerosis." *JAMA* 296 (23):2832-8. doi: 10.1001/jama.296.23.2832.

Murata, N., L. F. Gonzalez-Cuyar, K. Murata, C. Fligner, R. Dills, D. Hippe, and K. R. Maravilla. 2016. "Macrocyclic and Other Non-Group 1 Gadolinium Contrast Agents Deposit Low Levels of Gadolinium in Brain and Bone Tissue: Preliminary Results From 9 Patients With Normal Renal Function." *Invest Radiol* 51 (7):447-53. doi: 10.1097/RLI.0000000000000252.

Murata, N., K. Murata, L. F. Gonzalez-Cuyar, and K. R. Maravilla. 2016. "Gadolinium tissue deposition in brain and bone." *Magn Reson Imaging* 34 (10):1359-1365. doi: 10.1016/j.mri.2016.08.025.

Mutsaerts, H. J., J. W. van Dalen, D. F. Heijtel, P. F. Groot, C. B. Majoie, E. T. Petersen, E. Richard, and A. J. Nederveen.

2015. "Cerebral Perfusion Measurements in Elderly with Hypertension Using Arterial Spin Labeling." *PLoS One* 10 (8):e0133717. doi: 10.1371/journal.pone.0133717.

Nakada, T. 2007. "Clinical application of high and ultra high-field MRI." *Brain Dev* 29 (6):325-35. doi: 10.1016/j.braindev.2006.10.005.

Narayana, P. A., Y. Zhou, K. M. Hasan, S. Datta, X. Sun, and J. S. Wolinsky. 2014. "Hypoperfusion and T1-hypointense lesions in white matter in multiple sclerosis." *Mult Scler* 20 (3):365-73. doi: 10.1177/1352458513495936.

Nie, X. J., and Y. Olsson. 1996. "Endothelin peptides in brain diseases." *Rev Neurosci* 7 (3):177-86.

Nielsen, A. S., R. P. Kinkel, E. Tinelli, T. Benner, J. Cohen-Adad, and C. Mainero. 2012. "Focal cortical lesion detection in multiple sclerosis: 3 Tesla DIR versus 7 Tesla FLASH-T2." *J Magn Reson Imaging* 35 (3):537-42. doi: 10.1002/jmri.22847.

O'Connor, J. P., P. S. Tofts, K. A. Miles, L. M. Parkes, G. Thompson, and A. Jackson. 2011. "Dynamic contrast-enhanced imaging techniques: CT and MRI." *Br J Radiol* 84 Spec No 2:S112-20. doi: 10.1259/bjr/55166688.

Olerup, O., and J. Hillert. 1991. "HLA class II-associated genetic susceptibility in multiple sclerosis: a critical evaluation." *Tissue Antigens* 38 (1):1-15.

Ostrow, L. W., T. J. Langan, and F. Sachs. 2000. "Stretch-induced endothelin-1 production by astrocytes." *J Cardiovasc Pharmacol* 36 (5 Suppl 1):S274-7.

Ota, M., N. Sato, Y. Nakata, K. Ito, K. Kamiya, N. Maikusa, M. Ogawa, T. Okamoto, S. Obu, T. Noda, M. Araki, T. Yamamura, and H. Kunugi. 2013. "Abnormalities of cerebral blood flow in multiple sclerosis: a pseudocontinuous arterial spin labeling MRI study." *Magn Reson Imaging* 31 (6):990-5. doi: 10.1016/j.mri.2013.03.016.

Paling, D., E. Thade Petersen, D. J. Tozer, D. R. Altmann, C. A. Wheeler-Kingshott, R. Kapoor, D. H. Miller, and X. Golay. 2014. "Cerebral arterial bolus arrival time is prolonged in multiple sclerosis and associated with disability." *J Cereb Blood Flow Metab* 34 (1):34-42. doi: 10.1038/jcbfm.2013.161.

Papadaki, E. Z., V. C. Mastorodemos, E. Z. Amanakis, K. C. Tsekouras, A. E. Papadakis, N. D. Tsavalas, P. G. Simos, A. H. Karantanas, A. Plaitakis, and T. G. Maris. 2012. "White

matter and deep gray matter hemodynamic changes in multiple sclerosis patients with clinically isolated syndrome." *Magn Reson Med* 68 (6):1932-42. doi: 10.1002/mrm.24194.

Papadaki, E. Z., P. G. Simos, V. C. Mastorodemos, T. Panou, T. G. Maris, A. H. Karantanas, and A. Plaitakis. 2014. "Regional MRI perfusion measures predict motor/executive function in patients with clinically isolated syndrome." *Behav Neurol* 2014:252419. doi: 10.1155/2014/252419.

Papadaki, E. Z., P. G. Simos, T. Panou, V. C. Mastorodemos, T. G. Maris, A. H. Karantanas, and A. Plaitakis. 2014. "Hemodynamic evidence linking cognitive deficits in clinically isolated syndrome to regional brain inflammation." *Eur J Neurol* 21 (3):499-505. doi: 10.1111/ene.12338.

Patrikios, P., C. Stadelmann, A. Kutzelnigg, H. Rauschka, M. Schmidbauer, H. Laursen, P. S. Sorensen, W. Brück, C. Lucchinetti, and H. Lassmann. 2006. "Remyelination is extensive in a subset of multiple sclerosis patients." *Brain* 129 (Pt 12):3165-72. doi: 10.1093/brain/awl217.

Peng, S. L., P. Su, F. N. Wang, Y. Cao, R. Zhang, H. Lu, and P. Liu. 2015. "Optimization of phase-contrast MRI for the

quantification of whole-brain cerebral blood flow." *J Magn Reson Imaging* 42 (4):1126-33. doi: 10.1002/jmri.24866.

Peruzzo, D., M. Castellaro, M. Calabrese, E. Veronese, F. Rinaldi, V. Bernardi, A. Favaretto, P. Gallo, and A. Bertoldo. 2013. "Heterogeneity of cortical lesions in multiple sclerosis: an MRI perfusion study." *J Cereb Blood Flow Metab* 33 (3):457-63. doi: 10.1038/jcbfm.2012.192.

Petersen, E. T., I. Zimine, Y. C. Ho, and X. Golay. 2006. "Non-invasive measurement of perfusion: a critical review of arterial spin labelling techniques." *Br J Radiol* 79 (944):688-701. doi: 10.1259/bjr/67705974.

Peterson, J. W., L. Bö, S. Mörk, A. Chang, and B. D. Trapp. 2001. "Transected neurites, apoptotic neurons, and reduced inflammation in cortical multiple sclerosis lesions." *Ann Neurol* 50 (3):389-400.

Pitt, D., A. Boster, W. Pei, E. Wohleb, A. Jasne, C. R. Zachariah, K. Rammohan, M. V. Knopp, and P. Schmalbrock. 2010. "Imaging cortical lesions in multiple sclerosis with ultra-high-field magnetic resonance imaging." *Arch Neurol* 67 (7):812-8. doi: 10.1001/archneurol.2010.148.

Pizzini, F. B., P. Farace, P. Manganotti, G. Zoccatelli, L. G. Bongiovanni, X. Golay, A. Beltramello, A. Osculati, G. Bertini, and P. F. Fabene. 2013. "Cerebral perfusion alterations in epileptic patients during peri-ictal and post-ictal phase: PASL vs DSC-MRI." *Magn Reson Imaging* 31 (6):1001-5. doi: 10.1016/j.mri.2013.03.023.

Polman, C. H., S. C. Reingold, B. Banwell, M. Clanet, J. A. Cohen, M. Filippi, K. Fujihara, E. Havrdova, M. Hutchinson, L. Kappos, F. D. Lublin, X. Montalban, P. O'Connor, M. Sandberg-Wollheim, A. J. Thompson, E. Waubant, B. Weinshenker, and J. S. Wolinsky. 2011. "Diagnostic criteria for multiple sclerosis: 2010 revisions to the McDonald criteria." *Ann Neurol* 69 (2):292-302. doi: 10.1002/ana.22366.

Polman, C. H., S. C. Reingold, G. Edan, M. Filippi, H. P. Hartung, L. Kappos, F. D. Lublin, L. M. Metz, H. F. McFarland, P. W. O'Connor, M. Sandberg-Wollheim, A. J. Thompson, B. G. Weinshenker, and J. S. Wolinsky. 2005. "Diagnostic criteria for multiple sclerosis: 2005 revisions to the "McDonald Criteria"." *Ann Neurol* 58 (6):840-6. doi: 10.1002/ana.20703.

Pooley, R. A. 2005. "AAPM/RSNA physics tutorial for residents: fundamental physics of MR imaging." *Radiographics* 25 (4):1087-99. doi: 10.1148/rg.254055027.

Poonawalla, A. H., P. Hou, F. A. Nelson, J. S. Wolinsky, and P. A. Narayana. 2008. "Cervical Spinal Cord Lesions in Multiple Sclerosis: T1-weighted Inversion-Recovery MR Imaging with Phase-Sensitive Reconstruction." *Radiology* 246 (1):258-264. doi: 10.1148/radiol.2463061900.

Popescu, B. F., and C. F. Lucchinetti. 2012. "Meningeal and cortical grey matter pathology in multiple sclerosis." *BMC Neurol* 12:11. doi: 10.1186/1471-2377-12-11.

Purkayastha, S., and F. Sorond. 2012. "Transcranial Doppler ultrasound: technique and application." *Semin Neurol* 32 (4):411-20. doi: 10.1055/s-0032-1331812.

Puthenparampil, M., D. Poggiali, F. Causin, G. Rolma, F. Rinaldi, P. Perini, and P. Gallo. 2016. "Cortical relapses in multiple sclerosis." *Mult Scler* 22 (9):1184-91. doi: 10.1177/1352458514564483.

Radbruch, A., L. D. Weberling, P. J. Kieslich, O. Eidel, S. Burth, P. Kickingereder, S. Heiland, W. Wick, H. P. Schlemmer, and M. Bendszus. 2015. "Gadolinium retention in the dentate

nucleus and globus pallidus is dependent on the class of contrast agent." *Radiology* 275 (3):783-91. doi: 10.1148/radiol.2015150337.

Rashid, W., L. M. Parkes, G. T. Ingle, D. T. Chard, A. T. Toosy, D. R. Altmann, M. R. Symms, P. S. Tofts, A. J. Thompson, and D. H. Miller. 2004. "Abnormalities of cerebral perfusion in multiple sclerosis." *J Neurol Neurosurg Psychiatry* 75 (9):1288-93. doi: 10.1136/jnnp.2003.026021.

Riise, T., M. W. Nortvedt, and A. Ascherio. 2003. "Smoking is a risk factor for multiple sclerosis." *Neurology* 61 (8):1122-4.

Rodriguez-Vieitez, E., S. F. Carter, K. Chiotis, L. Saint-Aubert, A. Leuzy, M. Schöll, O. Almkvist, A. Wall, B. Långström, and A. Nordberg. 2016. "Comparison of Early-Phase 11C-Deuterium-l-Deprenyl and 11C-Pittsburgh Compound B PET for Assessing Brain Perfusion in Alzheimer Disease." *J Nucl Med* 57 (7):1071-7. doi: 10.2967/jnumed.115.168732.

Rosenbloom, M. H., and A. B. Singhal. 2007. "CT angiography and diffusion-perfusion MR imaging in a patient with ipsilateral reversible cerebral vasoconstriction after carotid endarterectomy." *AJNR Am J Neuroradiol* 28 (5):920-2.

Saindane, A. M., M. Law, Y. Ge, G. Johnson, J. S. Babb, and R. I. Grossman. 2007. "Correlation of diffusion tensor and dynamic perfusion MR imaging metrics in normal-appearing corpus callosum: support for primary hypoperfusion in multiple sclerosis." *AJNR Am J Neuroradiol* 28 (4):767-72.

Samaraweera, A. P., M. A. Clarke, A. Whitehead, Y. Falah, I. D. Driver, R. A. Dineen, P. S. Morgan, and N. Evangelou. 2017. "The Central Vein Sign in Multiple Sclerosis Lesions Is Present Irrespective of the T2* Sequence at 3 T." *J Neuroimaging* 27 (1):114-121. doi: 10.1111/jon.12367.

Sattar, A., G. Manousakis, and M. B. Jensen. 2010. "Systematic review of reversible cerebral vasoconstriction syndrome." *Expert Rev Cardiovasc Ther* 8 (10):1417-21. doi: 10.1586/erc.10.124.

Serdaru, M., J. Chiras, M. Cujas, and F. Lhermitte. 1984. "Isolated benign cerebral vasculitis or migrainous vasospasm?" *J Neurol Neurosurg Psychiatry* 47 (1):73-6.

Sethi, V., N. Muhlert, M. Ron, X. Golay, C. A. Wheeler-Kingshott, D. H. Miller, D. T. Chard, and T. A. Yousry. 2013. "MS cortical lesions on DIR: not quite what they seem?" *PLoS One* 8 (11):e78879. doi: 10.1371/journal.pone.0078879.

Sethi, V., T. A. Yousry, N. Muhlert, M. Ron, X. Golay, C. Wheeler-Kingshott, D. H. Miller, and D. T. Chard. 2012. "Improved detection of cortical MS lesions with phase-sensitive inversion recovery MRI." *J Neurol Neurosurg Psychiatry* 83 (9):877-82. doi: 10.1136/jnnp-2012-303023.

Silverman, D. H. 2004. "Brain 18F-FDG PET in the diagnosis of neurodegenerative dementias: comparison with perfusion SPECT and with clinical evaluations lacking nuclear imaging." *J Nucl Med* 45 (4):594-607.

Simpson, S., L. Blizzard, P. Otahal, I. Van der Mei, and B. Taylor. 2011. "Latitude is significantly associated with the prevalence of multiple sclerosis: a meta-analysis." *J Neurol Neurosurg Psychiatry* 82 (10):1132-41. doi: 10.1136/jnnp.2011.240432.

Singhal, A. B. 2004. "Postpartum angiopathy with reversible posterior leukoencephalopathy." *Arch Neurol* 61 (3):411-6. doi: 10.1001/archneur.61.3.411.

Singhal, A. B., and R. A. Bernstein. 2005. "Postpartum angiopathy and other cerebral vasoconstriction syndromes." *Neurocrit Care* 3 (1):91-7. doi: 10.1385/NCC:3:1:091.

Smith, S. M. 2002. "Fast robust automated brain extraction." *Human Brain Mapping* 17 (3):143-155.

Sowa, P., A. Bjørnerud, G. O. Nygaard, S. Damangir, G. Spulber, E. G. Celius, P. Due-Tønnessen, H. F. Harbo, and M. K. Beyer. 2015. "Reduced perfusion in white matter lesions in multiple sclerosis." *Eur J Radiol* 84 (12):2605-12. doi: 10.1016/j.ejrad.2015.09.007.

Sowa, P., G. O. Nygaard, A. Bjørnerud, E. G. Celius, H. F. Harbo, and M. K. Beyer. 2017. "Magnetic resonance imaging perfusion is associated with disease severity and activity in multiple sclerosis." *Neuroradiology* 59 (7):655-664. doi: 10.1007/s00234-017-1849-4.

Speciale, L., M. Sarasella, S. Ruzzante, D. Caputo, R. Mancuso, M. G. Calvo, F. R. Guerini, and P. Ferrante. 2000. "Endothelin and nitric oxide levels in cerebrospinal fluid of patients with multiple sclerosis." *J Neurovirol* 6 Suppl 2:S62-6.

Stary, J. M., B. H. Wang, S. J. Moon, and H. Wang. 2014. "Dramatic intracerebral hemorrhagic presentations of reversible cerebral vasoconstriction syndrome: three cases and a literature review." *Case Rep Neurol Med* 2014:782028. doi: 10.1155/2014/782028.

Steen, C., M. D'haeseleer, J. M. Hoogduin, Y. Fierens, M. Cambron, J. P. Mostert, D. J. Heersema, M. W. Koch, and J. De Keyser. 2013. "Cerebral white matter blood flow and energy metabolism in multiple sclerosis." *Mult Scler* 19 (10):1282-9. doi: 10.1177/1352458513477228.

Stevenson, V. L., and D. H. Miller. 1999. "Magnetic resonance imaging in the monitoring of disease progression in multiple sclerosis." *Mult Scler* 5 (4):268-72.

Tan, H., J. A. Maldjian, J. M. Pollock, J. H. Burdette, L. Y. Yang, A. R. Deibler, and R. A. Kraft. 2009. "A fast, effective filtering method for improving clinical pulsed arterial spin labeling MRI." *J Magn Reson Imaging* 29 (5):1134-9. doi: 10.1002/jmri.21721.

Tang, M. Y., T. W. Chen, X. M. Zhang, and X. H. Huang. 2014. "GRE T2∗-weighted MRI: principles and clinical applications." *Biomed Res Int* 2014:312142. doi: 10.1155/2014/312142.

Teeuwisse, Wouter M., Andrew G. Webb, and Matthias J. P. van Osch. 2010. Arterial Spin Labeling at Ultra-High Field: All That Glitters is Not Gold. Int J Imaging Syst Technol. 2010;20:62–70. doi: 10.1002/ima.20218.

Terasaki, P. I., M. S. Park, G. Opelz, and A. Ting. 1976. "Multiple sclerosis and high incidence of a B lymphocyte antigen." *Science* 193 (4259):1245-7.

Thompson, A. J., B. L. Banwell, F. Barkhof, W. M. Carroll, T. Coetzee, G. Comi, J. Correale, F. Fazekas, M. Filippi, M. S. Freedman, K. Fujihara, S. L. Galetta, H. P. Hartung, L. Kappos, F. D. Lublin, R. A. Marrie, A. E. Miller, D. H. Miller, X. Montalban, E. M. Mowry, P. S. Sorensen, M. Tintoré, A. L. Traboulsee, M. Trojano, B. M. J. Uitdehaag, S. Vukusic, E. Waubant, B. G. Weinshenker, S. C. Reingold, and J. A. Cohen. 2018. "Diagnosis of multiple sclerosis: 2017 revisions of the McDonald criteria." *Lancet Neurol* 17 (2):162-173. doi: 10.1016/S1474-4422(17)30470-2.

Tourdias, T., S. Rodrigo, C. Oppenheim, O. Naggara, P. Varlet, S. Amoussa, G. Calmon, F. X. Roux, and J. F. Meder. 2008. "Pulsed arterial spin labeling applications in brain tumors: practical review." *J Neuroradiol* 35 (2):79-89. doi: 10.1016/j.neurad.2007.11.007.

Trapp, B. D., and P. K. Stys. 2009. "Virtual hypoxia and chronic necrosis of demyelinated axons in multiple sclerosis." *Lancet Neurol* 8 (3):280-91. doi: 10.1016/S1474-4422(09)70043-2.

Truyen, L., J. H. van Waesberghe, M. A. van Walderveen, B. W. van Oosten, C. H. Polman, O. R. Hommes, H. J. Adèr, and F. Barkhof. 1996. "Accumulation of hypointense lesions ("black holes") on T1 spin-echo MRI correlates with disease progression in multiple sclerosis." *Neurology* 47 (6):1469-76.

Tzartos, J. S., M. A. Friese, M. J. Craner, J. Palace, J. Newcombe, M. M. Esiri, and L. Fugger. 2008. "Interleukin-17 production in central nervous system-infiltrating T cells and glial cells is associated with active disease in multiple sclerosis." *Am J Pathol* 172 (1):146-55. doi: 10.2353/ajpath.2008.070690.

Umutlu, L., M. E. Ladd, M. Forsting, and T. Lauenstein. 2014. "7 Tesla MR imaging: opportunities and challenges." *Rofo* 186 (2):121-9. doi: 10.1055/s-0033-1350406.

van der Zwaag, W., J. P. Marques, T. Kober, G. Glover, R. Gruetter, and G. Krueger. 2012. "Temporal SNR characteristics in segmented 3D-EPI at 7T." *Magn Reson Med* 67 (2):344-52. doi: 10.1002/mrm.23007.

van Gelderen, P., J. A. de Zwart, and J. H. Duyn. 2008. "Pittfalls of MRI measurement of white matter perfusion based on

arterial spin labeling." *Magn Reson Med* 59 (4):788-95. doi: 10.1002/mrm.21515.

Varga, A. W., G. Johnson, J. S. Babb, J. Herbert, R. I. Grossman, and M. Inglese. 2009. "White matter hemodynamic abnormalities precede sub-cortical gray matter changes in multiple sclerosis." *J Neurol Sci* 282 (1-2):28-33. doi: 10.1016/j.jns.2008.12.036.

Vitorino, R., S. P. Hojjat, C. G. Cantrell, A. Feinstein, L. Zhang, L. Lee, P. O'Connor, T. J. Carroll, and R. I. Aviv. 2016. "Regional Frontal Perfusion Deficits in Relapsing-Remitting Multiple Sclerosis with Cognitive Decline." *AJNR Am J Neuroradiol* 37 (10):1800-1807. doi: 10.3174/ajnr.A4824.

Wang, J., D. C. Alsop, L. Li, J. Listerud, J. B. Gonzalez-At, M. D. Schnall, and J. A. Detre. 2002. "Comparison of quantitative perfusion imaging using arterial spin labeling at 1.5 and 4.0 Tesla." *Magn Reson Med* 48 (2):242-54. doi: 10.1002/mrm.10211.

Washington, C. W., G. J. Zipfel, and Participants in the International Multi-disciplinary Consensus Conference on the Critical Care Management of Subarachnoid Hemorrhage. 2011. "Detection and monitoring of vasospasm and delayed

cerebral ischemia: a review and assessment of the literature." *Neurocrit Care* 15 (2):312-7. doi: 10.1007/s12028-011-9594-8.

Wattjes, M. P., B. W. van Oosten, W. L. de Graaf, A. Seewann, J. C. Bot, R. van den Berg, B. M. Uitdehaag, C. H. Polman, and F. Barkhof. 2011. "No association of abnormal cranial venous drainage with multiple sclerosis: a magnetic resonance venography and flow-quantification study." *J Neurol Neurosurg Psychiatry* 82 (4):429-35. doi: 10.1136/jnnp.2010.223479.

Wintermark, M., M. Sesay, E. Barbier, K. Borbély, W. P. Dillon, J. D. Eastwood, T. C. Glenn, C. B. Grandin, S. Pedraza, J. F. Soustiel, T. Nariai, G. Zaharchuk, J. M. Caillé, V. Dousset, and H. Yonas. 2005. "Comparative overview of brain perfusion imaging techniques." *J Neuroradiol* 32 (5):294-314.

Wu, W. C., M. Fernández-Seara, J. A. Detre, F. W. Wehrli, and J. Wang. 2007. "A theoretical and experimental investigation of the tagging efficiency of pseudocontinuous arterial spin labeling." *Magn Reson Med* 58 (5):1020-7. doi: 10.1002/mrm.21403.

Wu, W. C., S. F. Jiang, S. C. Yang, and S. H. Lien. 2011. "Pseudocontinuous arterial spin labeling perfusion magnetic resonance imaging--a normative study of reproducibility in the human brain." *Neuroimage* 56 (3):1244-50. doi: 10.1016/j.neuroimage.2011.02.080.

Wuerfel, J., J. Bellmann-Strobl, P. Brunecker, O. Aktas, H. McFarland, A. Villringer, and F. Zipp. 2004. "Changes in cerebral perfusion precede plaque formation in multiple sclerosis: a longitudinal perfusion MRI study." *Brain* 127 (Pt 1):111-9. doi: 10.1093/brain/awh007.

Wuerfel, J., F. Paul, and F. Zipp. 2007. "Cerebral blood perfusion changes in multiple sclerosis." *J Neurol Sci* 259 (1-2):16-20. doi: 10.1016/j.jns.2007.02.011.

Yeo, C. J. J., G. J. Hutton, and S. H. Fung. 2018. "Advanced neuroimaging in Balo's concentric sclerosis: MRI, MRS, DTI, and ASL perfusion imaging over 1 year." *Radiol Case Rep* 13 (5):1030-1035. doi: 10.1016/j.radcr.2018.04.010.

Yin, P., H. Xiong, Y. Liu, S. K. Sah, C. Zeng, J. Wang, Y. Li, and N. Hong. 2018. "Measurement of the permeability, perfusion, and histogram characteristics in relapsing-remitting multiple sclerosis using dynamic contrast-enhanced MRI with

extended Tofts linear model." *Neurol India* 66 (3):709-715. doi: 10.4103/0028-3886.232324.

Zajicek, J. P., M. Wing, N. J. Scolding, and D. A. Compston. 1992. "Interactions between oligodendrocytes and microglia. A major role for complement and tumour necrosis factor in oligodendrocyte adherence and killing." *Brain* 115 (Pt 6):1611-31.

Zamboni, P., R. Galeotti, E. Menegatti, A. M. Malagoni, G. Tacconi, S. Dall'Ara, I. Bartolomei, and F. Salvi. 2009. "Chronic cerebrospinal venous insufficiency in patients with multiple sclerosis." *J Neurol Neurosurg Psychiatry* 80 (4):392-9. doi: 10.1136/jnnp.2008.157164.

Zhang, X., I. Ronen, H. E. Kan, W. M. Teeuwisse, and M. J. van Osch. 2016. "Time-efficient measurement of multi-phase arterial spin labeling MR signal in white matter." *NMR Biomed* 29 (11):1519-1525. doi: 10.1002/nbm.3603.

Zhang, Y., M. Brady, and S. Smith. 2001. "Segmentation of brain MR images through a hidden Markov random field model and the expectation-maximization algorithm." *IEEE Trans Med Imag* 20 (1):45-57.

Zivadinov, R., N. Bergsland, M. Stosic, J. Sharma, F. Nussenbaum, J. Durfee, N. Hani, N. Abdelrahman, Z. Jaisani, A. Minagar, R. Hoque, F. E. Munschauer, and M. G. Dwyer. 2008. "Use of perfusion- and diffusion-weighted imaging in differential diagnosis of acute and chronic ischemic stroke and multiple sclerosis." *Neurol Res* 30 (8):816-26. doi: 10.1179/174313208X341003.

Zivadinov, R., M. Ramanathan, K. Dolic, K. Marr, Y. Karmon, A. H. Siddiqui, R. H. Benedict, and B. Weinstock-Guttman. 2011. "Chronic cerebrospinal venous insufficiency in multiple sclerosis: diagnostic, pathogenetic, clinical and treatment perspectives." *Expert Rev Neurother* 11 (9):1277-94. doi: 10.1586/ern.11.117.